EPA-600/4-79-012
February 1979

EFFECTS OF POLLUTANTS AND URBAN PARAMETERS ON ATMOSPHERIC DISPERSION AND TEMPERATURE

by

R. Viskanta and T. L. Weirich
School of Mechanical Engineering
Purdue University
West Lafayette, Indiana 47907

Grant No. R803514

Project Officer

Francis S. Binkowski
Meteorology and Assessment Division
Environmental Sciences and Assessment Laboratory
Research Triangle Park, North Carolina 27711

ENVIRONMENTAL SCIENCES RESEARCH LABORATORY
OFFICE OF RESEARCH AND DEVELOPMENT
U.S. ENVIRONMENTAL PROTECTION AGENCY
RESEARCH TRIANGLE PARK, NORTH CAROLINA 27711

DISCLAIMER

This report has been reviewed by Environmental Sciences and Assessment Laboratory, U. S. Environmental Protection Agency and approved for publication. Approval does not signify that the contents necessarily reflect the views and policies of the U. S. Environmental Protection Agency, nor does mention of trade names or commercial products constitute endorsement or recommendation for use.

ABSTRACT

A study of the effects of anthropogenic pollutants and urbanization on the thermal structure and pollutant dispersal in the planetary boundary layer showed that urbanization had a greater influence on the surface temperature excess between urban and rural locations than the radiatively active pollutants. The net effect of gaseous and particulate pollutants was to decrease the surface temperature around the noon hours and to increase the temperature during the rest of the diurnal cycle. The increase in the surface temperature was most significant for winter simulations with snow covered ground. The maximum temperature at the urban center for a simulation with radiatively active pollutants was about 1 K warmer than for a corresponding simulation without the radiatively active pollutants. As a result of warmer surface temperature, pollutant dispersal near the ground was improved. The feedback between radiatively active pollutants, temperature structure and pollutant dispersal was significant and resulted in a maximum of 25 percent reduction in pollutant concentrations for the winter simulations.

During wintertime the assumed rates of anthropogenic heat release in the city were found to play a more important role in the formation of the urban heat island than the radiatively active pollutants. Increase in heat release raised the surface temperature and caused the surface layer to become less stable which improved pollutant dispersal. Changes in such interface parameters as the surface roughness, moisture availability and solar albedo were found to have significant effect near-surface temperatures in the city and on the urban-rural temperature

differences. The findings indicate that a change in land use is a very important factor in climate and weather modification by urbanization and industrialization.

This report was submitted in fulfillment of Grant Number R 803514 by the School of Mechanical Engineering, Purdue University, West Lafayette, Indiana, under a partial sponsorship of the U. S. Environmental Protection Agency. This phase of the work was completed as of December 1977.

CONTENTS

FIGURES

TABLES

LIST OF SYMBOLS

a_s	Absorptance of soil, $a_s = 1 - r_s$
C_n	Concentration of species n
$\dot{C}_n$	Volumetric rate of production of species n
$C_{w,sat}$	Concentration of water vapor at saturated conditions
c_p	Specific heat at constant pressure
D_n	Diffusion coefficient of species n
E_n	Exponential integral function
e_t	Emittance (emissivity) of the air-soil interface in the thermal part of the spectrum
F	Net radiative flux defined by Eq. (22)
F^+	Radiative flux in the positive z-direction
F^-	Radiative flux in the negative z-direction
f	Coriolis parameter
g	Gravitational constant
H	Turbulent (sensible) heat flux at the air-soil interface, see Eq. (10)
Δh_g	Latent heat of vaporization of water
I_λ	Intensity of radiation
$I_{b\lambda}$	Planck's function
K_z	Turbulent eddy diffusivity in the z-direction
k	Thermal conductivity
ℓ	Mixing length, see Eq. (20)

L	Latent heat flux at the air-soil interface, see Eq. (11)
M	Halstead's moisture availability parameter, see Eq. (13)
m_p	Surface source of pollutant emissions, see Eq. (14)
NP	Refers to radiatively nonparticipating
p	Pressure
P	Refers to radiatively participating
p_λ	Scattering distribution function, see Eq. (17)
q_{an}	Anthropogenic heat emission source at the surface, see Eq. (10)
$\dot{q}$	Volumetric rate of heat generation
r_s	Albedo (reflectance) of the air-soil interface in the solar part of the spectrum
R	Relative humidity of soil or gas constant
Ri	Richardson number
T	Thermodynamic temperature
T_s	Temperature of the soil
t	Time
u	Horizontal north velocity component
v	Horizontal west velocity component
w	Vertical velocity component
x	Horizontal coordinate, see Figure 1
y	Horizontal coordinate
z	Vertical coordinate, see Figure 1
z_o	Surface roughness
α_s	Thermal diffusivity of soil
Θ	Potential temperature defined as $\Theta = T(p_o/p)^{R/c_p}$
κ	Absorption coefficient or the ratio of specific heat at constant pressure to specific heat at constant

	volume
λ	Wavelength
μ	Direction cosine
ν	Frequency
ρ	Density
σ	Scattering coefficient or Stefan-Boltzmann constant
ϕ	Azimuthal angle

Subscripts

n	Refers to species n
p	Refers to pollutants both aerosols and gases
w	Refers to water vapor
Δ	Refers to the bottom of the soil layer
δ	Refers to the edge of the planetary boundary layer
ν	Refers to frequency or per unit frequency
1	Refers to aerosol
2	Refers to pollutant gas
∞	Refers to top of the free atmosphere

Superscripts

M	Refers to turbulent eddy diffusivity of momentum
Θ	Refers to turbulent eddy diffusivity of heat
C_n	Refers to turbulent eddy diffusivity of mass of species n

ACKNOWLEDGMENTS

This work was supported by the Meteorology and Assessment Division, U. S. Environmental Protection Agency, under Grant No. R803514. The interest and support of Drs. James T. Peterson and Francis S. Binkowski, the Grant Project Officers, is acknowledged with sincere thanks. Computer facilities were made available by the National Center for Atmospheric Research which is supported by the National Science Foundation.

The authors also wish to acknowledge fruitful discussions with and contributions of Drs. R. W. Bergstrom, Jr., and A. Venkatram to this effort. Mr. Rodney A. Daniel has assisted with numerical calculations and data reduction. One of the authors (R. V.) held a Humbolt Award from the Alexander von Humbolt Foundation, Bonn, Federal Republic of Germany during 1976-1977. He also gratefully acknowledges the hospitality extended to him by the Technical University of Munich during his stay in the Federal Republic of Germany.

SECTION 1

INTRODUCTION

LOCAL WEATHER MODIFICATION

The rapid increase in industrialization over the past few decades has been accompanied by relatively significant changes in the local climate (Peterson, 1969; Landberg, 1975 and 1977). There is also considerable measure of agreement among investigators as to the nature and magnitude of inadvertant weather and climate modifications particularly on urban and meso scales. The modifications are manifested by observations of urban-rural differences in horizontal and vertical temperature, relative humidity, wind speeds, radiation, visibility, precipitation and other alterations. The differences in the various meteorological parameters are well documented and recent reviews are available (Garstang et al., 1975; Landsberg, 1977).

The temperature difference between urban and rural areas, known as the urban heat island effect, is satisfactorily understood (Landsberg, 1974). It is generally accepted that, in addition to the earth-surface properties and topography differences between urban and rural environs there are a number of physical processes which are known to contribute to the effects of urbanization on temperature, relative humidity and wind flow patterns. For example, the physical processes which are known to influence the urban heat island formation include: 1) reduction of low level winds due to buildings, 2) reduced evaporation cooling due to lower moisture availability in the city, 3) increased heat storage in concrete and buildings, 4) anthropogenic heat emissions due to human activity, and 5) alteration of the radiation

balance due to the presence of air pollutants in the urban atmosphere. The physics of the development and decay of the urban heat island is understood and the relative importance of these processes has been examined (Garstang et al., 1975).

The urban heat island is created by man's activity; therefore, phenomena associated with that activity accompany the heat island and may contribute to its unintended effects on weather and climate. A number of feedback mechanisms can also come into play as a result of anthropogenic effects. For example, radiative interaction with air pollutants in the planetary boundary layer (PBL) can affect the energy balance and the temperature structure in the boundary layer and, through this change, the pollutants can alter the mixed layer growth and turbulent diffusivities. In turn, these changes may modify the concentration and dispersion rate of pollutants near the ground. In addition, cumulative and synergistic effects may also arise as a result of changes in the pattern of land use, anthropogenic air pollutants, water vapor and heat emissions and radiative transfer. It is important to understand these mechanisms so that their contribution to the magnitude of the inadvertant weather modification in urban areas can be assessed.

The modification of the thermal structure by air pollutants is just one of the many effects of urbanization on the weather and climate of a city and its rural surroundings. Although observational data can provide, for example, information on the urban environment, it cannot explain the effects of various factors influencing the urban atmosphere. An understanding of the different effects of urbanization can be obtained only by isolating possible causative factors and studying their contributions one at a time. Such a procedure is not practical from the view of an observational program as it is not possible to manipulate environmental and meteorological conditions. Mathematical models, however, can be employed to advantage to help understand and extend observational data by numerically simulating the transport process in the atmosphere. To the extent

that the mathematical model simulates observations, it can become valuable. For example, the model can aid local weather prediction, interpretation of field data, forecasting of pollution episodes in urban areas, urban planning, estimation of air pollution dispersion, and identification of pollutants using remote sensing methods. In addition to the above, numerical modeling can also be a valuable guide to on-going observational programs such as METROMEX, SURE, MAP3S, MISTT and others. The main utility of numerical modeling lies in its ability to predict what will happen for any given set of changes in the urban parameters, meteorological, surface and/or initial conditions.

OBJECTIVES AND SCOPE OF STUDY

The primary effects of particulate and gaseous pollutants on urban climate is through their radiative interaction. Understanding the alteration of the visibility, insolation, ground and near ground temperature and wind patterns by aerosols and of the ground and of the near ground temperature and wind patterns by gaseous pollutants are of importance in being able to assess the impact of air pollutants on the anthropogenic contributions to the changes in the urban environment. Apart from the precise details by which gaseous and particulate matter might influence, for example, the energy balance in an urban atmosphere, an important aspect in understanding local climate modification and pollutant dispersion involves feedback mechanisms which could amplify the influence of variations in factors such as atmospheric stability, lapse rate, surface temperature, effective PBL albedo, mixed layer growth and others.

The primary objective of the research program was to enhance understanding of the effects of pollutants on the urban environment. To this end, the specific aims of the project were:

1. To perform short-term numerical experiments and sensitivity studies using an unsteady, two-dimensional transport model simulating transport processes in an urban PBL by accounting for anthropogenic pollutant and heat

emissions in the atmosphere as well as surface parameter variations along an urban area.

2. To determine the role of pollutants in modifying the temperature structure in the urban atmosphere.
3. To search for primary feedback mechanisms between pollutants, temperature structure and pollutant dispersion.

First, before proceeding with details of the model used and the discussion of results, some background material is presented which is relevant to the model. The available literature on the urban PBL models, surface characteristics, radiation characteristics of pollutants and anthropogenic pollutant, water vapor and heat emissions in the atmosphere are reviewed.

In the report emphasis is placed on the results and their discussion. The development of the model used for the numerical simulations is discussed adequately elsewhere (Viskanta et al., 1976) and changes made in the model since its initial development will be highlighted. Only results of numerical experiments which have not yet been published will be discussed in the report. Some phases of the overall project have been completed some time ago and the results are available in the published literature. The publications which have resulted from the work under the research grant are listed in APPENDIX.

URBAN PBL MODELS

During the past decade there has been considerable interest in developing improved understanding of the urban environment and a number of urban-PBL models have been developed. These models can be roughly divided into three groups based on the approaches taken. These groups are: 1) unsteady energy-budget studies of the urban surface (e.g. Myrup, 1969; Gertis and Wolseher, 1977) and for the surface plus mixing depth (e. g. Leahey and Friend, 1971; Oke and East, 1971), 2) dynamic models simulating air flow over heated surfaces but ignoring pollutants and surface characteristics (e. g. Estoque and Bhumralker, 1969; Olfe and Lee, 1971;

Vukovich, 1973; Bornstein, 1975) and those models which ignore pollutants but account for surface characteristics (e. g. Yu and Wagner, 1975; Gutman and Torrance, 1975) and 3) dynamic PBL models incorporating the radiative effects of anthropogenic air pollutant, water vapor and heat emissions. The third group of models is most relevant to this work and will be summarized in the following paragraphs.

The urban-PBL models which account for anthropogenic effects of radiatively interacting air pollutants, heat emissions and surface characteristics can be grouped into one-, two- and three-dimensional models. Some dynamic models which account for the presence of radiatively active pollutants in the urban PBL but ignore horizontal variations have been developed (Atwater, 1971a, 1971b, Zdunkowski and McQuage, 1972; Bergstrom and Viskanta, 1973a, 1973b; Zdunkowski et al., 1976; Venkatram and Viskanta, 1976). The earliest models (Atwater, 1971a, 1971b) neglected both convection and advection and specified the surface temperature independently of the boundary layer. In some later models, which could be considered as extensions of earlier work of Atwater, other investigators (Zdunkowski and McQuage, 1972; Bergstrom and Viskanta, 1973a; Venkatram and Viskanta, 1976; Zdunkowski et al., 1976) have incorporated radiative transfer and convective transport by eddy diffusion into time-dependent, one-dimensional models which produced vertical velocity, temperature, water vapor and pollutant concentration profiles. In these models radiative transfer is treated with different levels of detail, but the K-theory is used to model turbulent eddy diffusion.

More detailed time-dependent two-dimensional transport models in the urban PBL have also been developed and used to perform numerical simulations (Atwater, 1974; Viskanta et al., 1976; Venkatram and Viskanta, 1976; Viskanta et al., 1977a). In these models the variation of the surface characteristics and anthropogenic air pollution and heat emission parameters were accounted for. Perhaps the most detailed (e. g. as far as the geometry is concerned) three-dimensional PBL models developed to date are

those of Atwater (1975, 1977). The model accounts for changes in topography and incorporates radiation, convection, advection and diffusive transport as well as source emissions. The model parametrizes surface-atmosphere interactions for rural and urban land surfaces and calculates the surface temperature from an energy balance equation. Anthropogenic heat emission sources are accounted in the surface energy balance. Vertical transport is described by turbulent eddy diffusivity approach while the radiative transfer calculated using a simple approximate model (Atwater, 1971a, 1971b). A relatively crude (5 x 5 at 12.8 km intervals over Los Angeles) (Atwater, 1975) grid is used for the numerical calculations, apparently because of computer time requirements.

The sophistication of the urban PBL models for numerical simulations has increased in the past few years. However, the results are still ambiguous and must be treated with some skepticism. This is due, in large part, to several factors: 1) various surface parameters which enter the models are virtually unknown in urban area, 2) radiation absorption and scattering characteristics of anthropogenic aerosol and absorption coefficients of air pollutants are uncertain, 3) air pollution and heat emission during the diurnal cycle cannot be modeled with sufficient accuracy, 4) turbulence models are inadequate, and 5) the results of the models have received little verification because of the lack of comparison to actual urban data. The next few subsections will address some of these problem areas in greater detail.

SURFACE PARAMETERS

A rural surface is a combination of natural cover such as grass, vegetation, trees, bare dirt, water and some impervious cover such as roads. An urban surface is of course an amalgamation of impervious cover such as streets and buildings and natural cover, predominantly grass, vegetation and trees. The physical properties and the radiation characteristics of the substrate must be determined as an average of these types of

materials. However, the properties needed have not been established for common type soils (Eagleson, 1970) not to mention the large variety of materials encountered in different urban areas.

The amount of impervious cover in urban areas is a question of some importance to hydrologists and few studies have been carried out (Bartholomew, 1955; Abrams, 1966; Clawson, 1972). These studies indicate that at least 50 percent of the average large city is impervious cover. The studies of Bartholomew (1955) and Clawson (1972) are, however, biased towards high cover by their consideration of large cities with highly developed core and by predominantly eastern cities with high polulation densities. A statistical study (Stankowski, 1972) has developed a relationship between impervious cover and population density.

Model calculations have indicated that urban surface characteristics may play an important role in the formation of heat islands (Atwater, 1972). However, little has been done (Dabbert and Davis, 1974) to determine values for the surface parameters which are to be used in the numerical models. The values used by Atwater (1972) are taken, in large part, from the work of Myrup (1969) and represent educated guesses rather than actual experimental data. Other investigators (Yu and Wagner, 1975; Gutman and Torrance, 1975; Viskanta et al., 1977a) who have modelled the temperature structure used similar values.

RADIATION CHARACTERISTICS OF AIR POLLUTANTS

Particulate Pollutants

The atmospheric aerosols and their radiation absorption and scattering properties are characterized by their size distribution, chemical composition, and physical properties such as the density and the complex index of refraction. The problem of characterizing the aerosols is a difficult one and consequently any model of the radiation characteristics will be open to some criticism over the parameters used. An extensive (over several hundred literature citations) and up to date review of the tropospheric and stratospheric aerosols is available (Kondratayev,

1977) and will not be repeated. A few of the relevant topics will be discussed here.

Recent studies in St. Louis (Bhardwaja et al., 1974; Charlson et al., 1974; Dzuby and Stevens, 1975) suggest that the urban aerosols may be separated into two distinct distributions based on the size and the chemical composition of the aerosol particles. The first of these distributions consists generally of particles with radii greater than 2 μm. These particles are composed primarily of silcon oxides with substantial amounts of calcium and lesser amounts of iron oxides and metal chlorides. The second of these two distributions consists generally of particles which have radii less than 2 μm. These particles are chiefly anthropogenic in origin and are either produced directly as aerosol or by heterogeneous nucleation of gas-phase pollutants. Chemical analysis of these particles shows large concentrations of sulfur and carbon compounds with varying amounts of lead, zinc, arsenic and other metals. Chemical analysis of organic constituents (Kondratayev, 1977) suggests that organic acids are also present in submicron particles. Because of the hygroscopic nature of many of the chemical compounds present in the aerosol and the high humidities present in the urban areas, the particles are often composed largely of liquid water. The solution of water-soluble pollutants favors the formation of many pollutant species such as sulfuric acid, bisulfates, ammonium sulfate and nitrate as well as a host of other salts and acids (Kondratayev, 1977).

Measurements of size distributions in cities (Butcher and Charlson, 1972) indicate that plots of volume distributions versus particle diameter generally exhibit a bimodal structure with the two peaks occuring about 0.4 μm and 10 μm and the minimum between the peaks around 2 μm. The measurements also show a large variation in the relative magnitude of the two peaks. While the power law distributions are quite satisfactory for number density, they are quite unsatisfactory for volume distributions. Experimental data show variation in the aerosol particle size distribution with altitude in the troposphere as well as with the

type of the aerosol (Kunkel et al., 1975; Kondratayev, 1977).

The chemical complexity of the aerosol makes it extremely difficult to specify the spectral index of refraction, $\tilde{n}_\lambda = n_\lambda + ik_\lambda$, which together with the size distribution and density is needed to calculate the spectral absorption and scattering characteristics of the aerosol (Bergstrom, 1972). Measurements have, however, been reported for the larger, more homogeneous natural aerosol particles (Kondratayev, 1977). Because of the extreme chemical complexity of anthropogenic aerosol, it is not possible to relate its index of refraction to that of particular chemical compound as was done with natural aerosol. Measurements of urban aerosols (Hänel, 1968; Fischer, 1970; Charlson, et al., 1974; Kondratayev, 1977) suggest that the imaginary part of the complex index of refraction is small but not zero. However, there is a great deal of uncertainty associated with these measurements.

Gaseous Pollutants

There are hundreds of different waste gases emitted into the atmosphere in urban areas as a result of human activity. Leighton (1961) has presented the absorption coefficient in the solar part of the spectrum of some gases associated with photochemical reactions, including nitrogen dioxide, sulfur dioxide, ozone, nitric acid, ethyl nitrate, biacetyl, methyl propenyl keytone and hydrogen peroxide. Of these gases nitrogen dioxide has the greatest effect on the radiative transfer and energy budget in the atmosphere. The gas is a strong absorber in the short wave part of the spectrum and its concentrations in the urban atmospheres are sufficiently high (Kunkel et al., 1975). The absorption coefficients of gaseous pollutants in the long-wave part of the spectrum of such gases as sulfur dioxide, methane, ammonia, carbon monoxide, peroxyacetyl nitrate, ethylene, benzene, nitric oxide, nitrogen dioxide and ozone has been presented by Ludwig et al. (1969). A more recent survey of the gaseous pollutants and the measured range of the concentrations in the atmosphere is available (Kunkel et al., 1975).

SECTION 2

CONCLUSIONS

The conclusions of this study deal with the results of the numerical simulations and with the model itself. These two topics are related since the results obtained from the model can only be applied to the urban PBL in so far as the model represents the physical processes which occur in the urban atmosphere.

The results of the various numerical simulations performed for the assumed, meteorological conditions and urban parameters can be summarized into the following main points:

1. In general, urbanization has greater influence on the ground and near-ground temperature than radiatively active pollutants. The net effect of aerosols is to decrease the daytime surface temperature. The net effect of gaseous pollutants is to increase the nighttime surface temperature. The increase in the surface temperature is most significant during winter nights with snow covered ground (~ 1 K at urban center).
2. Radiatively active air pollutants in the PBL accentuate the nighttime and moderate the daytime urban heat island. During wintertime the assumed rate of anthropogenic heat releases are found to play a more important role in the formation of the urban heat island than radiatively active pollutants. Heat releases in the city increase the temperature excess between urban and rural environs.
3. Radiatively participating aerosols in the city generally give rise to cooling of the ground and warming

of the PBL. Whether there is a net cooling or warming of the earth-PBL system depends upon the surface albedo, the radiation absorption and scattering characteristics of the aerosol, aerosol loadings and vertical distribution and zenith angle (latitude, season and time of day). Because of the incomplete knowledge of aerosol radiative properties (e. g. primarily absorption) the conclusions about the effects on the radiation balance of the earth-atmosphere system have to be carefully tempered by statements about these properties.

4. From the results obtained it is clear that urban interface parameters such as the roughness height, moisture availability and solar albedo are more important in forming the urban heat island than radiatively active pollutants. This is particularly true during the day when solar irradiation and surface temperature are at their maximum. The findings indicate that urbanization and industrialization have a significant impact on the urban microclimate. It is possible that these microclimatic perturbations might lead to changes in large scale weather. Thus, it is evident that the modeling of atmospheric transport processes is a crucial step in urban planning.
5. Radiatively active air pollutants alter the local energy balance and through it modify the vertical temperature structure, stability and heat fluxes at the ground. The altered atmospheric stability produces feedback between pollutant concentrations, temperature structure and pollutant dispersion. The feedback is particularly significant during winter nights downwind of the urban center. It results in a reduction of a maximum of 25% in pollutant concentrations at a 2 m height for simulations

with radiatively active pollutants in comparison with radiatively inactive pollutants. The magnitude of the feedback correlates with the magnitude of the near-ground temperature difference between the two simulations.

6. Aerosol particles by absorbing and scattering solar radiation have a number of direct and indirect effects. They affect air quality and by modifying solar radiation they also influence the energy availability for solar energy utilization systems particularly in urban areas. Aerosols not only reduce direct solar flux reaching ground but also change the proportion of direct and diffuse radiation.
7. The urban heat island formed by urbanization and anthropogenic heat and pollutant emissions into the atmosphere may have some social and economic impact if it exceeds a few degrees Celsius. For example, the energy demand for space heating would be decreased. Taken over a diurnal cycle in summer, the net effect may be nullified. The energy demand for space cooling would be decreased but it may be increased at night because of warmer air temperatures.
8. A more complete understanding to what extent air pollutants modify the thermal structure and their own dispersion in an urban PBL will most likely come from better turbulence models, from more complete understanding of the absorption characteristics of anthropogenic aerosols and gases, and from more complete data on the properties of the urban interface. Observational data in urban atmospheres is essential for verifying the various models.

Before concluding it is worthwhile to emphasize the shortcomings of the model used in this study. The model is two-dimensional and cannot realistically simulate three-dimensional transport processes in the urban PBL. However, a truly detailed

and accurate treatment of the present problem is extremely difficult and beyond the capability of most present-day computers. Since the primary objective of the research is to simulate thermal structure, pollutant dispersion and radiative transfer, some details of the complicated urban flow field have been ignored. For example, the model cannot simulate diffusion within or between tall roughness elements such as buildings. In addition, the model of this study does not account for chemical and photochemical reactions either in the PBL or at the surface. Finally, the transport of pollutants by cumulus convection and interaction between could processes and the radiation field have been neglected by assuming that the atmosphere is cloudless. The two-dimensional model, however, should provide a more realistic description of transport processes in the urban PBL than one-dimensional models.

SECTION 3

RECOMMENDATIONS

This investigation involved modeling of a large number of physical processes. Although every attempt was made to model the physical processes as realistically as possible, the wide scope of this study made it impossible to give equal attention to all the processes. Two types of specific recommendations are made here for future work. First, problem areas are identified which require additional research effort for the purpose of improving the transport model. Second, specific research topics are suggested which could be investigated using the model.

Some of the problem areas which should receive attention in connection with the development of a dynamic two-dimensional transport model are the following:

1. An improved turbulence model is needed. This is particularly critical in the simulation of the outer PBL where the production-dissipation equilibrium assumption, which forms the basis for eddy diffusivity correlations, is not valid. A first step towards an improvement of turbulence modeling would be the incorporation of a two-equation (Launder and Spalding, 1974) model.
2. A radiative transfer model which accounts for the presence of clouds as well as for air pollutants in an urban atmosphere should be developed and incorporated in the two-dimensional transport model. In this model the shadowing caused by buildings should be considered. Some research effort in this direction has been reported at a recent symposium (e. g. Avaste and Vainikko,

1977; Davies and Weinman, 1977). Models which consider clouds and radiation interaction with them are needed for examining numerically various feedback mechanisms and attempting to understand the higher order nonlinear interactions of the various atmospheric constituents with the radiation field.

3. An improved procedure should be developed to account for the absorption and emission of thermal radiation of a combination of pollutant gases. A realistic pollutant model should include the most important pollutants found in an urban atmosphere. Such a model should also provide a procedure to account for the overlap between the pollutant gas bands. As narrow band models are too time consuming for dynamic calculations, it is necessary to modify the wide band models to account for overlap.
4. Realistic procedures for modeling the spatial and temporal variation of anthropogenic pollutant, heat and water vapor emissions in the urban atmosphere must be developed. For example, it is important to model the variation of the pollutant sources along the urban area with time of the day since the location of pollutant sources determines whether radiative interaction by pollutants increases or decreases pollutant concentrations.
5. Simple operational urban PBL models incorporating direct and indirect radiation effects (e. g. in a parametrized manner) should be developed for performing studies on urban and meso scales. The models should be sufficiently flexible to allow, for example, modeling in urban areas with large variations in topography and/or near large bodies of water.

While a number of problem areas remain, the dynamic two-dimensional transport model can simulate time-dependent

distributions of meteorological variables in the urban PBL. The model can be used to study various feedback mechanisms and synergistic effects which may be important in understanding inadvertent weather modification on micro and macro scales. Specifically, it is recommended that the following topics be investigated using the model.

1. The limited results of this study indicate the important role of the surface parameters in determining the effect of radiatively active pollutants on the temperature in the urban atmosphere. Systematic sensitivity studies should be conducted to focus attention on the interface parameters and their variation along the urban area.
2. The cumulative and synergistic effects of changes in the pattern of land use and anthropogenic heat and pollutant emissions within an urban area should be investigated. For example, the model can be used as a component of a study evaluating the total environmental change resulting from a proposed siting in an existing urban area of a new large scale industrial and/or residential development on weather, climate and air quality. This type of input would be useful to those developing strategies for land use, economic and social development of an urban area.
3. Urbanization and industrialization, including heat and pollutant emissions, modifies temperature and winds near the ground. This may affect energy demand for space heating and/or cooling over a diurnal cycle or for a season. The net effect of modification of environment on the energy demand is by no means clear, and more complete investigation appears to be warranted. The energy use in an urban area has a direct effect on air quality and emission control planning.
4. The role of the turbulence model in determining pollutant induced changes of pollutant dispersal should be

investigated. This can be accomplished by performing a series of simulations with identical conditions and sources but with different turbulence models. Use of different models on the sensitivity of the vertical temperature structure have been investigated (Zdunkowski et al., 1976). Atmospheric turbulence is still incompletely understood and conclusions based on results of simulations which examine the effect of the choice of the turbulence model will find acceptance.

SECTION 4

THE URBAN PBL MODEL

DYNAMIC TWO-DIMENSIONAL TRANSPORT MODEL

The dynamic two-dimensional transport model of the urban PBL utilized for the numerical simulations is described elsewhere (Viskanta et al., 1976) and is only highlighted here. Only changes of substance in that model will be discussed below.

A schematic representation of the urban environment and coordinate system is illustrated in Figure 1. In the model the earth-atmosphere system is assumed to be composed of four layers: (1) the "free (natural) atmosphere" which is not affected

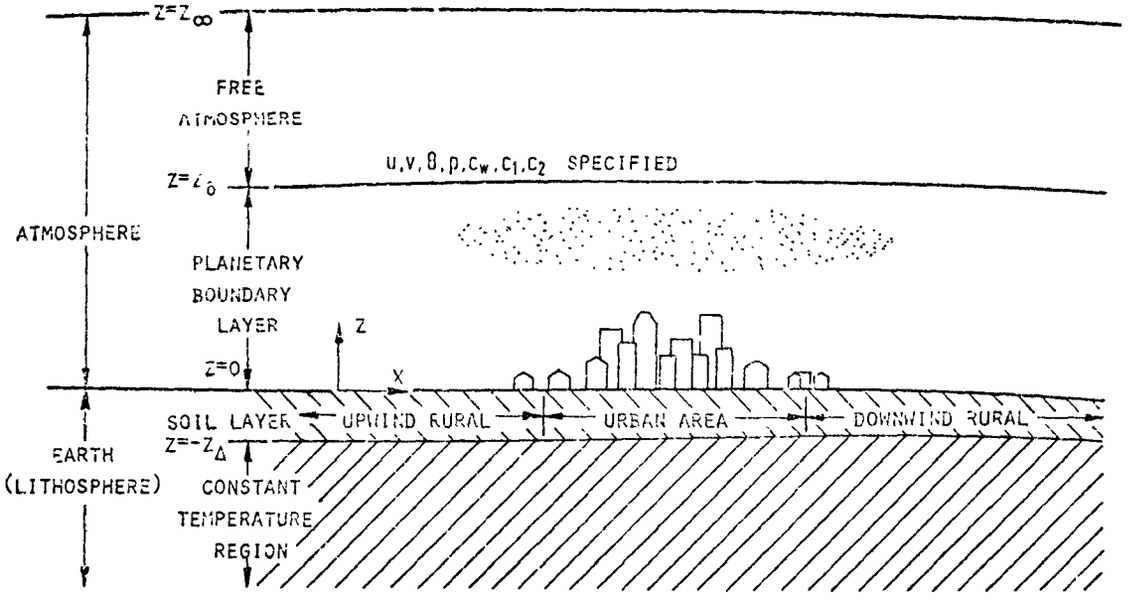

Figure 1. Schematic representation of urban environment and coordinate system.

greatly by surface processes and where meteorological variables are considered to be time independent; (2) the "polluted" atmosphere (the PBL) where the meteorological variables such as the horizontal, vertical, and lateral wind velocities, temperature, water vapor and pollutant concentrations are functions of height, time, and distance along the urban area; (3) the soil layer where the energy transport is one-dimensional (with depth only), but the soil properties and the radiation characteristics are considered to vary in the horizontal direction; and (4) the lithosphere where the temperature below the "soil layer" is assumed to be constant during the simulation period. Variation in the topography of the urban area is neglected, and the atmosphere is assumed to be cloud free.

Model Equations

In the polluted transition layer, the boundary-layer equations expressing mass, momentum, energy, and species* conservation are:

Mass:

$$\frac{\partial(\rho u)}{\partial x} + \frac{\partial(\rho w)}{\partial z} = 0 \qquad (1)$$

Momentum (x-direction):

$$\frac{\partial u}{\partial t} + u\frac{\partial u}{\partial x} + w\frac{\partial u}{\partial z} = f(v - v_g) + \frac{\partial}{\partial z}\left(K_z^M \frac{\partial u}{\partial z}\right) \qquad (2)$$

Momentum (y-direction):

$$\frac{\partial u}{\partial t} + u\frac{\partial v}{\partial x} + w\frac{\partial v}{\partial z} = -f(u - u_g) + \frac{\partial}{\partial z}\left(K_z^M \frac{\partial v}{\partial z}\right) \qquad (3)$$

Momentum (z-direction):

$$0 = +\frac{\partial p}{\partial z} + \rho g \qquad (4)$$

Energy:

$$\frac{\partial \Theta}{\partial t} + u\frac{\partial \Theta}{\partial x} + w\frac{\partial \Theta}{\partial z} = \frac{\partial}{\partial z}\left(K_z^{\Theta} \frac{\partial \Theta}{\partial z}\right) - \left[\frac{\partial F}{\partial z} - \dot{q}\right](p_o/p)^{R/c_p}/\rho c_p \qquad (5)$$

*The specific humidity is not conserved but the water vapor concentration, partial pressure and density are conservable quantities.

Species:

$$\frac{\partial C_n}{\partial t} + u \frac{\partial C_n}{\partial x} + w \frac{\partial C_n}{\partial z} = \frac{\partial}{\partial z} \left(K_z \, C_n \frac{\partial C_n}{\partial z}\right) + \dot{C}_n \qquad (6)$$

In the soil layer the energy equation is

$$\frac{\partial T_s}{\partial t} = \alpha_s \frac{\partial^2 T_s}{\partial z^2} \qquad (7)$$

Boundary Conditions

At the top of the PBL, the dependent meteorological variables are specified and held constant during the simulation. This assumes that the large scale flow (i.e., synoptic scale weather pattern) remains constant during the simulation period. The temperature at the lower sub-soil boundary is specified and is independent of time. Temperature, humidity, and pressure are specified above the PBL in the "free atmosphere" for radiative transfer calculations.

At the atmosphere-land interface ($z = 0$) the velocities are assumed to vanish,

$$u(t,x,z) = v(t,x,z) = w(t,x,z) = 0 \qquad (8)$$

The temperatures in the air and the soil are coupled through an energy balance at the interface ($z = 0$). This energy balance requires that the sum of the heat fluxes at any horizontal position x along the interface vanish, i.e.,

$$a_s F_s^- + a_t F_t^- - e_t \sigma T^4 - H - L + S = 0 \qquad (9)$$

where a_s ($= 1 - r_s$, with r_s being the solar albedo) is the solar absorptance, a_t is the thermal absorptance and e_t is the thermal emittance. In this equation, the first two terms account for absorption of solar (short-wave, F_s^-) and thermal (long-wave, F_t^-) radiation, the third term represents thermal emission, and the fourth and fifth terms account for sensible and latent heat transfer by turbulent diffusion, and the sixth term represents heat conduction into the ground. The anthropogenic heat source

has not been included in the energy balance at the interface since it is considered to be released directly into the air above and not at the surface. The turbulent sensible (H) and latent (L) heat fluxes are given by

$$H = - \rho c_p K_z^{\Theta} \frac{\partial \Theta}{\partial z} \tag{10}$$

and

$$L = - \Delta h_g K_z^{C_w} \frac{\partial C_w}{\partial z} \tag{11}$$

where Δh_g is the latent heat of vaporization. The sensible heat flux in the soil is determined from

$$S = - k_s \frac{\partial T_s}{\partial z} \tag{12}$$

where k_s is the thermal conductivity of the soil (substrate).

The water vapor concentration at the surface is prescribed by Halstead's moisture availability parameter M (Halstead et al., 1957) using the expression

$$C_w = MRC_{w,sat} + (1 - M)C_w(z_1) \tag{13}$$

where R is the relative humidity of the interface, and $C_{w,sat}$ is the water vapor concentration at a saturation condition. The values of the parameter R range from unity for water to zero for dry soil.

The interface boundary conditions for the pollutant concentration is written as

$$m_p \equiv - K_z^{C_p} \frac{\partial C_p}{\partial z}, \quad p = 1, 2 \tag{14}$$

Physically, this condition implies that there is a source of pollutants at the earth surface. Pollutant emissions will also be accounted in the volumetric source $\dot{C}_n$ included in Eq. (6).

The horizontal variation of the urban interface parameters such as ground solar albedo, thermal emittance, surface roughness, thermal diffusivity and conductivity of the soil, moisture

availability and relative humidity parameters are prescribed functions of position along the urban area. There is lack of data for these parameters and their variation along urban areas. For example, the moisture parameter M, the fraction of surface area which is covered with vegetation depends on soil type, root distribution, water table depth, and other variables (Halstead et al., 1957). Also, the soil in urban areas is partly covered by buildings, pavement, etc., and this fraction varies from one area urban area to another and cannot be readily estimated. More detailed models than the one utilized in this study for predicting temperature distribution in the soil and evaporation from the earth's surface are available (Sasamori, 1970). Unfortunately, hydraulic and physical properties of soil such as moisture potential, effective permeability (hydraulic conductivity), and moisture content as well as thermal diffusivities are not known for the soil types and textures encountered in urban areas (Eagelson, 1970).

At the upwind rural boundary, the meteorological variables are predicted from the one-dimensional model of Bergstrom and Viskanta (1973a). This assumes that the flow into the urban area is fully developed, parallel, and possesses no vertical velocity. Downwind of the city (i.e., in the rural area) it is assumed that all the meteorological and air pollution variables change slowly, or,

$$\frac{\partial \phi}{\partial x} = 0 \qquad \text{at } x = L \tag{15}$$

This condition implies that the downwind rural area is far away from the city center and that nearly fully developed conditions have been reached. At the initial time the variables are specified everywhere and are assumed to be independent of the horizontal coordinate x.

RADIATIVE TRANSFER MODEL

The radiative transfer model used is an extension of the earlier non-dynamical model of Bergstrom and Viskanta (1973c).

Since multidimensional radiative transfer is quite complex and the absorption and scattering characteristics of aerosols are not known to sufficient accuracy (Coulson and Fraser, 1975), it is assumed that the transport of radiation can be approximated by a quasi-two-dimensional field based on the vertical temperature, water vapor and pollutant distributions at several predetermined horizontal positions along the urban area. The radiative fluxes and flux divergences can then be evaluated at these prescribed horizontal locations. Suitable interpolation is then used to determine the desired quantities between these locations. This approach appears to be justifiable because the radiation properties, the ground albedo and pollutant emission sources along the urban area are not known presently with sufficient accuracy. The computational effort, which would be needed for a more sophisticated treatment, does not warrant multidimensional radiative transfer analysis.

The urban atmosphere is considered to be cloudless, plane-parellel, and consist of two layers: (1) the free atmosphere and (2) the urban PBL where most pollutants are concentrated. From below, the polluted PBL is bounded by an opaque earth's surface which not only emits but also reflects the incident radiation diffusely. The emission characteristics and albedo of the ground are arbitrary but prescribed functions of wavelength. The radiative transfer between the free atmosphere and the polluted PBL are coupled. The solar radiation incident on the free atmosphere is scattered by gases (Rayleigh scattering) and absorbed by such natural constituents as water vapor, carbon dioxide, ozone and other trace gases. Solar energy absorption by NO_2 is generally small, except during certain times in urban areas like Los Angeles and will therefore be neglected. The solar radiation is also scattered by the natural aerosols in the free atmosphere. In the polluted PBL the solar radiation is absorbed and scattered by gases and aerosols, both natural and pollutant. In the model the natural aerosol is considered nonabsorbing and the absorption is accounted by the pollution aerosol. Thermal

radiation is emitted and absorbed by natural atmospheric gases in both layers and by pollutant gases in the lower layer. Additional computational details can be found in the literature (Viskanta et al., 1977b).

The solution of the radiative transfer equation was accomplished by dividing the entire electromagnetic spectrum into the short wave solar part ($0.3 \leq \lambda \leq 4$ μm) and the long wave thermal part ($4 \leq \lambda \leq 50$ μm). This separation is natural and allows considerable simplification in the analysis and evaluation of the radiative fluxes and flux divergences.

It should be emphasized that the radiation transfer model utilized is not as detailed as the more recent models which are available (Ackerman et al., 1976; Welch and Zdunkowski, 1976). Effects of multiple scattering by aerosols in the window region (Balkan and Quenzel, 1976) do not appear to be sufficiently significant to warrant inclusion in the radiative transfer calculations even for highly polluted atmospheres. In addition, since the absorption and scattering characteristics of pollution aerosols are not known with sufficient accuracy (Coulson and Fraser, 1975), little data is available for the variation of the solar albedo and thermal emittance along the urban area, and the fact that radiative transfer in the urban PBL is not one-dimensional are the primary reasons justifying the use of a less detailed model for dynamic calculations.

Solar Spectrum

In the solar part of the spectrum emission by atmospheric constituents is neglected, and following Chandrasekhar (1960) the intensity $I_\lambda(\tau_\lambda,\mu,\phi)$ at optical depth τ_λ and direction μ,ϕ can be expressed as a sum of directly transmitted part I_λ^t and of scattered part I_λ^s such that $I = I_\lambda^t + I_\lambda^s$. The directly transmitted intensity can be immediately calculated from

$$I_\lambda^t(\tau_\lambda,\mu_o,\phi_o) = F_{\infty,\lambda}(\mu_o,\phi_o)\exp[-(\tau_{\infty,\lambda} - \tau_\lambda)/\mu_o]\delta(\mu - \mu_o)\delta(\phi - \delta_o) \quad (16)$$

where $F_{\infty,\lambda}$ is the spectral flux at the top of the free atmosphere, $\tau_{\infty,\lambda}$ is the optical thickness of the entire (free + polluted) atmosphere, τ_λ is the optical depth measured from the surface of the earth, and δ is the Dirac delta function. The equation for scattered intensity I_λ^s when emission is neglected becomes

$$\mu \frac{dI_\lambda^s}{d\tau_\lambda} = - I_\lambda^s + \frac{\omega_\lambda}{4\pi} \int_{-1}^{+1} \int_0^{2\pi} I_\lambda^s (\tau_\lambda, \mu', \phi') \, p_\lambda(\mu', \phi' \to \mu, \phi) d\mu' d\phi'$$

$$+ \left(\frac{\omega_\lambda}{4}\right) F_{\infty,\lambda}(\mu_o, \phi_o) \exp[-(\tau_{\infty,\lambda} - \tau_\lambda)/\mu_o] p_\lambda(\mu_o, \phi_o \to \mu, \phi) \quad (17)$$

where $\mu (= \cos\theta)$ is the direction cosine, ω_λ is the albedo for single scattering, and p_λ is the scattering distribution function. The advantages of separating and then solving the radiative transfer equation in this manner are that the scattered intensity I_λ^s may be orders of magnitude smaller than the directly transmitted I_λ^t and that the latter is assumed to be a collimated beam (plane wave) which does not have a continuous angular variation.

It is assumed that the scattering distribution function p_λ can be expanded in a series of Legendre polynomials (P_ℓ) and can be written as

$$p_\lambda (\cos\Theta) = \sum_{\ell=0}^{N} p_\ell P_\ell(\cos\Theta) \quad (18)$$

where Θ is the angle between the incident (μ', ϕ') and scattered (μ, ϕ) beams. If Eq. (18) is substituted into Eq. (17), the addition theorem of spherical harmonics (Irving and Mullineaux, 1959) is employed, the resulting equation is integrated over ϕ from 0 to 2π, and there results

$$\frac{d\hat{I}_\lambda^s}{d\tau_\lambda} = - \hat{I}_\lambda^s + \frac{\omega_\lambda}{2} \int_{-1}^{+1} \hat{I}_\lambda^s(\tau_\lambda, \mu') \sum_{\ell=0}^{N} p_\ell P_\ell(\mu') d\mu' P_\ell(\mu)$$

$$+ \frac{\omega_\lambda}{2} \hat{I}^t_\lambda(\tau_\lambda,\mu_o) \sum_{\ell=0}^{N} p_\ell P_\ell(\mu) P_\ell(\mu_o) \tag{19}$$

where

$$\hat{I}^s_\lambda(\tau_\lambda,\mu) \equiv \int_0^{2\pi} I_\lambda(\tau_\lambda,\mu,\phi)\,d\phi \tag{20}$$

Assuming a solution for $I^s_\lambda(\tau_\lambda,\mu)$ in the form

$$\hat{I}^s_\lambda(\tau_\lambda,\mu) = \sum_{k=0}^{N} a_k(\tau_\lambda) P_k(\mu) \tag{21}$$

substituting into Eq. (19), integrating over μ from -1 to 1, and manipulating yields a system of N + 1 (n = 0, 1, 2, ... N) ordinary differential equations for the coefficients a_n. These equations together with the boundary conditions are solved analytically and the details can be found elsewhere (Bergstrom and Viskanta, 1973c).

Once the radiation field I_λ has been determined, the radiative flux F_λ and its divergence follow immediately from the definitions

$$F_\lambda(z) = \int_0^{2\pi}\int_{-1}^{1} I_\lambda(z,\mu,\phi)\,\mu\,d\mu\,d\phi \tag{22}$$

and

$$-\frac{\partial F_\lambda}{\partial z} = H_\lambda(z) = \kappa_\lambda \int_0^{2\pi}\int_{-1}^{1} I_\lambda(z,\mu,\phi)\,d\mu\,d\phi \tag{23}$$

respectively, where κ_λ is the spectral absorption coefficient.

The spectral absorption and scattering coefficients and the scattering distribution function of the aerosols in the polluted PBL were predicted using Mie electromagnetic theory by specifying the size distribution (Deirmendijian's Haze L distribution). The complex indices of refraction of the urban air pollution aerosols were taken from the model proposed by Bergstrom (1972). The resulting absorption and extinction

coefficients agreed well with the values based on the bulk mean indices of refraction of a dry aerosol found over the industrial sector of Mainz, West Germany (Fischer, 1973).

The P_3-approximation of the spherical harmonics method was used in the numerical computations. The predictions of radiative transfer in a polluted atmosphere using this approximation have been previously made (Bergstrom and Viskanta, 1974) and found to agree well with the results based on much more detailed and time consuming calculations. The solar fluxes predicted using this method (but somewhat different aerosol properties and spectral integration) were also in good agreement with observations in the St. Louis, Missouri metropolitan area for relatively clean atmosphere (Bergstrom and Peterson, 1977). The fact that the radiative transfer calculations were not too time consuming was an important consideration because of the diurnal nature of the transport processes to be modeled in the atmosphere. The integration over the wavelengths was carried out by dividing the spectrum into twelve bands.

Thermal Spectrum

In the thermal part of the spectrum scattering is neglected in comparison to absorption. As a first approximation this simplification appears to be justifiable. The presence of scattering would increase only slightly the importance of absorption by increasing the optical path. Assuming that emission and reflection from the earth's surface is isotropic (diffuse), the total radiative flux $F(z)$ can be expressed as a difference between the upward $F^+(z)$, and downward $F^-(z)$, directed fluxes,

$$F(z) = F^+(z) - F^-(z) \tag{24}$$

where

$$F^+(z) = 2\int_0^\infty \{[\pi e_\lambda I_{b\lambda}(0) + r_\lambda F_\lambda^-(0)]E_3(\tau_\lambda) + \pi\int_0^{\tau_\lambda} I_{b\lambda}(\xi)\frac{d}{d\xi}E_3(\tau_\lambda - \xi)d\xi\}d\lambda \tag{25}$$

and

$$F^{-}(z) = 2\pi\int_0^{\infty}\int_{\tau_\lambda}^{\tau_{\infty\lambda}} I_{b\lambda}(\xi)\frac{d}{d\xi} E_3(\xi - \tau_\lambda)d\xi d\lambda \qquad (26)$$

where e_λ and r_λ are the emittance and reflectance of the earth surface, $I_{b\lambda}(T)$ is Planck's function, $E_n(\xi)$ is the exponential integral function (Chandrasekhar, 1960), and the optical depth and thickness are defined respectively as

$$\tau_\lambda = \int_0^z \kappa_\lambda dz \text{ and } \tau_{\infty\lambda} = \int_0^{z_\infty} \kappa_\lambda dz \qquad (27)$$

The radiative flux divergence follows immediately from Eq. (24) and becomes

$$-\frac{\partial F}{\partial z} = H(z) = 2\int_0^{\infty}\kappa_\lambda\{\pi e_\lambda I_{b\lambda}(0) + r_\lambda F_\lambda^{-}(0)E_2(\tau_\lambda) +$$

$$\pi\int_0^{\tau_{\infty\lambda}} I_{b\lambda}(\xi)\frac{d}{d\xi} E_2(|\tau_\lambda - \xi|)d\xi\}d\lambda \qquad (28)$$

The thermal radiative flux, Eq. (24), and its divergence, Eq. (28), were evaluated with the help of the emissivity data for the absorbing atmospheric gases. The emissivity concept is well established in the meteorology literature (Goody, 1964; Kondratayev, 1969) and is the most efficient method for predicting the radiative fluxes and flux divergences. For water vapor the emissivity data from Kuhn (1963) were used. This data simplify the means of accounting for the overlap of the water and carbon dioxide bands since the carbon dioxide contribution has been subtracted out. For carbon dioxide the emissivity data of Shekter (Kondratayev, 1969) was used. In the calculations multiple scattering was neglected, and it was assumed that the influence of gaseous pollutants was confined to the 8-12 μm spectral region due to the relatively large opacity of the H_2O and CO_2 bands. Ethylene was chosen to simulate the net radiative effects of the gaseous pollutants since Ludwig et al. (1969)

considered it to be representative of a typical hydrocarbon and since it has strong absorption in the atmospheric window (8-12 μm). Obviously, other gases such as ammonia or gas mixtures could have been used to simulate the actual polluted conditions; however, a more detailed description of gaseous pollutants was considered unwarranted.

TURBULENT EDDY EXCHANGE COEFFICIENTS

Specification of turbulent eddy exchange coefficients in connection with numerical modeling of the PBL is a very difficult task and has been the subject of a recent review (Shir and Bornstein, 1977). The semi-empirical eddy exchange coefficient correlations employed (Viskanta et al., 1977a) were not completely satisfactory because different correlations for K_z^M had to be used which depended on the flow regime and stability conditions. This has sometimes led to sharp discontinuities in the values of K_z^M under some conditions which was undesirable. For this reason an attempt was made to use the turbulent kinetic energy model to calculate the eddy exchange coefficient which was successfully employed in the numerical simulations of the one-dimensional PBL (Venkatram and Viskanta, 1976). However, the approach was not successful for two-dimensional simulations because of the stability and time step restrictions involved in the numerical solution of the turbulent kinetic energy equation and was therefore abandoned.

The turbulent eddy coefficients for momentum exchange were predicted from the stability-dependent correlations (Estoque and Bhumralkar, 1969)

$$K_z^M = \ell^2 \left[\left(\frac{\partial u}{\partial z} \right)^2 + \left(\frac{\partial v}{\partial z} \right)^2 \right]^{1/2} \begin{cases} (1 - 3Ri) & \text{for } Ri \leq 0 \\ (1 - 3Ri)^{-1} & \text{for } Ri > 0 \end{cases} \tag{29}$$

where the mixing length ℓ is given by Blackadaar (1962)

$$\ell = \kappa(z + z_o)/[1 + \kappa(z + z_o)/\lambda] \tag{30}$$

Here λ represents a constant mixing length. To avoid unreasonably low values of K_z^M under stable conditions, an average Richardson number, $\overline{Ri}$, is used for the lowest 50 m. The eddy diffusion coefficients for heat and species transport are assumed to be given by

$$K_z^{\Theta} = K_z^{C_n} = \alpha K_z^M \tag{31}$$

where α ($= K_z/K_z^M$) is taken to be the neutral value of 1.35 (Businger, 1972). Equations (29) and (30) for the turbulent eddy exchange coefficients are not completely satisfactory. However, the sensitivity studies of Zdunkowski et al. (1976) (on the choice of a turbulence model) show that the choice of the model on the computed temperature, concentration, and wind profiles is not critical but has some effect on the model computations. These findings provide a partial justification for using Eqs. (16) and (18) until more appropriate correlations become available to model turbulence.

POLLUTANT, WATER VAPOR, AND HEAT EMISSION SOURCES

Because it is not practical to consider individual sources in the simulations, the pollutant emissions into the urban PBL were modeled as surface sources (Viskanta et al., 1976). The physical limitations of this type of formulation are recognized, and therefore the volumetric pollutant emission sources in the present calculations were approximated by

$$\dot{C}_p(x,z,t) = f_p(t)g_p(x)e^{-(z - z_{e,p})^2/2\sigma_p^2} \; ; \quad p = 1, 2 \tag{32}$$

In writing Eq. (32) it was assumed that individual pollutant sources are distributed continuously. The functions f(t) and g(x) approximating the variation of pollutant emissions with time of the day and the distance along the city, as well as the discharge height $z_{e,p}$ of the various sources will be specified later by making reasonable assumptions.

There are anthropogenic water vapor emissions in the

atmosphere due to combustion of hydrocarbons and other human activities. However, because of lack of quantitative observational data these vapor sources have been neglected.

In the past the anthropogenic heat emission sources were represented by surface fluxes (Yu and Wagner, 1975; Viskanta et al., 1976). In this work the man-caused heat emissions are approximated by a volumetric source given by the function

$$\dot{q}(x,z,t) = F(t)G(x)e^{-(z/\sigma_q)^2} \qquad (33)$$

According to this expression the highest heat emission occurs at the surface and decreases exponentially. The specific functions and parameters in Eq. (33) will be specified later.

SECTION 5

CASE STUDY AND NUMERICAL MODEL

For specific numerical calculations it is necessary to prescribe an urban geometry. An urban area 40 km in extent was simulated. There were 17 equally spaced grid points: 3 in the upwind, 4 in the downwind and 10 in the city. The city starts at x = 5 km and ends at x = 30 km, with the center being at x = 17.5 km. The top of the PBL was arbitrarily chosen at a height of 2000 m. For the meteorological conditions used in the simulations the mixed layer height even for the summer days never exceeded a height of 1600 m. This suggests that the top of the PBL at 2000 m was adequate for the numerical experiments. There were a total of 22 grid points in the vertical direction. Near the ground they were distributed logarithmically to improve resolution, and above 600 m the points were distributed linearly, see Table 1. The bottom of the soil layer is at a depth of 0.5 m

TABLE 1. GRID SPACING IN THE VERTICAL (z) DIRECTION

J	z(m)	J	z(m)
1	0	12	190.00
2	2.00	13	275.00
3	4.78	14	400.00
4	8.65	15	600.00
5	14.04	16	800.00
6	21.52	17	1000.00
7	31.94	18	1200.00
8	46.43	19	1400.00
9	65.58	20	1600.00
10	94.92	21	1800.00
11	133.62	22	2000.00

which is below the penetration depth of the daily temperature wave. There were 11 equally spaced grid points in the soil.

In the numerical simulations the city of St. Louis, Missouri (38.5° North Latitude) was taken as an example. Both a summer day (solar declination δ = 14°) and a winter day (solar declination δ = -21°) were modeled. The declination angle of 14° corresponds to mid-August and an angle of -21° refers to mid-January. These times of year were chosen because most of the serious pollution episodes occur then and because insolation is large or near its minimum. Cloudiness was assumed to be absent as often experienced in episodes of heavy pollution.

Table 2 lists the values of the atmosphere-soil interface parameters for the "base" winter simulations. There is a large uncertainty in the parameters listed in Table 2. The horizontal distribution of the surface characteristics was established by selecting the values of the parameters at the rural and urban center locations, and for the lack of better data or information, a Gaussian distribution curve was then fitted between these two points. The values of parameters given in Table 2 appear to be reasonable and similar to data that have been used by other investigators (Atwater, 1975; Yu and Wagner, 1975).

The diurnal variation of pollutant emissions assumed is illustrated in Figure 2. This approximation is based on observations in Cologne (Kunkel et al., 1975). In the numerical simulations the anthropogenic heating was assumed to occur within 2 m (first node) of the surface, i.e., $q_{an} \simeq \int_0^{2m} \dot{q} dz$. The variation of the heat releases with time or air temperature above ground has been ignored, and an average value was used throughout the day. It is recognized (Torrance and Shum, 1976) that the heat releases vary during the diurnal cycle, but the lack of knowledge of the variations along the city did not warrant this more detailed treatment. Based on the parameters given in Table 2 the anthropogenic heat flux for the summer simulations corresponds to an average value of 25 W/m^2. This is in a range of values that have been estimated for some cities such as Cincinnati, Ohio (Torrance and Shum, 1976). The anthropogenic sources and sinks

TABLE 2. SUMMARY OF INTERFACE PARAMETER FOR THE "BASE" NUMERICAL SIMULATIONS AT THE UPWIND RURAL (UR) AND URBAN CENTER (UC) LOCATIONS

Parameter	Summer		Winter	
	UR	UC	UR	UC
Surface albedo, r_s	0.25	0.15	0.25	0.125
Thermal emittance, e_t	0.96	0.94	0.96	0.94
Soil thermal conductivity, k_s(W/m-K)	0.50	2.00	0.50	2.00
Soil thermal diffusivity, α_s(10^6 x m^2/s)	0.55	2.20	0.50	2.00
Surface roughness, z_o(m)	0.10	1.00	0.10	1.00
Halstead's moisture parameter, M	0.75	0.20	0.80	0.20
Relative humidity of soil, R	0.20	0.15	0.20	0.20
Aerosol source, g_1(μg/m^2-s)	0.02	1.25	0.02	0.56
Gaseous source, g_2(μg/m^2-s)	0.02	1.25	0.02	0.56
Effective emission height, $z_{e,1} = z_{e,2}$ (m)	2.00	40.00	2.00	40.00
Pollutant emission variance, $\sigma_1 = \sigma_2$ (m)	2.00	40.00	2.00	40.00
Anthropogenic heat emissions, G(W/m^3)	0.28	28.00	0.56	56.00
Heat emissions variance, σ_q(m)	1.00	1.00	1.00	1.00
Lower soil boundary temperature, T_Δ(K)	296.00	296.00	274.00	274.00
Thermodynamic temperature at the top of the PBL, T_δ(K)	283.36	283.38	268.00	268.00

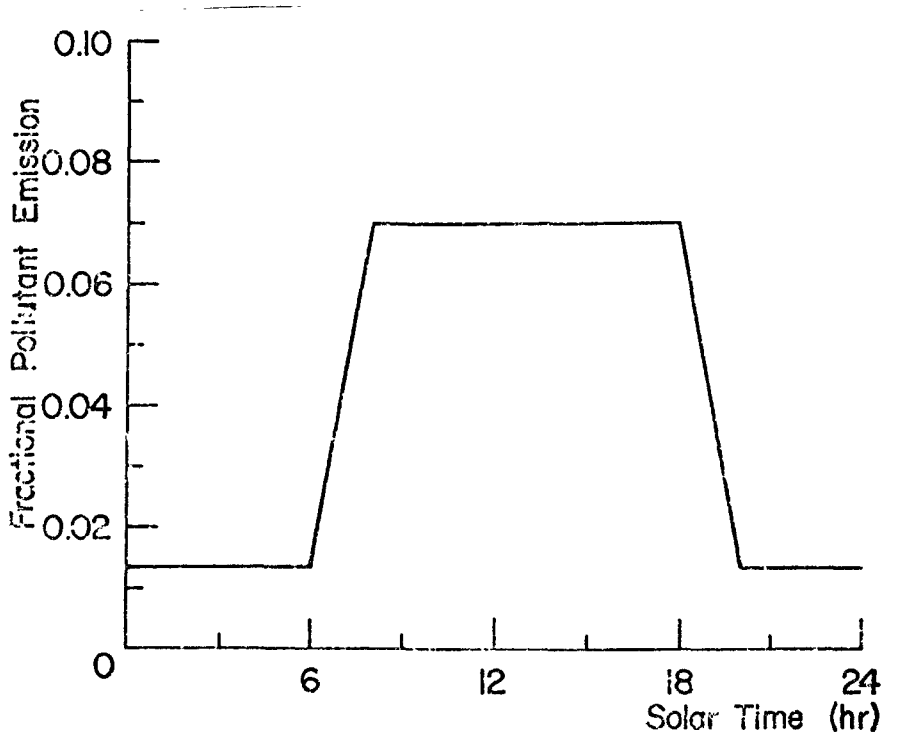

Figure 2. Fractional pollutant emissions during the diurnal cycle.

of water vapor in the atmosphere were neglected because they have been estimated to be insignificant for summer daytime mesoscale influences on the atmospheric water balance of the urban area (Sisterson and Dirks, 1977).

The simulations were started at 6:00 in the morning and were continued (depending on interest) for a period of 30 hours until noon of the second day. The initial conditions were representative for the two seasons. For the summer the initial temperature and water vapor concentration profiles used were based on the observations of Spangler and Dirks (1974) for the metropolitan area of St. Louis, Missouri and were imposed over the entire city (no x-variation), while for the winter the initial temperature and water vapor concentration profiles were similar to those employed by Atwater (1972). The initial wind profiles were decreased by a factor 3 from those given by Lettau and Davidson (1957) for the Great Plains Turbulence

TABLE 3. SUMMARY OF NUMERICAL SIMULATIONS: u_g = 4 m/s AND v_g = 3.0 m/s, ϕ = 38.5°. VARIATIONS FROM THESE AND OTHER PARAMETERS ARE GIVEN IN TABLE 2 ARE INDICATED BELOW

Simulation No.	Season	Radiative Interaction	Remarks
W1	Winter	NP	Base simulation
W2	"	P	"
W3	"	P	$q_{an,UR}$=10 W/m^2, $q_{an,UC}$=100 W/m^2
W4	"	P	Exponentially distributed $\dot{q}$
W5	"	NP	Snow covered ground: $r_{s,UR}$=0.8, $r_{s,UC}$=0.6, $\varepsilon_{t,UR}$=0.98, $\varepsilon_{t,UC}$=0.96 $k_{s,UR}$=0.171 W/mK, $k_{s,UC}$=0.537 W/m-K $\alpha_{s,UR}$=0.41x10^{-6} m^2/s, $\alpha_{s,UC}$= 0.82/10^{-6} m^2/s, $q_{an,UR}$=10 W/m^2, $q_{an,UC}$=100 W/m^2
W6	"	NP	As W5 except $q_{an,UR}$=5 W/m^2, $q_{an,UC}$=50 W/m^2
W7	"	P	As W6 except P
W8	"	P	$q_{an,UR}$=$q_{an,UC}$=0
W9	"	P	$z_{o,UR}$=0.1 m, $z_{o,UC}$=2.0 m
S1	Summer	NP	Base simulation
S2	"	P	"
S3	"	P	10% weight carbon aerosol
S4	"	P	$q_{an,UR}$=$q_{an,UC}$=0
S5	"	P	$r_{s,UR}$=0.3, $r_{s,UC}$=0.1
S6	"	P	M_{UR}=0.5, M_{UC}=0
S7	"	NP	$r_{s,UR}$=0.15, $r_{s,UC}$=0.1
S8	"	P	Same as S7 except P

Study. The initial pollutant concentrations assumed had an exponential decrease with height from the ground to the top of the PBL and a Gaussian variation along the urban area. The initial aerosol and gaseous pollutant concentrations at the surface were taken as 20 $\mu g/m^3$ and 100 $\mu g/m^3$ at the rural area and the urban center, respectively.

The numerical experiments are designed to examine:

1. The effects of urbanization on the planetary boundary layer.
2. The effects of radiatively active pollutants in modifying the temperature structure and dispersion in the PBL.
3. The effects of anthropogenic heat releases in modifying urban temperatures.
4. The modification in temperature and pollutant concentrations resulting from changes of interface parameters in the presence of radiatively active pollutants.

For ease of reference the numerical experiments which have been performed are listed in Table 3. The detailed discussion of the results obtained is given in the next section of the report.

SECTION 6

RESULTS AND DISCUSSION

ENERGY BALANCE COMPONENTS ALONG THE URBAN SURFACE

The surface temperature is a very important parameter in "forcing" the model. Thus, a comparison of the energy budget components along the urban area is of considerable interest. For this reason the energy fluxes for the "base" winter simulations W1 and W2 and the winter simulations W6 and W7 are presented in Figures 3 and 4, respectively. Note in each case the simulation with radiatively nonparticipating pollutants is represented by a solid line. In each case the fluxes are presented at noon (12:00) and midnight (24:00) along the urban area. According to the definition a positive heat flux indicates energy input into the soil while a negative heat flux indicates a loss to the atmosphere.

Referring first to Figure 3a (for simulation W1 and W2 at noon) it is seen that the absorbed solar flux (q_{as}) is the largest component, while the emitted (q_e), absorbed thermal (q_{at}), turbulent convection (q_c), and latent (q_ℓ) fluxes are all important components in the energy balance. The soil conduction flux (q_s) is important at the urban center where it is approximately 70% larger than in the rural areas. This is due primarily to the larger thermal conductivity of the soil compared to the rural environs, see Table 2. The absorbed solar flux q_{as} is a maximum at the urban center as the solar albedo (r_s) of the ground is a minimum there. The turbulent convective flux q_c shows large variations along the urban area primarily because of the changes in the surface roughness

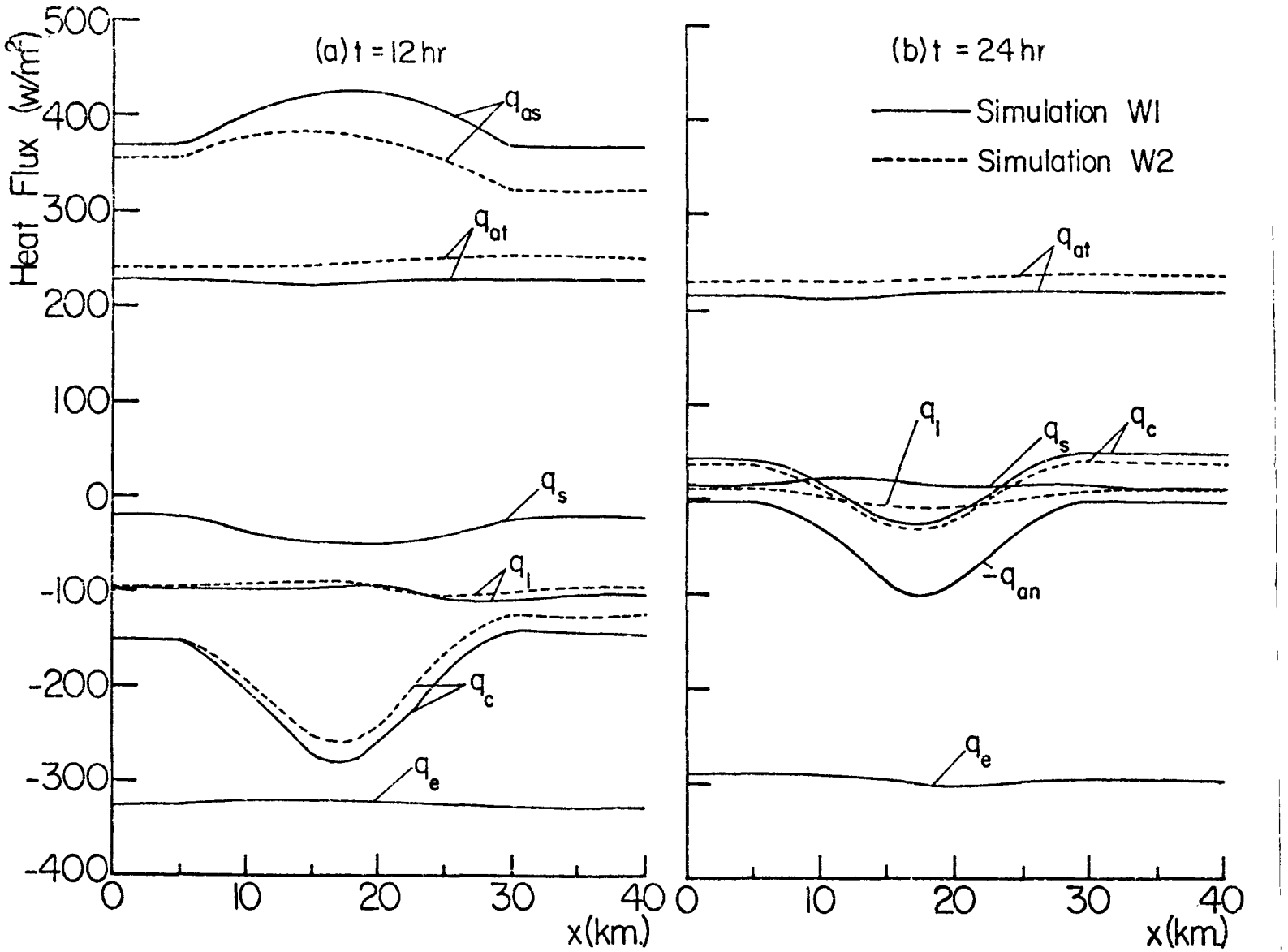

Figure 3. Comparison of energy flux components at the surface between simulations W1 and W2.

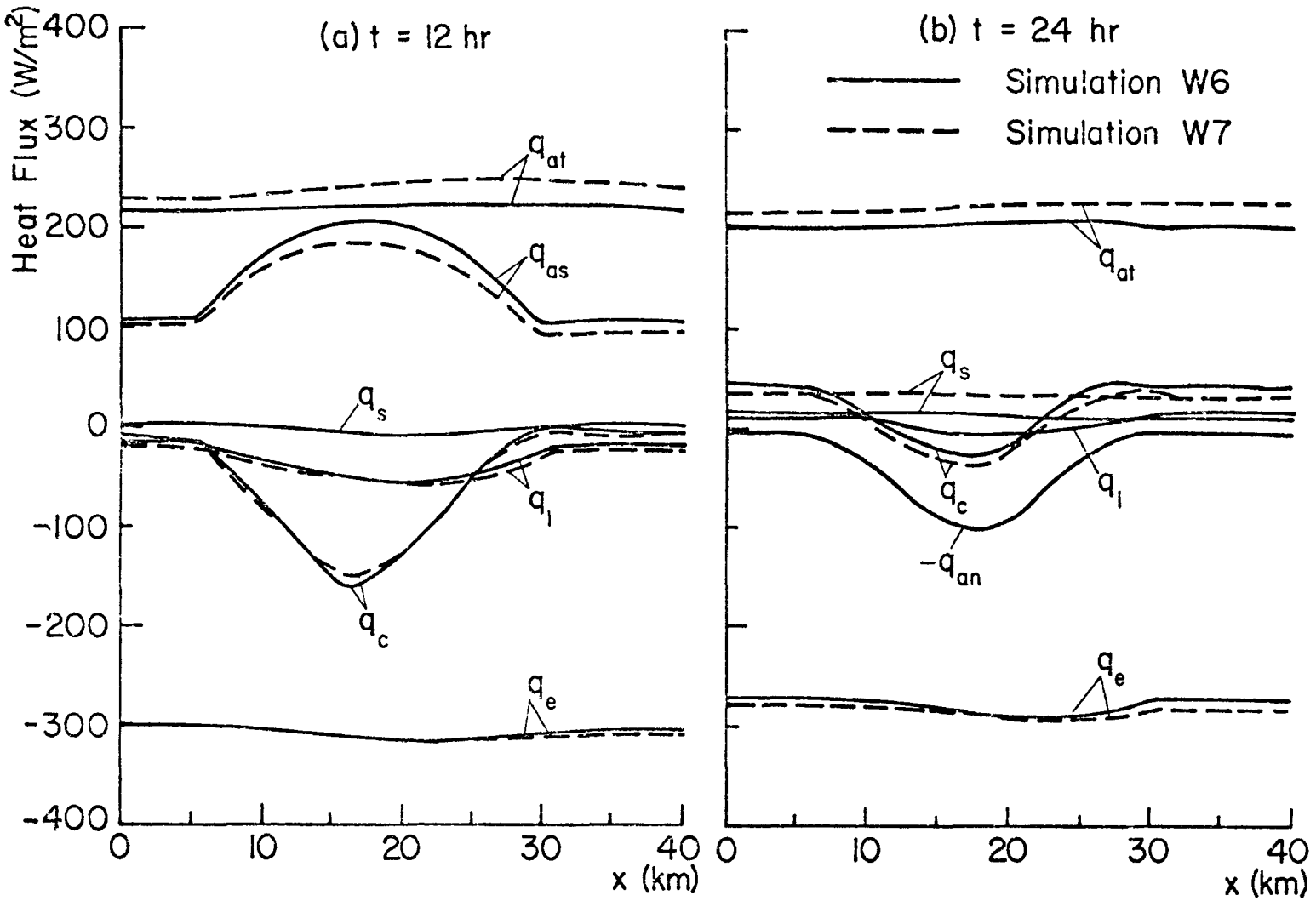

Figure 4. Comparison of energy flux components at the surface between simulations W6 and W7.

parameter z_o which affects greatly the turbulent eddy diffusivity near the ground.

At midnight the emitted (q_e) and absorbed thermal (q_{at}) fluxes dominate the energy budget as the turbulent (q_t), latent (q_ℓ), and soil conductive (q_s) fluxes are an order of magnitude smaller. The anthropogenic heat flux q_{an} is also included in the figure for the purpose of comparison even though in the model this energy is not released at the surface but within the first two meters above the ground. This flux is given by

$$q_{an}(x,t) = \int_0^{2m} \dot{q}(x,z,t)dz \tag{34}$$

Note that the turbulent (q_c) and latent (q_ℓ) energy fluxes change their sign during the diurnal cycle.

For the winter simulations with snow ground cover (W6 and W7) some important changes in the energy budget can be observed. Referring to Figure 4a, the most apparent difference at noon is that q_{as} is not the largest component in the energy budget. Comparing simulation W7 with simulation W2 (see Figure 2a) it is seen that q_{as} has decreased from about 425 to 200 W/m^2 depending upon the location in the urban area. This is due to the high solar albedo of the snow, which was assumed to be freshly fallen. The latent energy and soil conductive fluxes are also smaller due to changes in the soil conductivity and Halstead's moisture parameter. As expected, at midnight (Figure 4b), the fluxes are comparable to those found for simulations W1 and W2.

Examination of Figure 5 reveals that, compared to the winter simulations, the corresponding heat fluxes along the urban area are larger for the summer simulations. During the day, the latent heat flux (q_ℓ) is of much greater importance due to the higher temperatures than for the winter simulations. The latent heat flux reaches a minimum in the urban area due to decreased evaporation (reduction in Halstead's moisture availability parameter M) which is controlled by M. Note the decrease in the

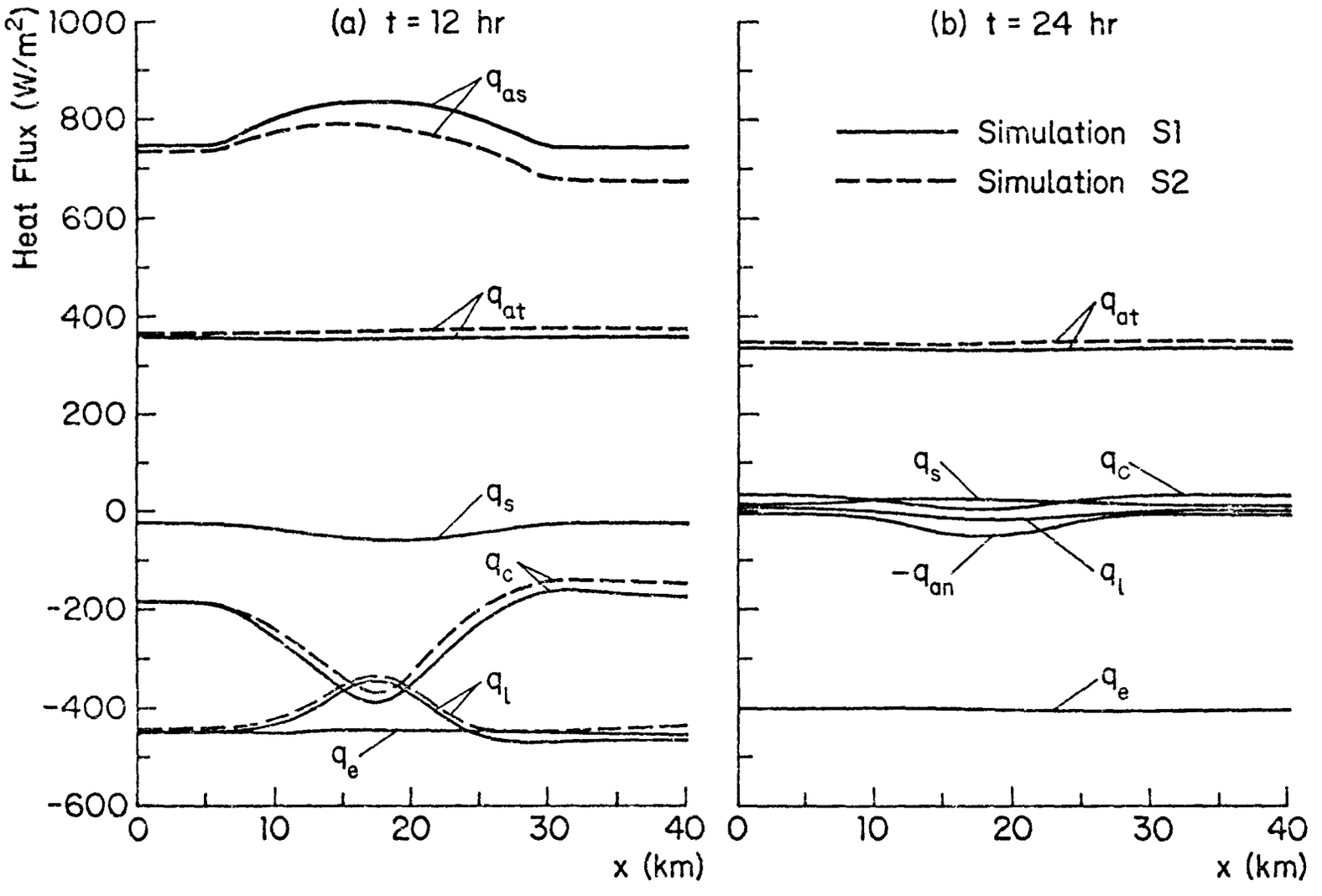

Figure 5. Comparison of energy flux components at the surface between simulations S1 and S2

relative importance of the anthropogenic heat flux (q_{an}) shown in Figure 5a when compared to the winter simulations. This indicates that q_{an} is a much less important contribution for the summer than for the winter.

All three figures (Figures 3, 4 and 5) indicate that radiatively interacting pollutants reduce the absorbed solar flux (q_{as}) while increasing the absorbed thermal flux (q_{at}). As an example, radiatively active pollutants in simulation S2 decrease the absorbed solar flux at noon by approximately 9% at the urban center while increasing the absorbed thermal flux by about 7% when compared to the noninteracting pollutants. The reason q_{as} is lower downwind of the urban center is because the pollutant concentration are highest. The turbulent and latent heat fluxes are about 7 and 4% smaller at the urban center for simulation S2 than for S1, respectively. The net flux heating (or cooling) the surface is therefore not very much different for the two simulations. As a result, the effect of radiatively active pollutants on the surface temperature which is determined from the energy balance Eq. (9) is not expected to be very large either during the day or the night.

RADIATIVE TRANSFER

Understanding of radiative transfer in the atmosphere is essential because solar radiation "drives" the PBL model during the day and thermal radiation cools the atmosphere at night. Therefore, before discussing the detailed model results it is desirable to discuss the effects of aerosols and gaseous pollutants on the radiative fluxes in the solar and thermal parts of the spectrum. Also, the radiative flux divergence $\partial F/\partial z$ [or the net heating/cooling rate $(\partial F/\partial z)/\rho c_p$] is an important component of the local energy balance for determing the temperature distribution in the atmosphere, and it is therefore of interest to determine how it is modified by urbanization and air pollution. In the urban PBL the vertical transport of energy by radiation can be of the same order of magnitude or

larger than energy transport by turbulence (Viskanta et al., 1976).

Solar Fluxes and Effective PBL Albedo

A schematic diagram illustrating the radiative fluxes for simulations S1 and S2 at noon are compared in Figures 6a and 6b, respectively. The diagram shows the effect of absorbing aerosol particles on the fluxes and indicates increased attenuation of solar radiation in the PBL from 0.918 for simulation S1 with radiatively nonactive anthropogenic aerosols (Figure 6a) to 0.861 for simulation S2 with radiatively active anthropogenic aerosols (Figure 6b). Absorbing aerosol causes an increase in atmospheric absorption by a factor of two, from 0.054 to 0.102. There is no appreciable increase in the effective albedo of the earth-PBL system. The effective albedos, rounded off to a three significant figure accuracy, are the same for the two

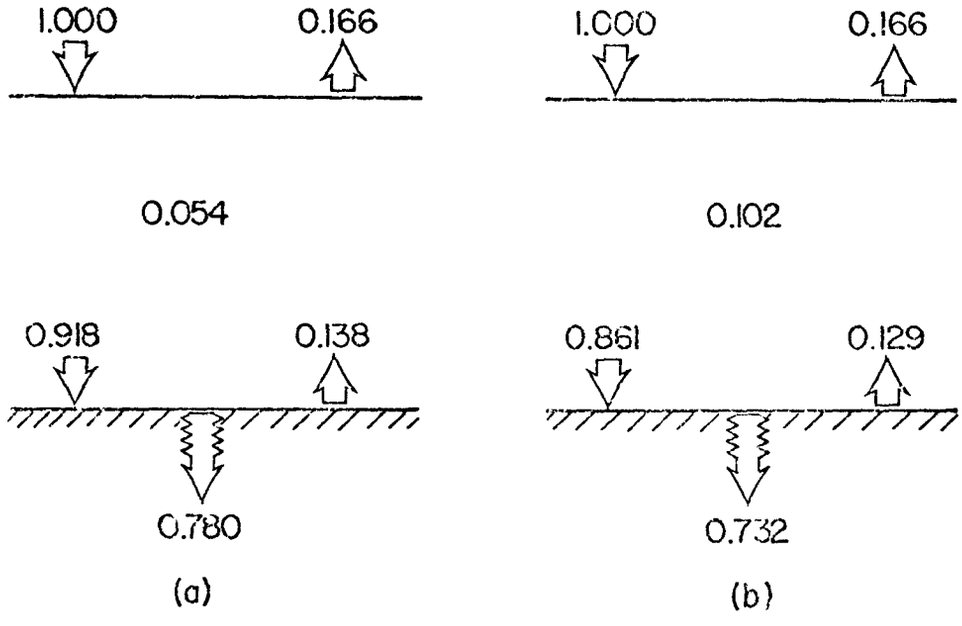

Figure 6. Schematic solar radiant energy balance diagram on the PBL at the urban center: a) simulation S1 with radiatively nonparticipating aerosol and b) simulation S2 with radiatively participating aerosol

simulations. There is, however, a corresponding decrease in the absorption of solar radiation by the ground. One can conclude from the results that there is no difference in the energy loss from the earth-PBL system for the two simulations, but there is some redistribution of the absorbed solar energy.

The effects of the absorbing pollutant aerosol on the radiative fluxes for the winter simulations W1 and W2 (Figures 7a and 7b) are similar to those for the summer simulations (Figure 6). The major difference is seen to be the increase in the effective albedo of the ground-PBL system for the simulation W2 with radiatively active aerosols. The effective albedo is increased from 0.212 to 0.228 which represents an energy loss from the ground-PBL system. This loss is at the expense of decreased absorption of solar radiation by the ground. On the contrary, the loss in energy from the ground-PBL system is smaller for simulations W7 in comparison to simulation W6, see Figure 7d and 7c. This is due primarily to the larger solar albedo of the snow covered ground. The results show that the tendency of warming of the PBL increases due to multiple reflection effects. This is consistent with the conclusions of Mitchell (1971).

The effective PBL albedo is defined as the ratio of the upward solar flux to the incident solar flux at the top of the PBL (2000 m). The effective albedo is a result of complex interactions of solar radiation with aerosols and gases in the atmosphere. It also depends on the solar zenith angle, ground albedo, as well as the concentration and distribution of pollutants. The diurnal variation at three urban locations of the effective PBL albedo for nonparticipating simulations S1 and S7 are shown in Figure 8. The ground albedo r_s (see Table 3) is similar to values reported by Dabbert and Davis (1974) over St. Louis. The results are in general agreement with those measured by White and Eaton (1977). The effective PBL albedo predicted for large solar zenith angles (i.e., early morning and late evening) is too high as shading effects are not

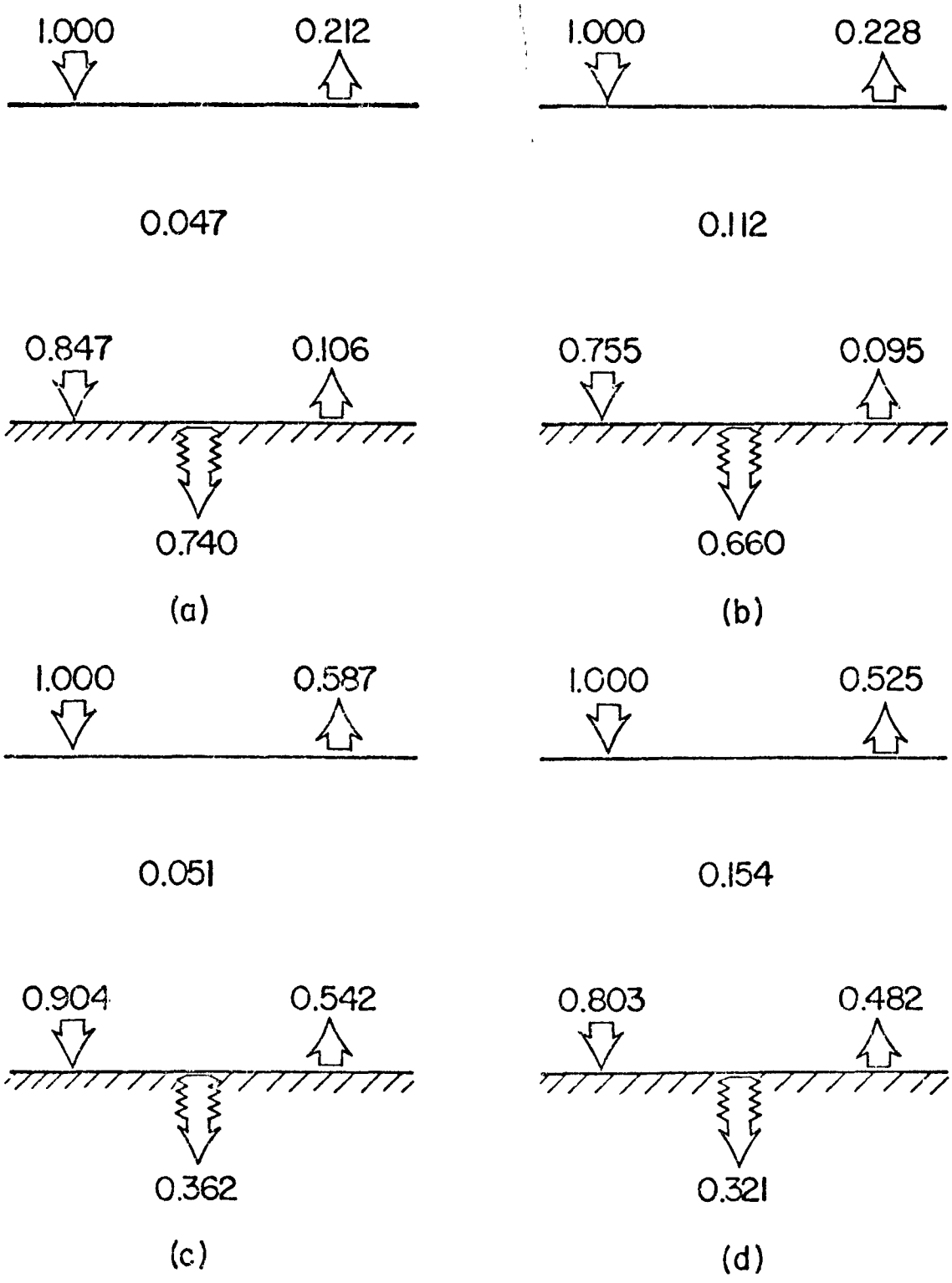

Figure 7. Schematic solar radiant energy balance diagram on the PBL at the urban center: a) simulation W1 with radiatively nonparticipating aerosol, b) simulation W2 with radiatively participating aerosol, c) simulation W6 with radiatively nonparticipating aerosol, and d) simulation W7 with radiatively participating aerosol.

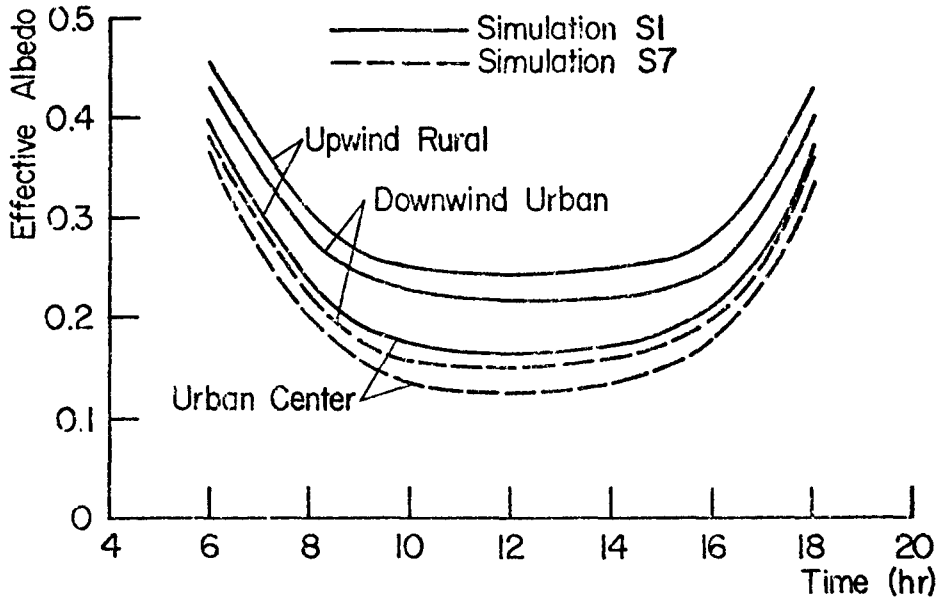

Figure 8. Diurnal variation of the effective PBL albedo.

considered in the model. Higher values for surface albedo were assumed for simulation S1 (see Table 2), as well as a greater difference between the rural and urban values. The results show a higher effective PBL albedo as well as a greater difference between urban locations than measured (White and Eaton, 1977).

The addition of radiatively participating pollutants has some effect on the effective albedo. For example, the solar albedo at the urban center at noon for participating simulation S8 is 4% greater than for nonparticipating simulation S7. While aerosol, water vapor, and carbon dioxide absorption tend to decrease the albedo, aerosol and Rayleigh scattering tend to increase the albedo. The results show that the effective albedo is most sensitive to the zenith angle and ground albedo and to a smaller degree by the presence of participating pollutants. This agrees with the recent results of Liou and Sasamori (1975).

On the basis of the results obtained, the effect of radiatively active aerosols in the city atmosphere is to cool the ground and warm the PBL. The net effect of the aerosols on the ground-PBL system is greater during the winter than the summer.

Conclusions about aerosol effects have to be carefully tempered by statements about solar albedo, aerosol concentrations, solar zenith angle (time of the day and year) and other factors.

Thermal Fluxes

A schematic diagram illustrating the effect of radiatively interacting gaseous pollutants on the net upward thermal flux at the ground and at the top of the PBL are illustrated in Figure 9 for the winter simulations W2 and W1 at midnight. Note that there is a decrease in the net flux (emitted minus absorbed) at the ground in the presence of the radiatively active gaseous pollutants (e.g. compare results for simulations W2 and W1), while there is an increase in the net radiant energy loss from the PBL for simulation W2 as compared to W1. The net effect of the radiatively active pollutants is to decrease the radiant energy loss from the ground-PBL system. The net modification of the radiant energy balance by pollutants at night is to reduce the cooling of the ground and of the system but to increase the

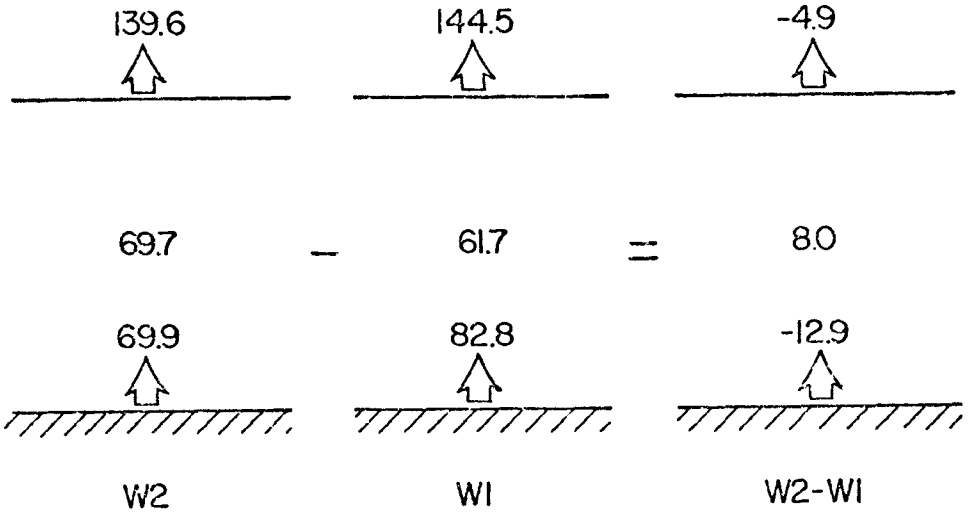

Figure 9. Schematic thermal radiant energy balance diagram (in W/m^2) on the PBL at the urban center for the winter simulations W1 and W2 at the urban center at midnight.

cooling of the PBL.

A summary of results for other simulations and both midnight and noon is given in Table 4. The effects indicated are seen to be identical to those already discussed. Again, it should be strongly emphasized that the conclusions reached regarding the modifications of the radiative fluxes by the pollutant gases are valid, strictly speaking, for the particular conditions considered. This is because the thermal radiative fluxes depend not

TABLE 4. SUMMARY OF NET UPWARD THERMAL RADIATIVE FLUXES (IN W/m^2) AT THE URBAN CENTER

a) Noon, 12:00

	W1	W2	W2-W1	S1	S2	S2-S1
Net flux at ground	97.8	78.8	-19.4	92.3	75.6	-17.7
Net loss from PBL	54.3	69.4	15.1	76.9	89.4	12.5
Net flux at top of PBL	152.1	147.6	-4.5	169.2	156.0	-4.2

b) Midnight, 24:00

Net flux at ground	82.8	69.9	-12.9	67.1	55.9	-11.2
Net loss from PBL	61.7	69.7	8.0	89.6	96.7	7.1
Net flux at top of PBL	144.5	139.6	-4.9	156.7	152.6	-4.1

only by pollutant gas and water vapor concentrations and their distributions but also on the vertical temperature structure in the PBL which is affected by urbanization.

Radiative Flux Divergences

The isopleths of solar flux divergence perturbations

(divergence in the upwind rural location) at noon for simulations W1 and S1 are presented in Figures 10a and 11a, respectively. In the absence of radiatively active pollutants the divergences over the city are smaller than in the rural area. The variations shown in the figures are due to urbanization, e.g., smaller solar albedo and evapotranspiration at the surface in the city compared to that in the upwind rural area. As expected, the perturbation is greater for the summer than for the winter simulation because of larger insolation during the summer.

The isopleths of the solar flux divergence differences between simulations W2 and W1 and between S2 and S1 are depicted in Figures 10b and 11b, respectively. The divergences are larger (more negative) for simulations with radiatively active pollutans. The greatest differences occur near the surface and downwind of the urban center where the aerosols are concentrated. The isopleths shown in the figures reflect the aerosol plume which develops downwind of the city center as a result of pollutant emissions near the ground and their transport by turbulent diffusion and advection. The results obtain are consistent with those reported in the literature (Viskanta et al, 1977b) under unstable meteorological conditions.

The net (solar plus thermal) flux divergences for some representative simulations are summarized in Table 5. The results show that the radiatively active pollutants increase the heating rate in the PBL, while during the night the gaseous pollutants increase the cooling rate, except in the immediate vicinity of the ground where there is an increase. The higher solar albedo for simulations W7 and W6 with snow covered ground than for simulations W2 and W1 with the bare ground result in larger differences during the day because of the larger solar albedo for the former two cases. For particular meteorological conditions, urban surface parameters, pollutant concentrations, heat and pollutant the net effect of radiatively active pollutants is to warm the PBL during the day and cool the PBL at night.

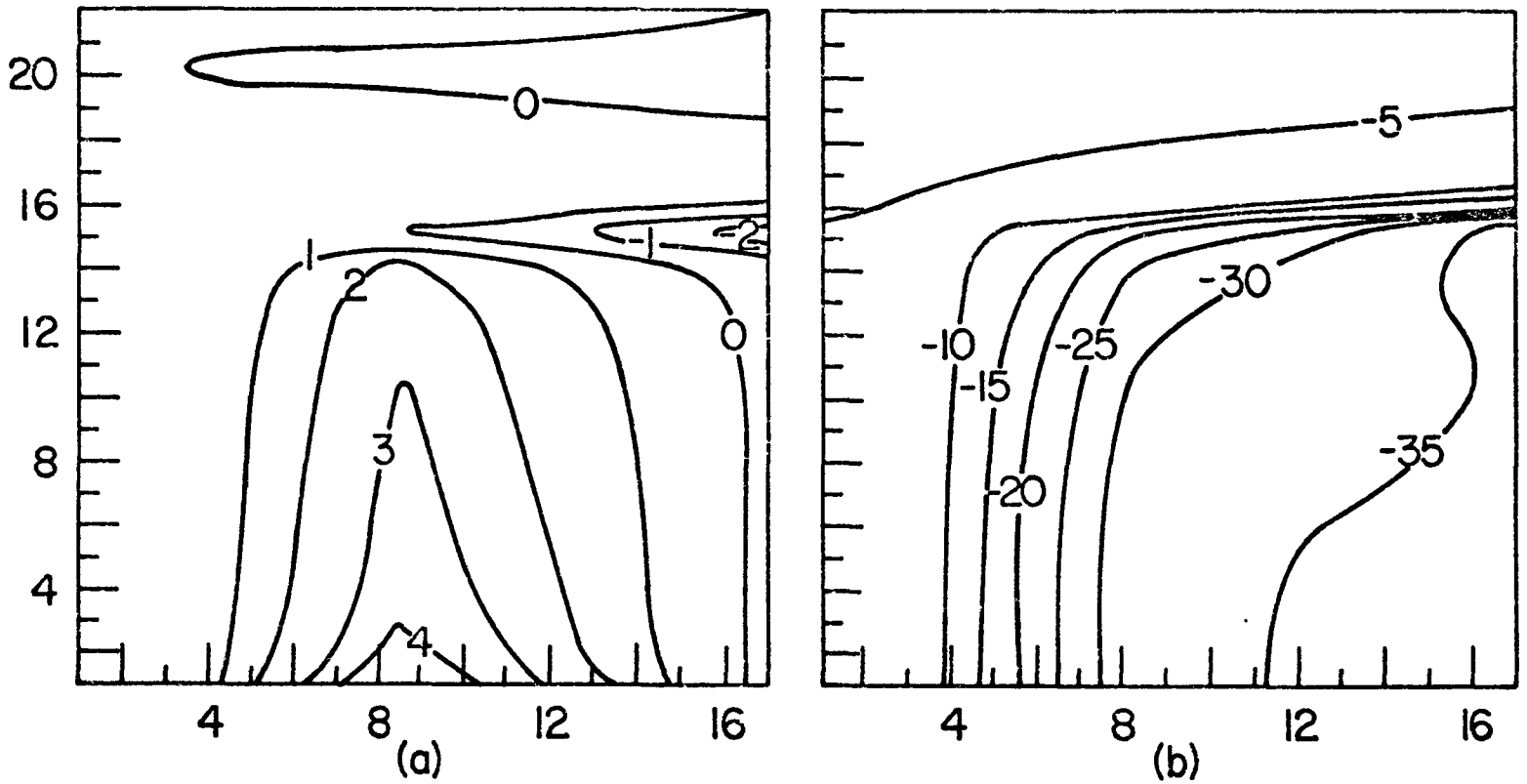

Figure 10. Isopleths of solar flux divergence perturbation (in $W/m^3 \times 10^3$) in the PBL for simulation W1 (a) isopleths of solar flux divergence difference (in $W/m^3 \times 10^3$) in the PBL between simulation W2 and W1 (b) at noon. (The abscissa represents the horizontal grid point along the urban area and the ordinate denotes the vertical grid point).

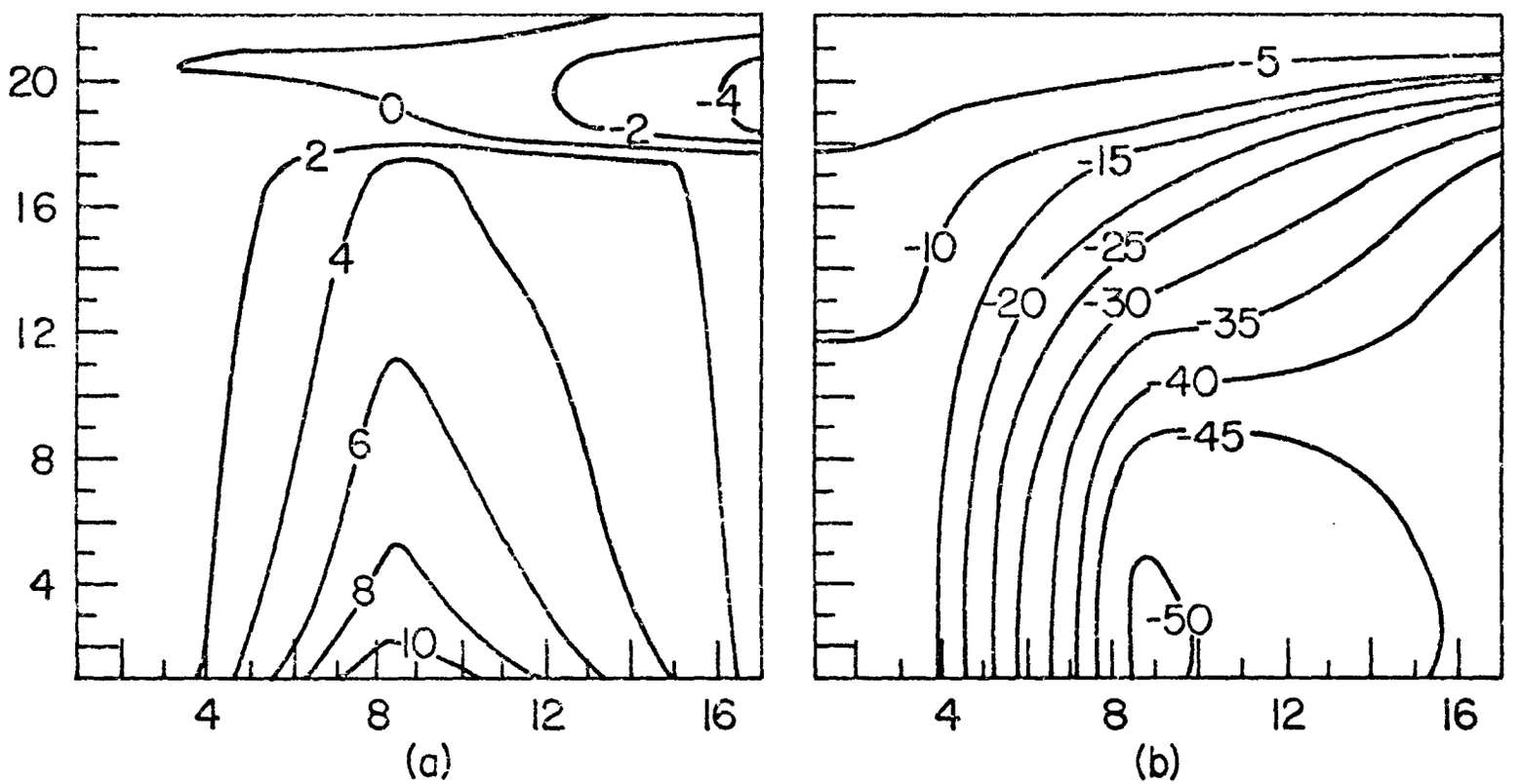

Figure 11. Isopleths of solar flux divergence perturbation (in $W/m^3 \times 10^3$) in the PBL for simulation S1 (a) and isopleths of solar flux divergence difference (in $W/m^3 \times 10^3$) in the PBL between simulation S2 and S1 at noon.

TABLE 5. NET RADIATIVE FLUX DIVERGENCE DIFFERENCES ($W/m^3 \times 10^2$) FOR REPRESENTATIVE SIMULATIONS AT THE URBAN CENTER

a) Noon, 12:00

z(m)	W2-W1	W7-W6	S2-S1
0	-11.97	-13.60	-17.14
5	-3.01	-7.53	-5.18
25	-2.72	-7.48	-4.99
50	-2.59	-7.22	-4.61
100	-2.14	-6.51	-3.89
500	-0.75	-0.45	-2.11
2000	-0.02	-0.02	-0.01

b) Midnight, 24:00

0	-4.64	-1.37	-6.47
5	0.50	1.26	0.45
25	0.72	1.29	0.69
50	0.64	1.19	0.49
100	1.10	1.59	0.94
500	0.30	0.26	0.05
2000	0.62	0.59	0.49

TURBULENT EDDY DIFFUSIVITIES

The vertical distribution of turbulent eddy diffusivities for simulation S1 without active pollutants is shown in Figure 12. Inspection of the figure reveals large variations in K_z^M during the diurnal cycle particularly for $z > 50$ m. For meteorologically very stable conditions when the vertical potential gradient $\partial\theta/\partial z$ exceeded 4 K/km, the turbulent eddy diffusivity K_z^M was arbitrarily set to a small value of 0.01 m^2/s. The diffusivities become maximum early in the afternoon and reach a minimum during the night. The magnitude of K_z^M of about 100 m^2/s is in agreement with the values reported by other investigators (Orlanski et al., 1974). From about 14:00 hours the

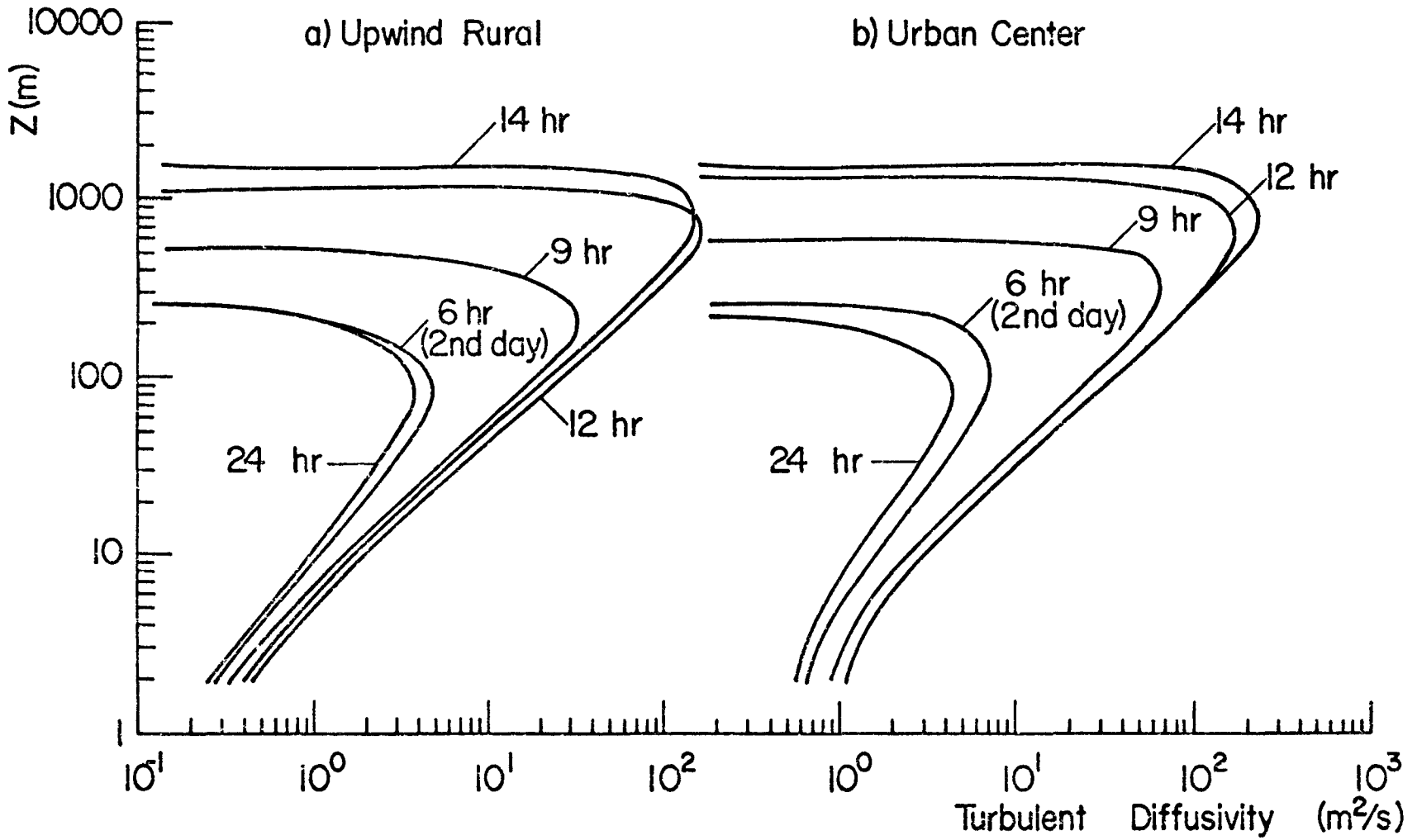

Figure 12. Vertical turbulent eddy diffusivity profiles for momentum transport (K_z^M) for simulation S1

diffusivities decay rapidly and there is a rapid decrease in the mixed layer height. By about 18:00 hours turbulence is practically extinguished in a large portion of the PBL. The K_z^M profile for 18:00 hours is not drawn as it is virtually identical with the profile at 24:00 hours. This type of behavior of PBL has been observed by Kaimal et al. (1975). Zdunkowski et al. (1976) has found that there is considerable variation in the magnitude of the eddy diffusivity particularly at greater heights from one formula to another but there are only minor variations in the vertical temperature profiles. The reason for this behavior, according to Zdunkowski et al., is that the temperature field is strongly controlled by the heat fluxes near the earth's surface where the diffusivities do not differ greatly.

The variation of the eddy diffusivity at the first grid point (z = 2 m) with time and position along the urban area is shown in Figure 13. An initial transient is noted during the early part (from 06:00 to about 09:00 hours) of the simulation. This is due to the fact that the assumed initial velocity, temperature and water vapor concentrations were too "far" away from the quasi-steady solutions induced by the diurnal cycle, and it took the system about 2 to 3 hours to adjust. The diffusivity is largest at the urban center (x = 17.5 km) where the surface roughness is maximum.

The diurnal variation of the eddy diffusivity at 2 m and 100 m for the summer simulations S1 and S2 and for the winter simulations W1 and W2 are shown in Figures 14 and 15, respectively. At the upwind rural location separate curves could not be drawn for either S1 and S2 or W1 and W2. At the urban center the radiatively active pollutants modify the diffusivities by altering the atmospheric stability through the temperature structure near the ground. However, the net effect is relatively modest. Due to the opposing influences the trends indicated are quite complex.

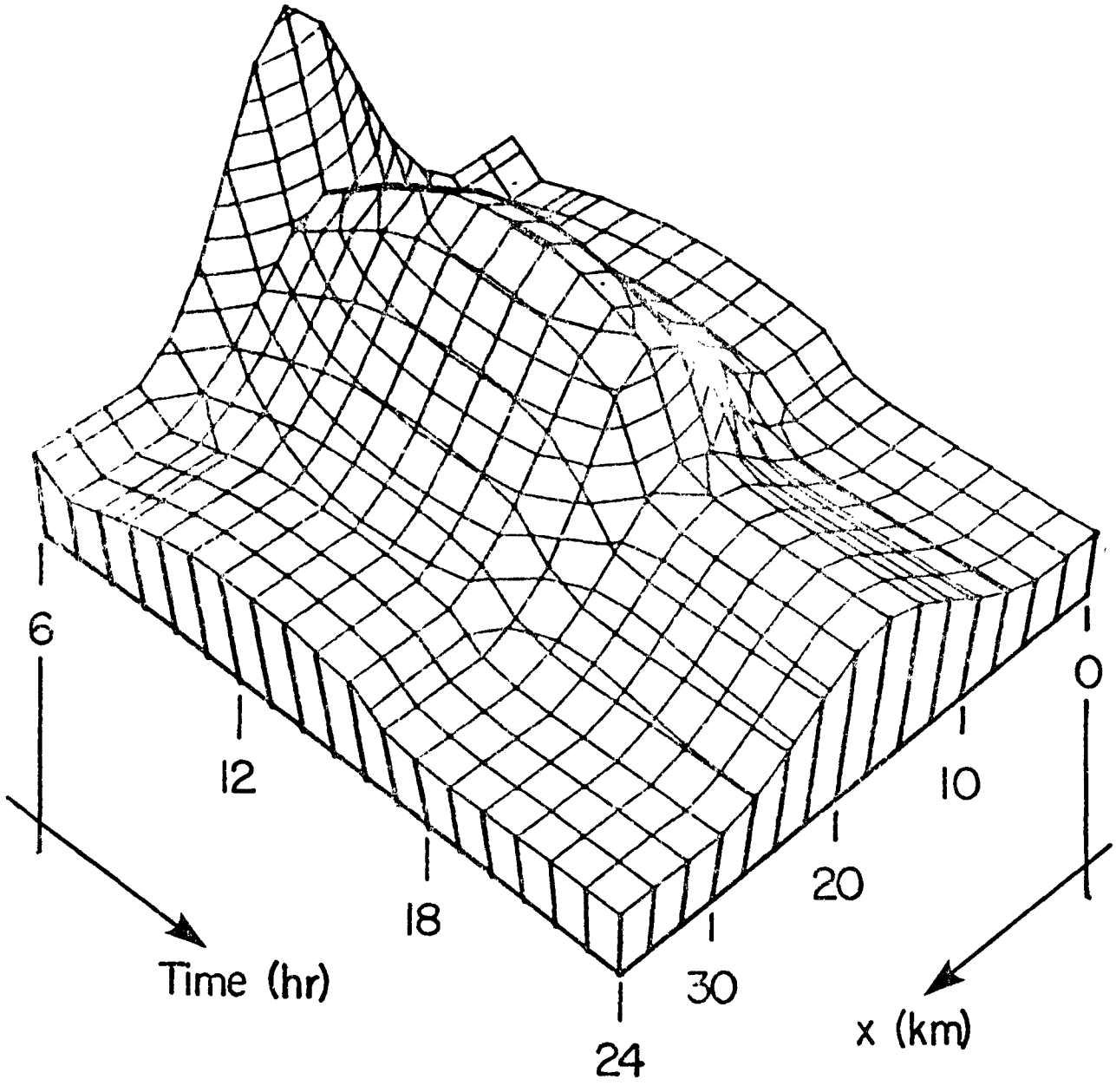

Figure 13. Variation of turbulent eddy diffusivity for momentum transport at z = 2 m with time and distance along the city for simulation S1.

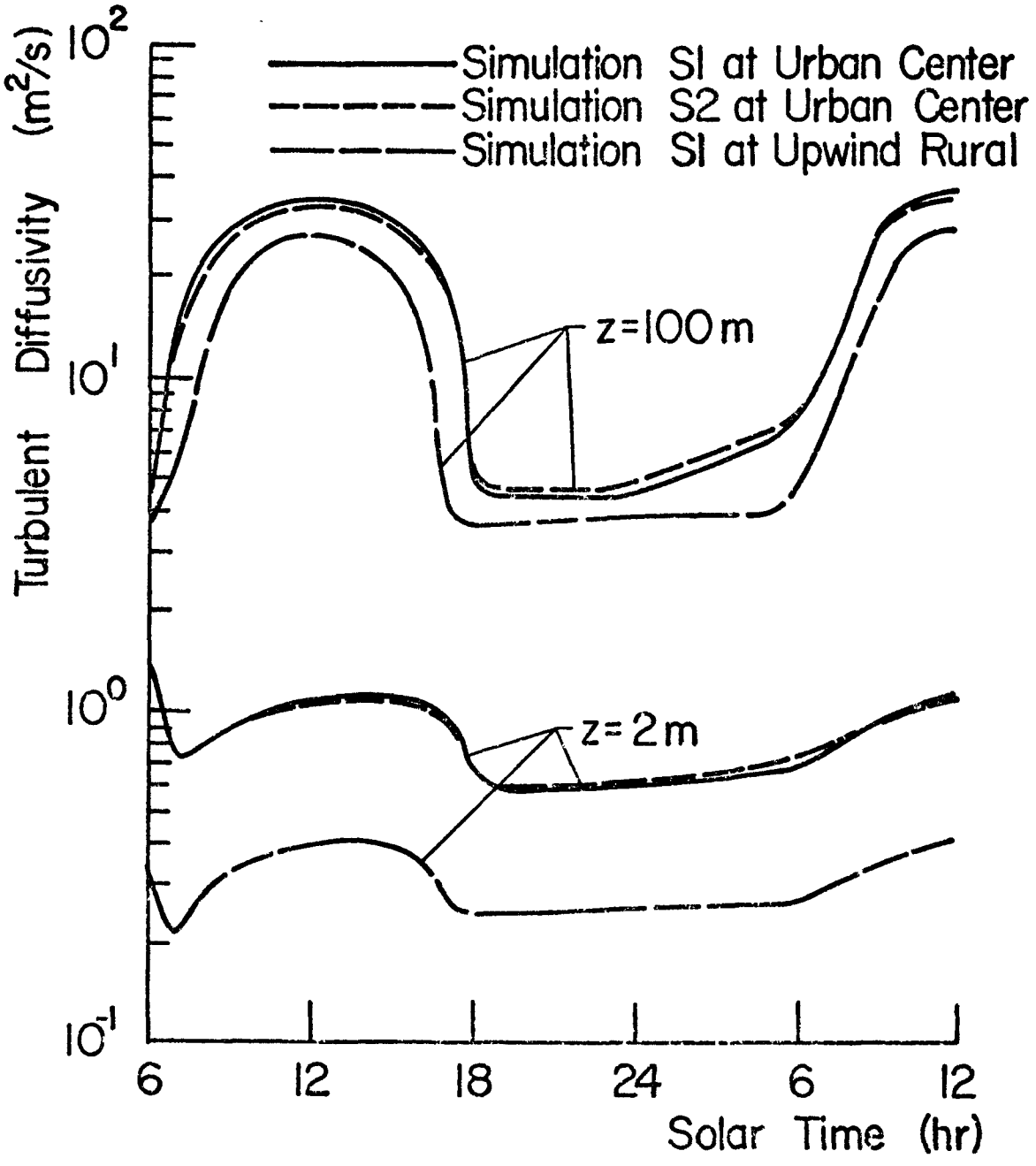

Figure 14. Comparison of turbulent eddy diffusivities for momentum transport between simulations S1 and S2.

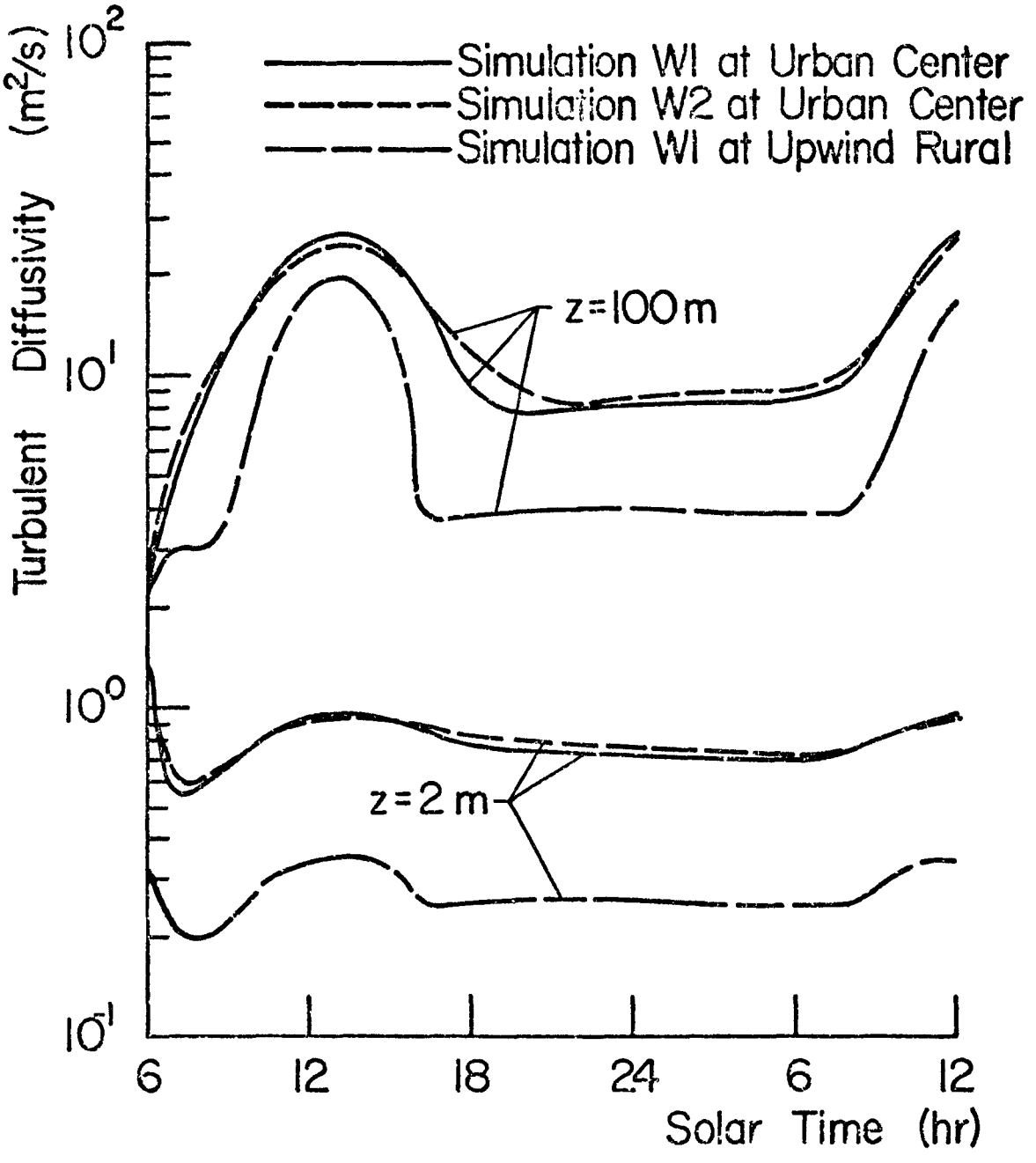

Figure 15. Comparison of turbulent eddy diffusivities for momentum transport between simulations W1 and W2.

DIURNAL VARIATION OF THE SURFACE ENERGY FLUX COMPONENTS

The diurnal variation of the energy flux components at the surface is important in understanding the surface temperature behavior during the daily cycle and in the dynamics of the PBL. For this reason some typical results which shed light on the salient nature of the transport processes at the ground are presented and discussed in this subsection.

Incident Solar and Thermal Fluxes

Figure 16 illustrates the variation of the solar flux incident on the surface q_{si} at noon for simulations W1 and W2. The radiatively participating simulation W2 shows a marked decrease in q_{si} (approximately 12% at the urban center) compared to the radiatively nonparticipating simulation W1 due to the attenuation of the incident solar flux by aerosols. Note that the effect becomes greater along the urban area due to the build-up in aerosol concentrations. The solar flux is attenuated by about 14% at x = 40 km for simulation W2 as compared to simulation W1. The solar albedo of the ground and the attenuation of solar radiation by aerosols in the atmosphere are factors in determining the solar flux incident along the urban area incident solar flux. Note that q_{si} is slightly decreased at the urban center compared to the rural areas for simulation W1 due to the lower solar albedo assumed (see Table 2). A fraction of the incident solar flux reflected from the ground is then scattered back by the natural (nonabsorbing) aerosols in the planetary boundary layer. However, this is only a second order effect. An examination of Figure 17 shows that, for simulations S1 and S2, the effect of radiatively active pollutants is similar. At noon, the solar flux incident on the ground has been reduced by about 6%. This is well within the range of observed reduction of solar fluxes in an urban area (Landsberg, 1977). It should be noted that carbon dioxide and water vapor in both P and NP simulations absorb solar radiation. For example, for

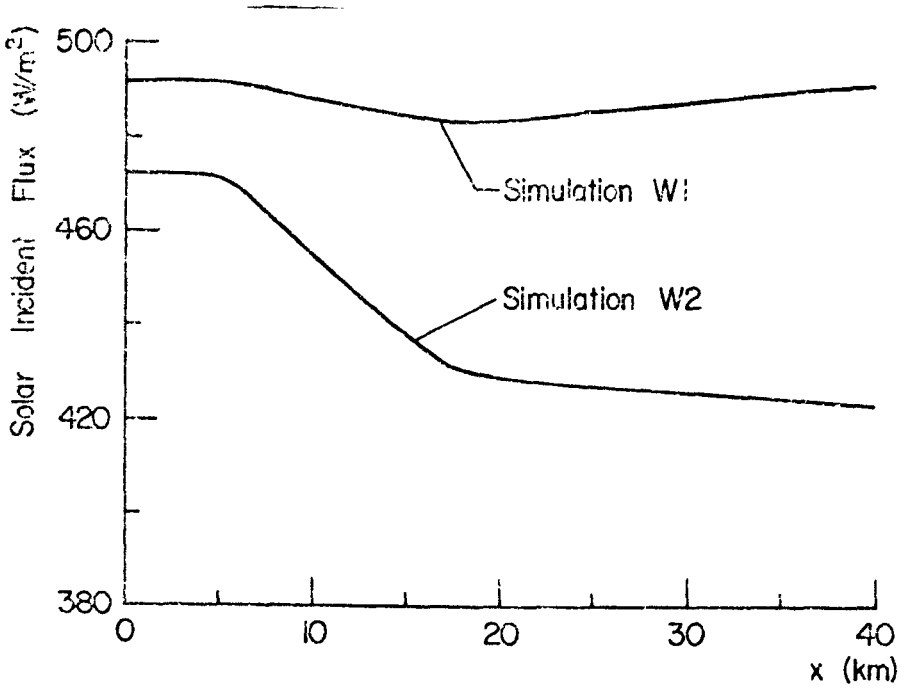

Figure 16. Comparison of solar incident flux along the urban area at noon between simulations W1 and W2.

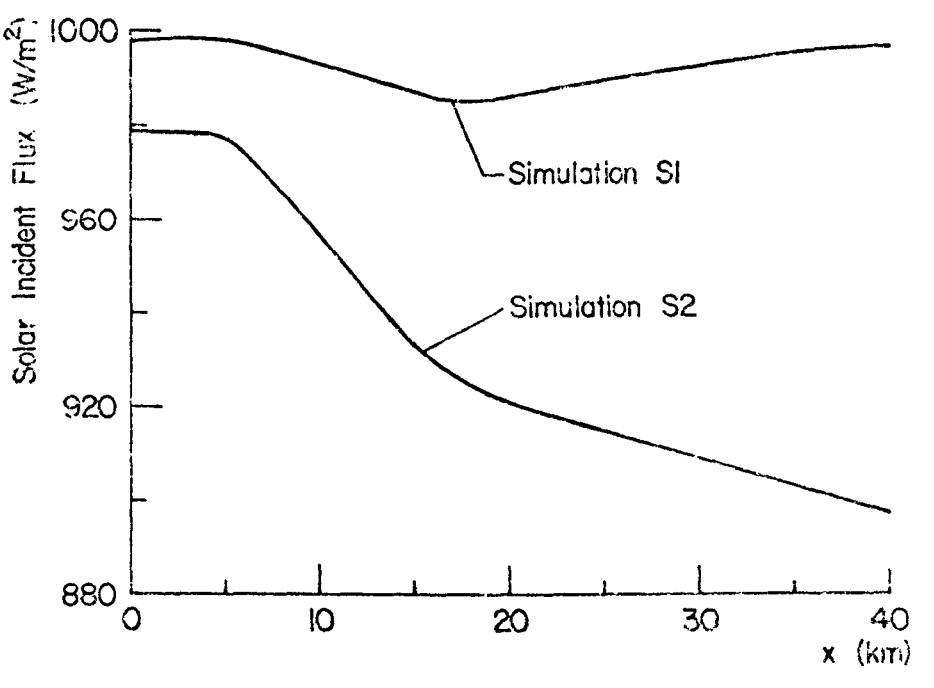

Figure 17. Comparison of solar incident flux along the urban area at noon between simulations S1 and S2.

the NP simulation S1, the downward solar flux has been attenuated by 7% from 2000 meters to the ground level. This is attributed to scattering by the natural aerosols and absorption by the carbon dioxide and water vapor in the PBL.

Figure 18 shows the diurnal variation of the solar incident flux at the urban center for some typical winter simulations. Comparing the radiatively participating (W2 and W7) with the nonparticipating (W1 and W6) simulations, the attenuation of solar flux by the radiatively active pollutants is apparent. Figure 19 illustrates the diurnal variation of q_{si} for simulations S1 and S2. The trends are similar to those for the winter simulations. The attenuation of solar radiation by pollutants is greatest for large zenith angles such as early morning and late afternoon as a result of an increase in the optical path. For instance, comparing simulations S1 and S2 at 7:00, the solar incident flux is attenuated 14% by participating pollutants, while at noon the attenuation is 6%.

Insolation measured in such cities as London and Vienna showed typical deficits of 10 and 20 percent below rural areas (Robinson, 1962). An 11% daily average decrease in the global insolation compared to rural areas was observed (Peterson and Flowers, 1977) during the more recent measurements (autumn 1973) in the Los Angeles area. In St. Louis area, however, smaller urban-rural differences were observed (Bergstrom and Peterson, 1977). The difference in behavior among St. Louis and Los Angeles and European urban areas appears to involve a decreased urban and increased rural attenuation. St. Louis may be atypical in this respect in that neither the city of St. Louis nor its surroundings over a wide area modify solar radiation in a manner typical of other locations.

Examination of Figure 20 shows a substantial increase in incident thermal flux for simulation W2 with radiatively active pollutants when compared to the simulation W1 with radiatively noninteracting ones. The average increase is about 7 percent.

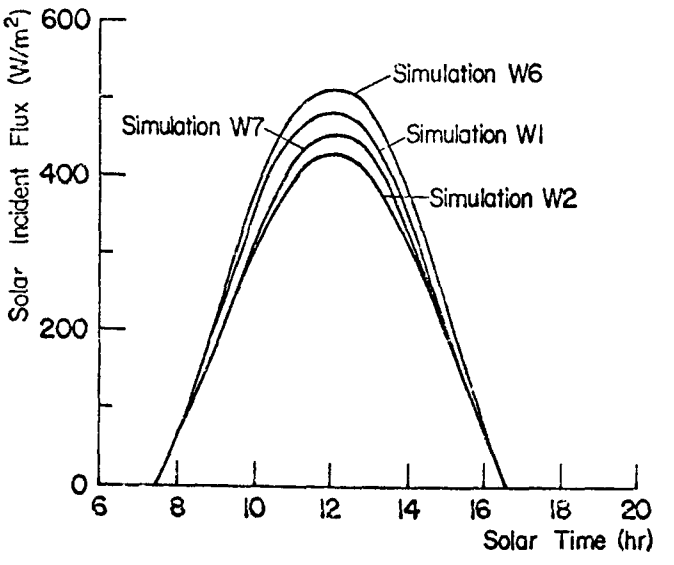

Figure 18. Diurnal variation of solar incident flux at urban center for winter simulations W1, W2, W6 and W7.

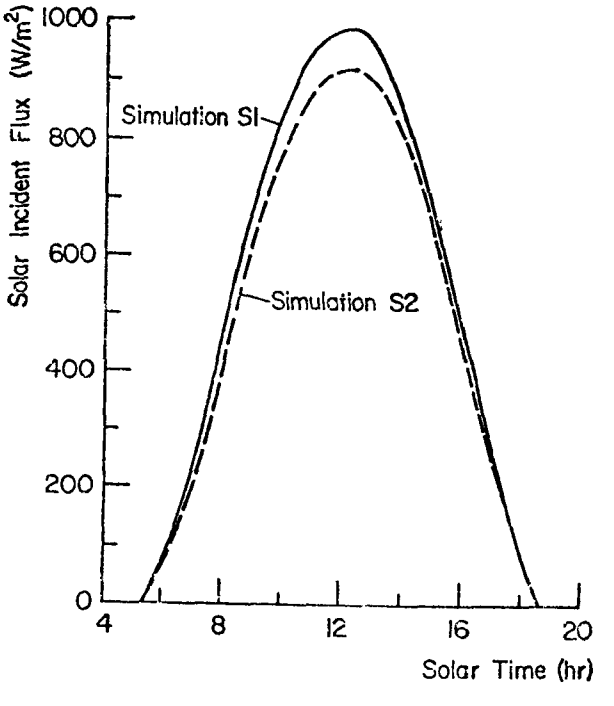

Figure 19. Diurnal variation of solar incident flux at urban center for summer simulations S1 and S2.

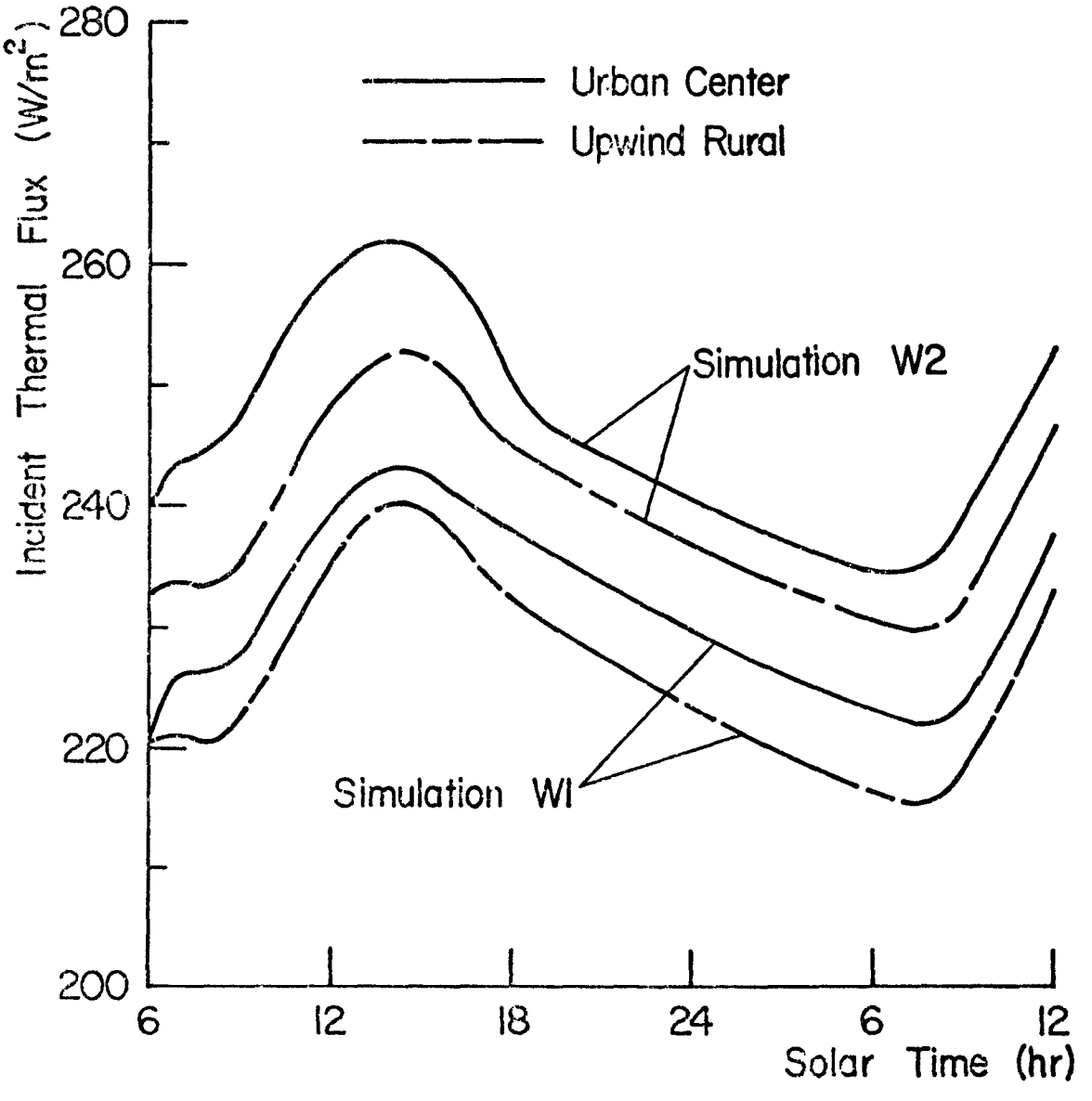

Figure 20. Comparison of thermal incident fluxes at upwind rural location and urban center for simulations W1 and W2.

Also note that, for both simulations, the incident thermal flux is greater at the urban center. This is due to higher temperatures and pollutant concentrations in the PBL than at the upwind rural location. Referring to participating simulation W2, the incident thermal flux is 4.4% greater at the urban center than at the upwind rural location. At midnight, this increase is only 1.3%. These trends are consistent with measurements of Rouse, et al. (1973). However, a meaningful comparison between the fluxes predicted in this study and those observed is not possible without a knowledge of the pollutant concentrations in the urban atmosphere. Inspection of Figures 20 and 21 reveals that the difference caused by radiatively active pollutants is relatively greater between simulations W6 and W7 than for W1 and W2. The variation of the thermal flux incident on the surface for the summer simulations S1 and S2, shown in Figure 22, is seen to be similar in trends to the winter simulations. The magnitudes are greater due to warmer PBL temperatures. The irregular trends in the incident thermal flux near the start (from 06:00 to about 09:00 hours) of the simulations are a result of the initial transient and will be explained when discussing the surface temperatures.

At night, the model predicts that the thermal radiation flux incident on the surface is slightly greater at the urban center than in the surrounding rural areas. However, this increase is slightly more than compensated for by an increase in radiation emitted by the surface. Thus, the surface net longwave radiation balance for the urban area is slightly more negative than for its rural surroundings. The difference is generally less than 10 W/m^2. These results are in agreement with measurements made by Oke and Fuggle (1972) in Montreal. This finding suggests that radiative exchange should play a relatively small role in the urban/rural surface energy balance differences at night.

It should be noted that the decrease in the solar fluxes

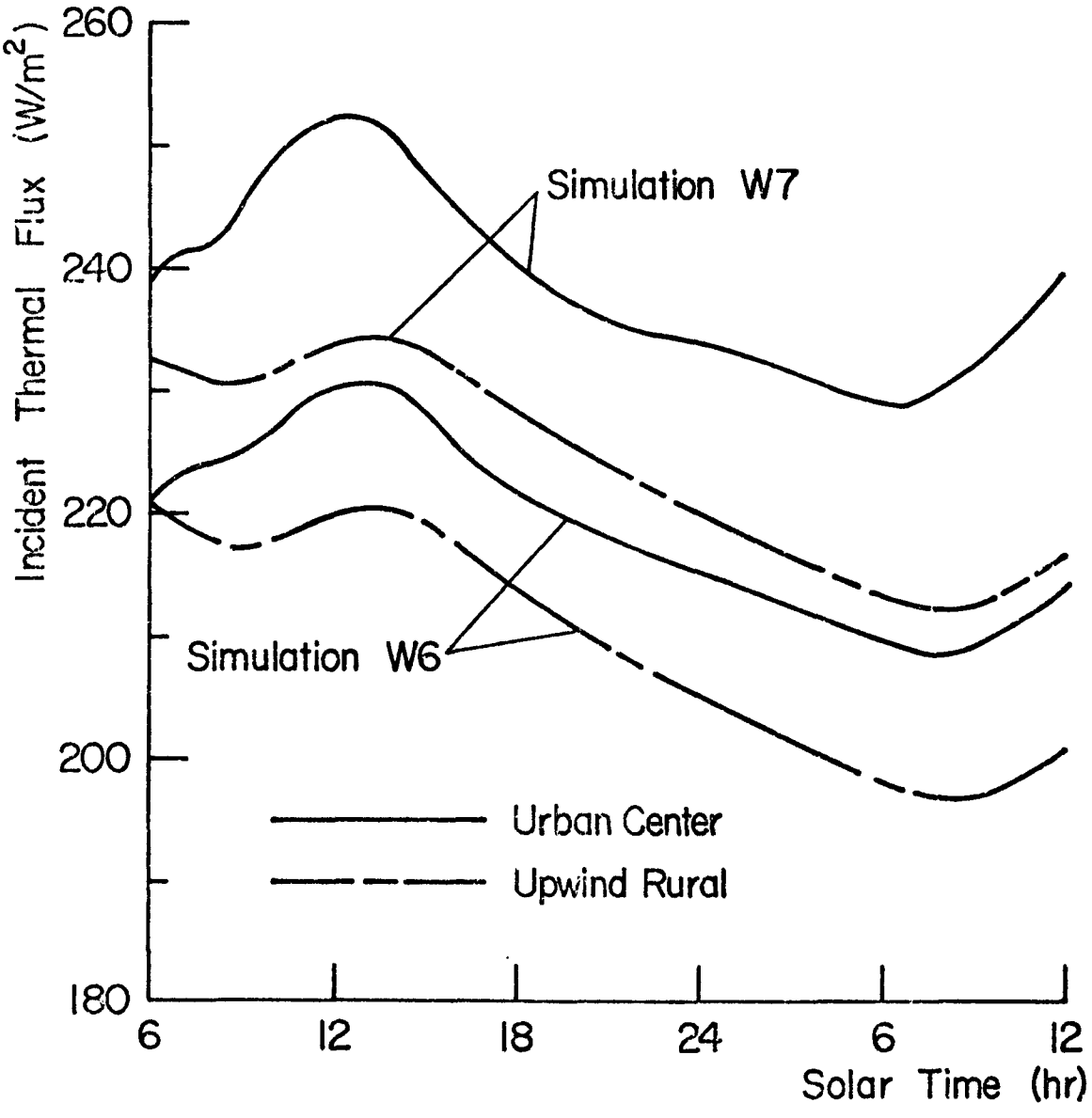

Figure 21. Comparison of thermal incident fluxes at upwind rural location and urban center for simulations W6 and W7.

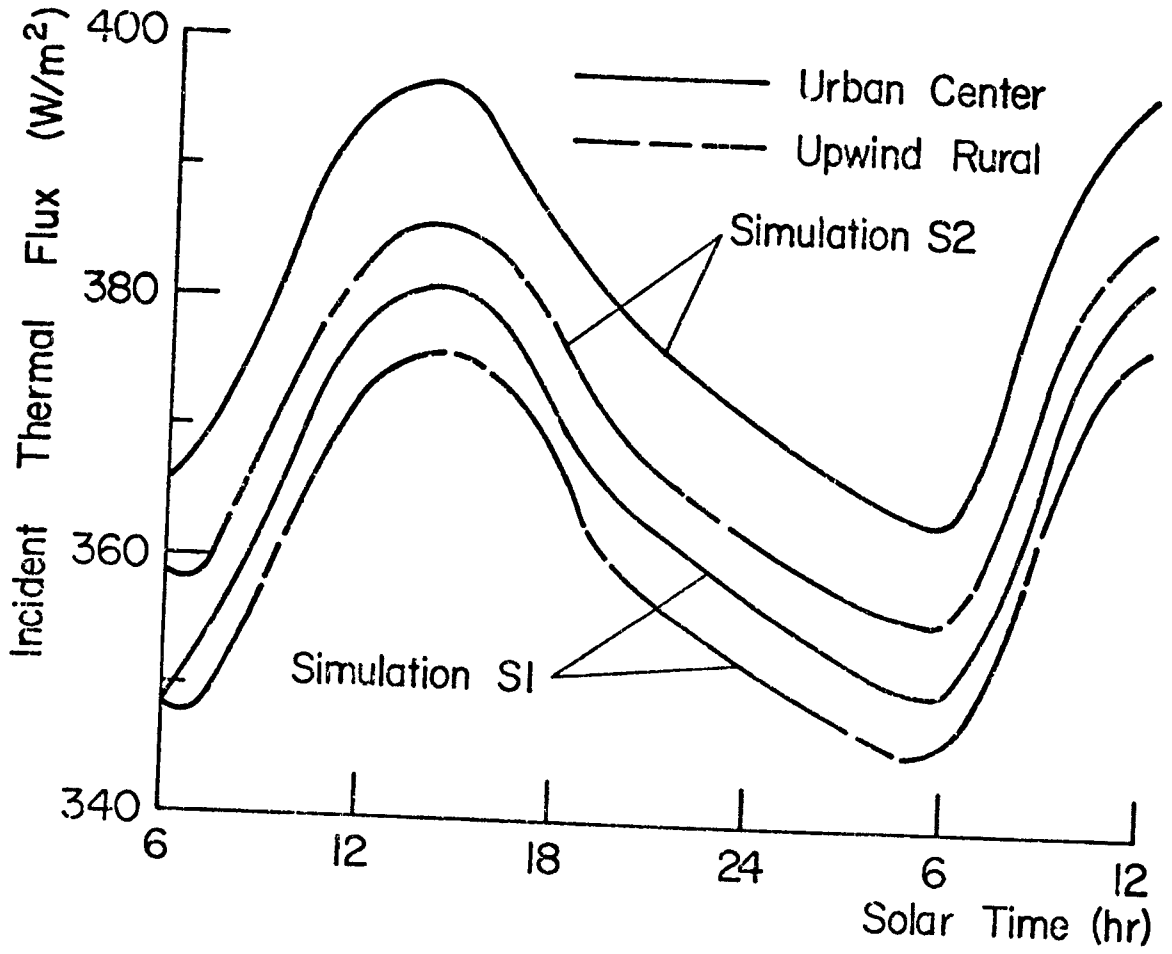

Figure 22. Comparison of thermal incident fluxes at upwind rural location and urban center for simulations S1 and S2.

is greater than the increase in thermal fluxes for simulations with radiatively participating pollutants during the daylight hours. For example, at noon the total (solar plus thermal) radiant energy flux incident on the surface for simulations W2, W7 and S2 is about 4, 5 and 3 percent, respectively, lower at the urban center as compared to the upwind rural location. The results disagree with observation by Rouse et al. (1973) in and around Hamilton, Ontario. At noon, a 2% increase in total radiant energy was observed when the industrial areas were compared to a relatively clean control site. Solar flux measurements in combination with information about the aerosol and gaseous pollutant concentration profiles, temperature structure and surface properties are not readily available. Thus, it is not possible to check the validity of the radiation model by comparing predictions with observed data.

Turbulent Fluxes

The variation of the turbulent heat flux for simulations W1, W6 and S1 with radiatively nonactive pollutants are presented in Figures 23, 24 and 25, respectively. Except for the magnitude of the fluxes, the trends indicated in the figures are similar. During the daylight hours the turbulent flux is negative (directed way from the surface) and indicates that turbulent convection tends to cool the surface. The reason the flux is largest near the noon hours is because the surface temperature and the turbulent diffusivity are highest at that time of the diurnal cycle. Depending on the location along the urban area considered, there may be reversal in the sign of the turbulent heat flux before the sunset and after the sunrise. Comparison of the results in Figure 25 with those reported elsewhere (Viskanta et al., 1976) indicates that the turbulent heat flux is quite sensitive to the meteorological conditions (particularly the wind speed) and is also influenced by the choice of the turbulence model used.

Comparison of the turbulence fluxes, particularly at the

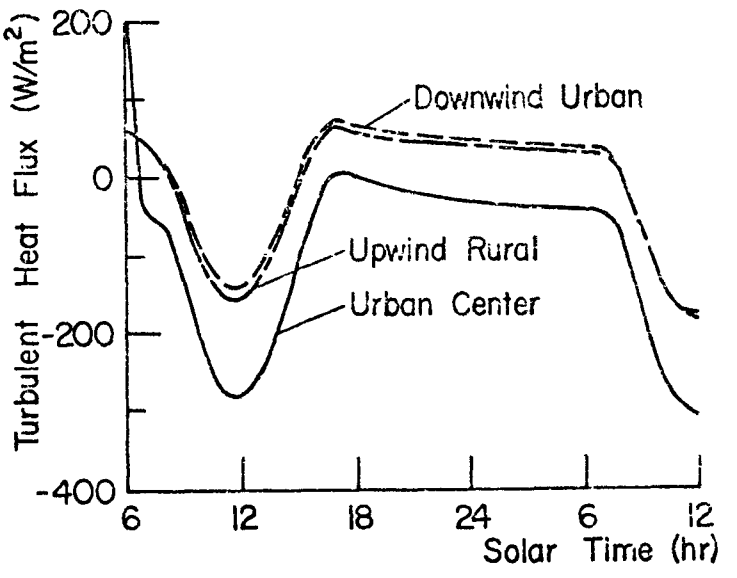

Figure 23. Diurnal variation of turbulent heat flux at upwind rural (x = 0), urban center (x = 17.5 km) and downwind urban (x = 30 km) locations for simulation W1.

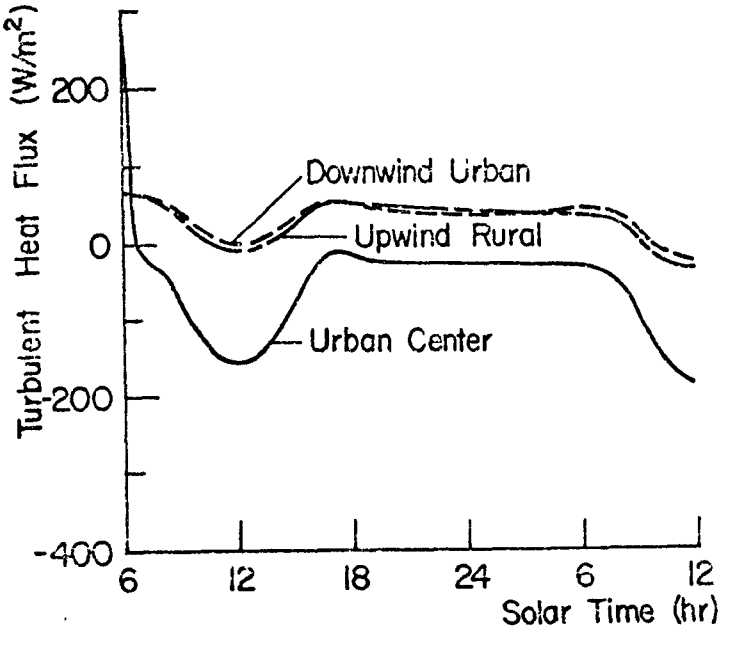

Figure 24. Diurnal variation of turbulent heat flux at upwind rural, urban center and downwind urban locations for simulation W6.

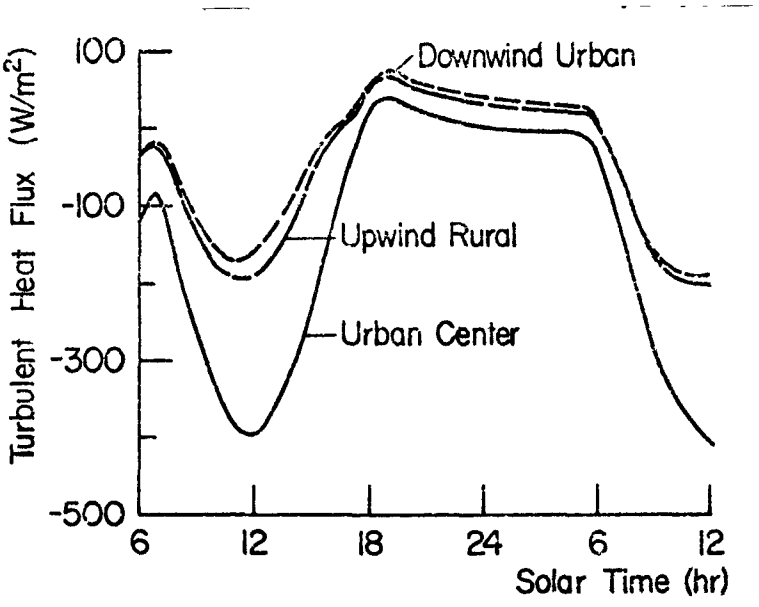

Figure 25. Diurnal variation of turbulent heat flux at upwind rural, urban center and downwind urban locations for simulation S1.

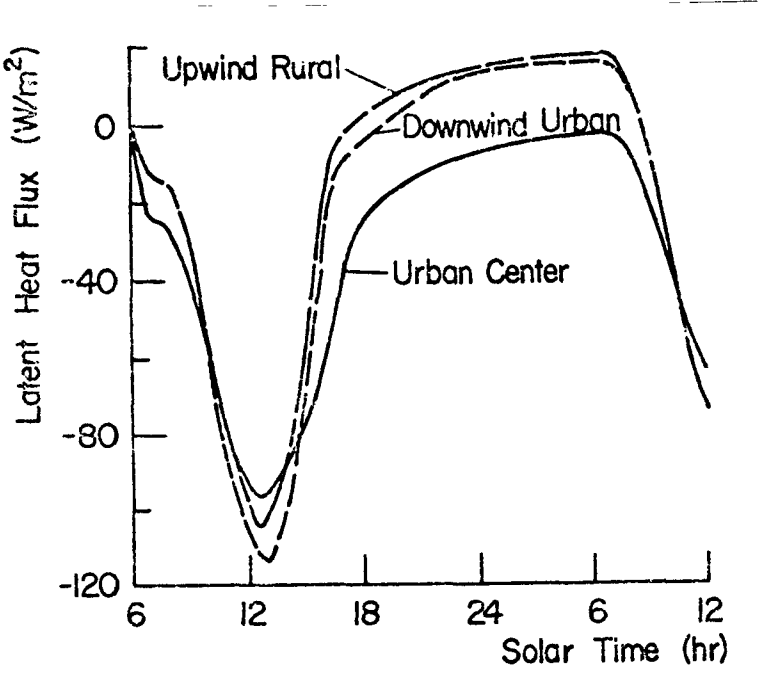

Figure 26. Diurnal variation of latent heat flux at upwind rural, urban center and downwind urban locations for simulation W1.

urban center during the day, for simulations S1 and W1 shows a 39% greater flux for the summer conditions. This is due to higher temperatures near the ground as a result of solar input and greater tubulent diffusivities for the summer than the winter simulations.

Latent Fluxes

Figure 26 illustrates the variation of the latent heat flux for simulation W1 with radiatively nonactive pollutants. Note that latent heat flux is greatest (shortly after noon) at the downwind urban center, in spite of the lower turbulent eddy diffusivity, due to the relative warmth (0.53 K greater than the upwind rural location) and the fact that Halstead's moisture availability parameter M is larger than at the urban center. At night the loss at the urban center is approximately 10 W/m^2 or less compared with 94 W/m^2 at noon. This is attributed to the cooler temperatures and smaller turbulent diffusivities. At the upwind rural and downwind urban locations the flux changes signs at night, indicating condensation at the surface. The value at the upwind rural node is slightly higher (on the order of 2 W/m^2) due to the cooler surface temperature. The variation of the latent heat flux for the simulation W6 with snow covered ground is shown in Figure 27. Note that the magnitude of the flux is more than 50% smaller during the day than that for simulation W1 with bare ground. This is attributable to the cooler surface temperatures for simulation W6.

Because of warmer surface temperatures and hence much larger water vapor concentrations at the ground $RC_{w,sat}$, the latent energy fluxes during the day for the summer simulation S1 are about a factor of four larger than for the corresponding winter simulation W1, see Figures 26 and 28. This suggests that the surface temperatures should be much more sensitive to the urban interface parameters, such as M and R, affecting q_ℓ for the summer than for the winter seasons.

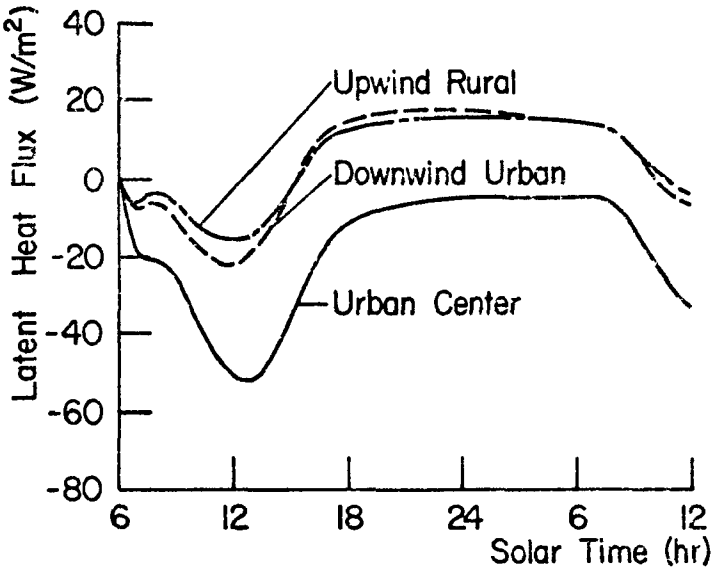

Figure 27. Diurnal variation of latent heat flux at upwind rural, urban center and downwind urban locations for simulation W6.

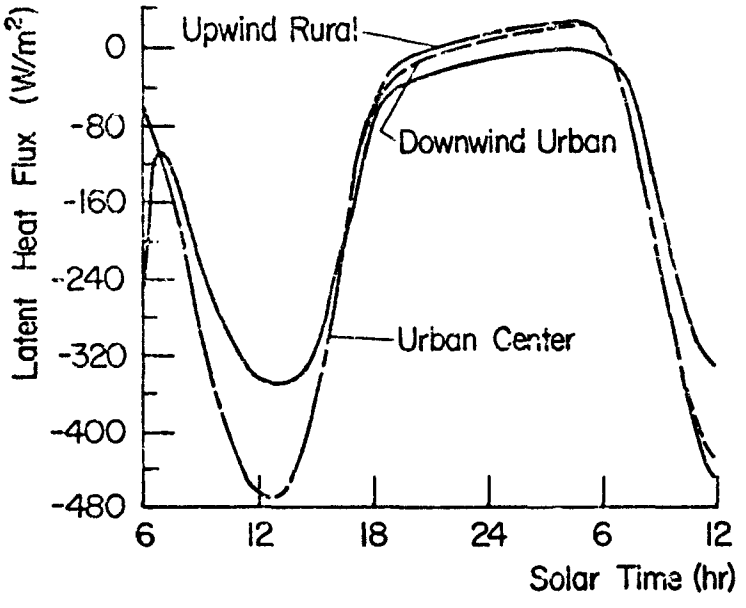

Figure 28. Diurnal variation of latent heat flux at upwind rural, urban center and downwind urban locations for simulation S1.

Conductive Fluxes

The conductive heat flux variations during the diurnal cycle for simulations W1, W6 and S1 are shown in Figures 29, 30 and 31, respectively. The conductive flux for simulation W6 is the smallest because the thermal conductivity of the snow was assumed to be about 25% lower than for the bare ground. Comparison of the results in these figures with those of Figures 23 through 28 shows that the conductive flux is the smallest component of the energy budget at the surface. Except for the magnitude and direction, the diurnal trends indicated are the same for the three numerical experiments discussed.

The conductive heat flux is largest at the urban center because the thermal conductivity os the bare ground is larger in the city than the rural environs. For these similations the maximum conductive heat flux occurs before noon and changes direction (sign) in the afternoon about 16:00 hours. The trends for the summer simulation S1 indicated in Figure 31 for upwind rural agree with results of other investigators (Myrup, 1969; Gertis and Wolfseher, 1977) and with observations (Sasamori, 1970).

Sensitivity of Turbulent, Latent and Conductive Fluxes to Changes in Urban Parameters

The sensitivity of the turbulent, latent and conductive heat fluxes in the city to changes in the urban parameters can be determined from Tables 6, 7 and 8, respectively. The difference in fluxes between corresponding simulations, with only a single parameter changed, are presented. The differences W2-W1, W7-W6, S2-S1 and S7-S6 show the effect of radiatively participating pollutants. The differences W3-W2, W8-W2 and S4-S2 indicate the effects of anthropogenic heat releases. The results for W9-W2 and S6-S2 illustrate the sensitivity to the surface roughness z_o and moisture availability parameter M changes, respectively.

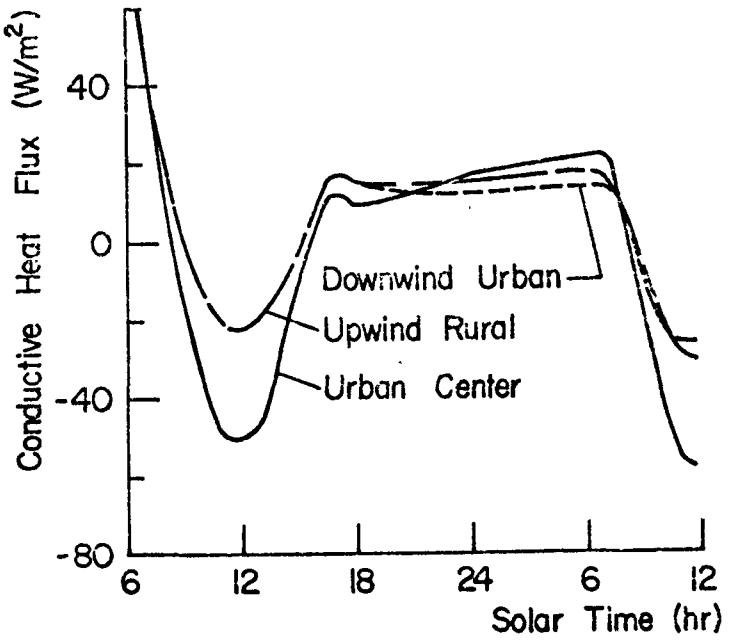

Figure 29. Diurnal variation of soil conductive heat flux at upwind rural, urban center and downwind urban locations for simulation W1.

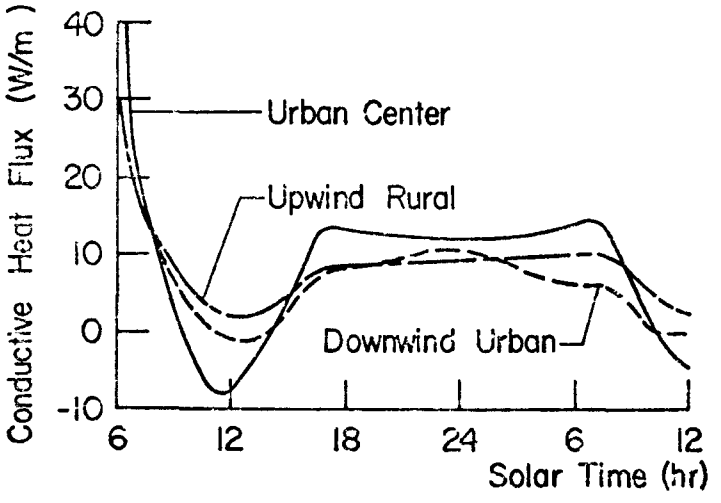

Figure 30. Diurnal variation of soil conductive heat flux at upwind rural, urban center and downwind urban locations for simulation W6.

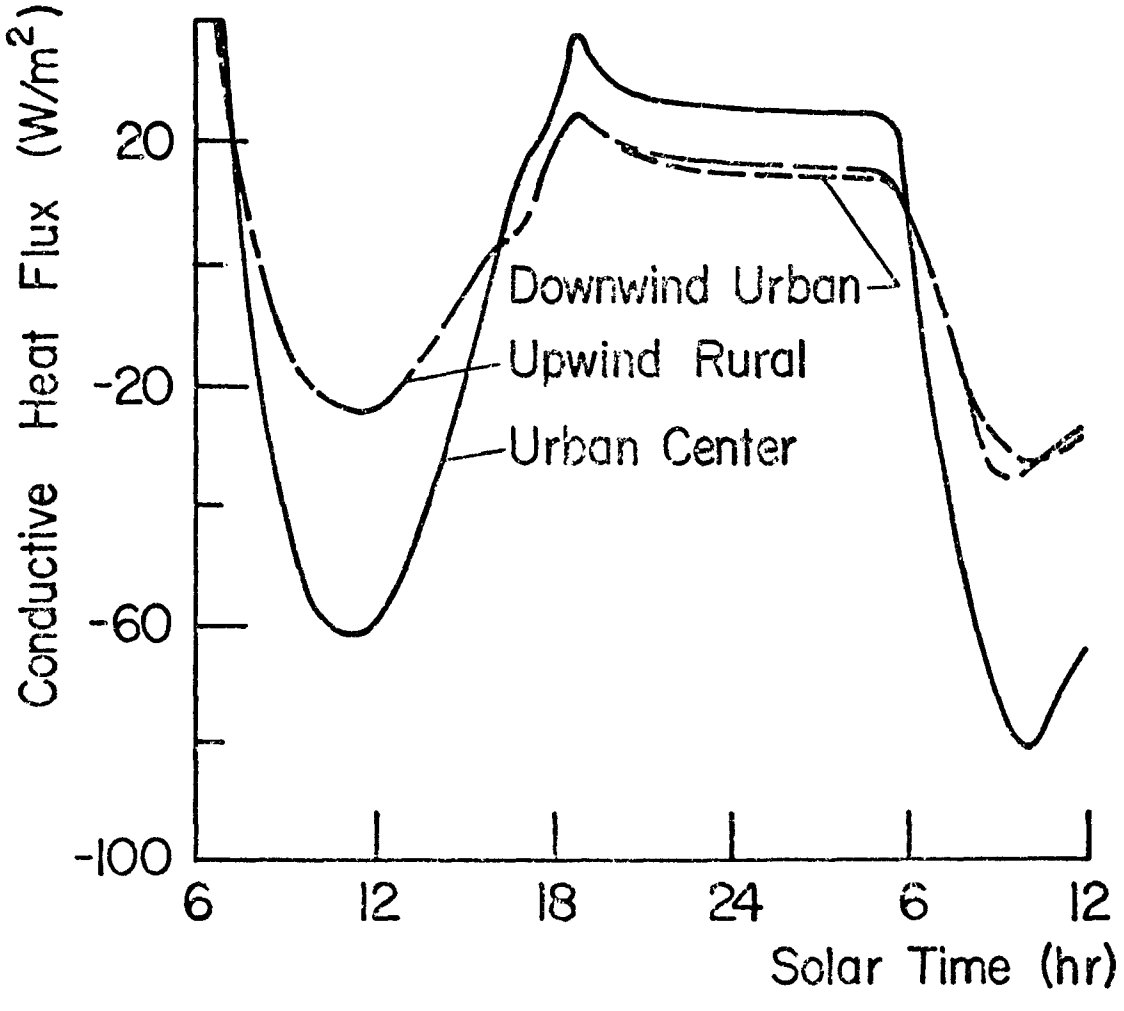

Figure 31. Diurnal variation of soil conductive heat flux at upwind rural, urban center and downwind urban locations for simulation S1.

TABLE 6. TURBULENT HEAT FLUX DIFFERENCES (IN W/m^2) AT THE URBAN CENTER FOR DIFFERENT SIMULATIONS

Time (hr)	W2-W1	W7-W6	S2-S1	W3-W2	W8-W2	S4-S2	W9-W2	S6-S2
06	0	0	0	0	0	0	0	0
08	5.8	9.3	-15.7	66.5	-59.1	-28.6	-7.2	120.6
10	-12.4	-2.2	-28.1	71.2	-75.5	-33.0	-14.7	226.2
12	-20.9	-5.8	-25.4	77.1	-85.2	-30.4	-26.4	310.7
14	-12.9	-2.6	-21.1	75.9	-78.1	-30.3	-31.1	251.5
16	3.4	7.0	-36.3	73.2	-59.3	-9.1	-22.5	258.2
18	7.6	9.5	-1.2	69.9	-49.3	-21.0	-8.7	92.1
20	5.8	8.6	5.2	66.5	-54.8	-21.9	-6.8	35.8
22	6.9	9.0	4.6	67.7	-59.9	-22.4	-5.3	25.2
24	6.6	9.2	4.0	71.0	-62.8	-22.4	-3.5	19.0
02	7.8	9.8	4.2	72.5	-65.0	-22.6	-2.3	15.4
04	7.0	10.1	9.7	75.2	-66.3	-23.4	-1.4	11.6
06	6.8	8.9	1.1	73.7	-67.1	-25.9	-0.9	14.5
08	4.9		-23.7					
10	-19.6		-37.0					
12	-26.2		-23.8					

TABLE 7. LATENT HEAT FLUX DIFFERENCES (IN W/m^2) AT THE URBAN CENTER FOR DIFFERENT SIMULATIONS

Time (hr)	W2-W1	W7-W6	S2-S1	W3-W2	W8-W2	S4-S2	W9-W2	S6-S2
06	0	0	0	0	0	0	0	-212.9
08	1.9	2.5	-6.0	16.6	-15.4	-15.4	10.8	-150.2
10	-1.5	1.5	-10.6	20.6	-20.8	-19.1	22.1	-261.8
12	-3.6	3.3	-8.8	19.6	-23.4	-18.0	29.6	-333.9
14	27.7	2.0	-7.2	20.2	-20.2	-17.7	32.3	-343.7
16	1.7	2.9	-6.8	18.9	-31.5	-17.9	20.5	-248.7
18	4.5	3.5	0.0	20.8	-27.5	-18.3	6.4	-89.4
20	3.9	2.9	2.8	24.2	-20.9	-15.1	5.9	-41.2
22	2.4	2.3	3.2	17.5	-18.3	-15.5	4.5	-26.9
24	2.2	2.3	4.0	16.0	-16.6	-16.4	3.2	-18.7
02	1.3	2.0	3.9	14.7	-15.3	-17.1	2.1	-13.4
04	1.8	1.8	3.7	12.5	-14.8	-16.8	1.2	-8.9
06	1.6	2.1	2.7	13.2	-13.8	-17.3	1.3	-13.9
08	1.4	2.2	-5.9					
10	-1.1	1.7	-7.8					
12	-1.7	1.9	-8.6					

TABLE 8. CONDUCTIVE HEAT FLUX DIFFERENCES (IN W/m^2) AT THE URBAN CENTER FOR DIFFERENT SIMULATIONS

Time (hr)	W2-W1	W7-W6	S2-S1	W3-W2	W8-W2	S4-S2	W9-W2	S6-S2
06	0	0	0	0	0	0	0	0
08	2.1	1.3	-3.1	14.4	-22.9	-5.5	-3.7	25.0
10	-6.2	-0.5	-2.7	6.9	-8.8	1.2	-9.3	29.7
12	-2.2	-0.8	-0.6	4.4	-3.9	-1.5	-7.3	13.5
14	-0.2	1.0	-0.5	3.8	-2.9	-1.7	-2.2	2.9
16	2.6	2.1	-0.1	5.9	-7.9	-2.4	2.0	0.4
18	3.2	2.4	2.9	6.6	-17.9	-9.3	2.4	-9.0
20	3.5	2.3	3.7	6.2	-17.9	-10.6	0.6	-0.9
22	4.6	2.2	3.3	11.4	-16.1	-9.7	0.3	-2.5
24	4.0	2.0	3.1	9.4	-15.4	-8.8	-0.4	-3.6
02	3.5	1.9	2.7	9.5	-14.8	-7.6	-0.2	-4.4
04	3.3	2.0	2.7	8.9	-13.7	-7.0	0.0	-4.3
06	3.9	2.9	1.1	9.9	-13.8	-4.7	-0.1	-1.7
08	2.5	1.9	-5.2					
10	-3.4	1.0	-5.3					
12	-3.2	1.5	-1.4					

The results how that the radiatively active pollutants decrease the daytime and increase the nighttime turbulent fluxes. The decrease of the turbulent flux during the sunlight hours is due primarily to the decrease of the surface temperature for simulations with radiatively participating versus the nonparticipating pollutants. The opposite is true at night. Generally the latent and conductive fluxes follow the same diurnal trends but their differences are smaller.

Examination of the tables shows that turbulent fluxes are quite sensitive to the anthropogenic heat releases. The larger the q_{an} the greater is q_c. The results also reveal, that q_c is the most sensitive and q_s is the least sensitive flux to the increase in q_{an}. The flux differences between simulations W9 and W2 indicate that increasing the surface roughness height z_o decreases the turbulent and increases the latent flux. Of all the changes in the urban parameters considered, the turbulent and latent fluxes are most sensitive to the moisture availability parameter M. The differences S6-S2 indicate that a decrease in M results in a decrease in q_ℓ and an almost equal increase

in q_c. The parameter M affects the latent heat flux and through the partitioning of the energy balance at the surface changes the turbulent flux. As a consequence of these compensating trends there is only a relatively small increase in conductive heat flux into the soil.

SURFACE TEMPERATURES

Surface Temperature Variation Along Urban Area

The surface temperature variation along the urban area for the base winter simulation W1 and the base summer simulation S1 with radiatively inactive pollutants are presented in Figures 32 and 33, respectively. For the particular surface parameters and anthropogenic heat emissions assumed in the simulations, the results show that urbanization increases the surface temperature in the city in comparison with rural environs. The temperature downwind of the city is higher than that upwind because of the heating of the air as it flows over the warm city. The difference is more pronounced at night than during the day. As expected, because of the larger anthropogenic heat releases into the atmosphere the difference is larger for the winter than for the summer simulation.

The difference in the surface temperatures between the urban and upwind rural locations is an indication of the intensity of the urban heat island. Comparison of the results in Figures 32 and 34 shows that the anomaly is greater for the winter simulation W6 with snow covered ground than for simulation W1 with bare ground. This is due to the fact that the anthropogenic heat releases in the city are a relatively more important contribution to the surface energy balance for simulation W6 because of decreased total radiative flux incident on the surface than for simulation W1.

Figures 35 and 36 depict the daily course of the temperature at the earth's surface at three different locations along the urban area for simulations W1 and S1, respectively. The

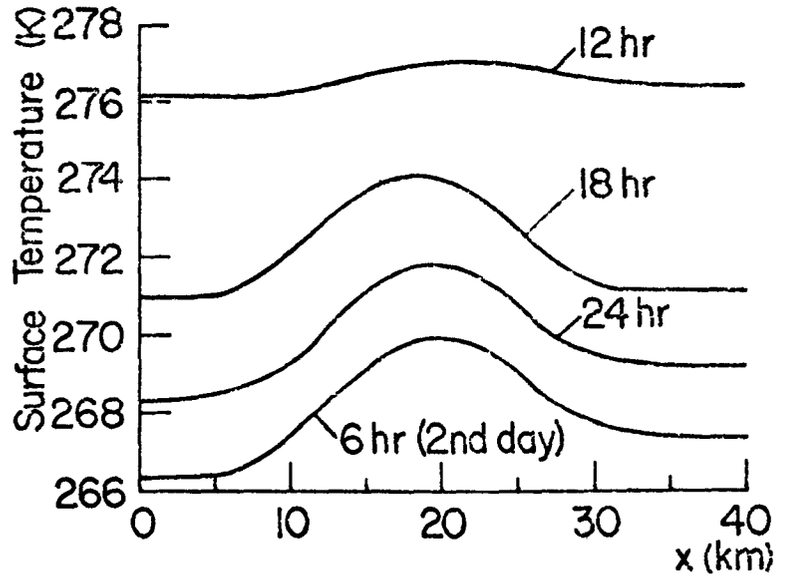

Figure 32. Surface temperature variation along the urban area for simulation W1.

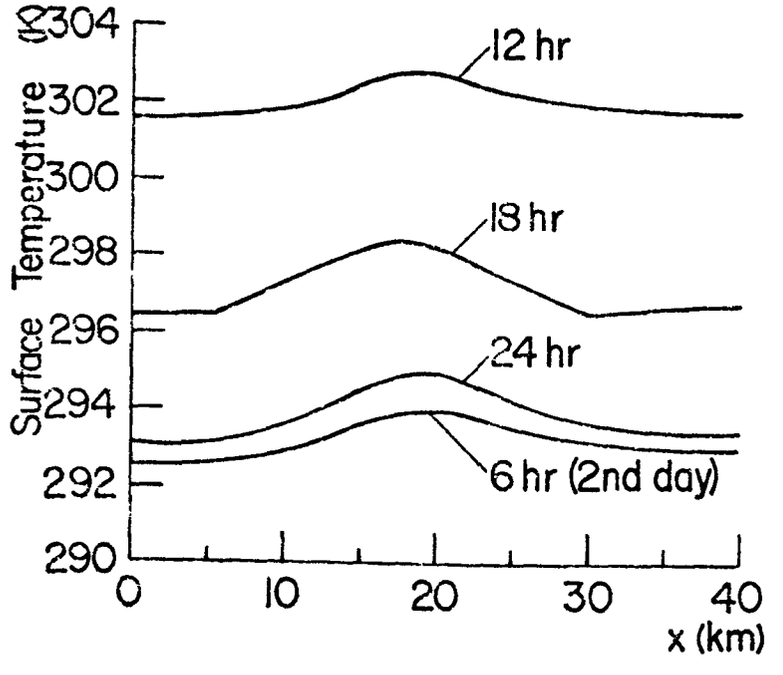

Figure 33. Surface temperature variation along the urban area for simulation S1.

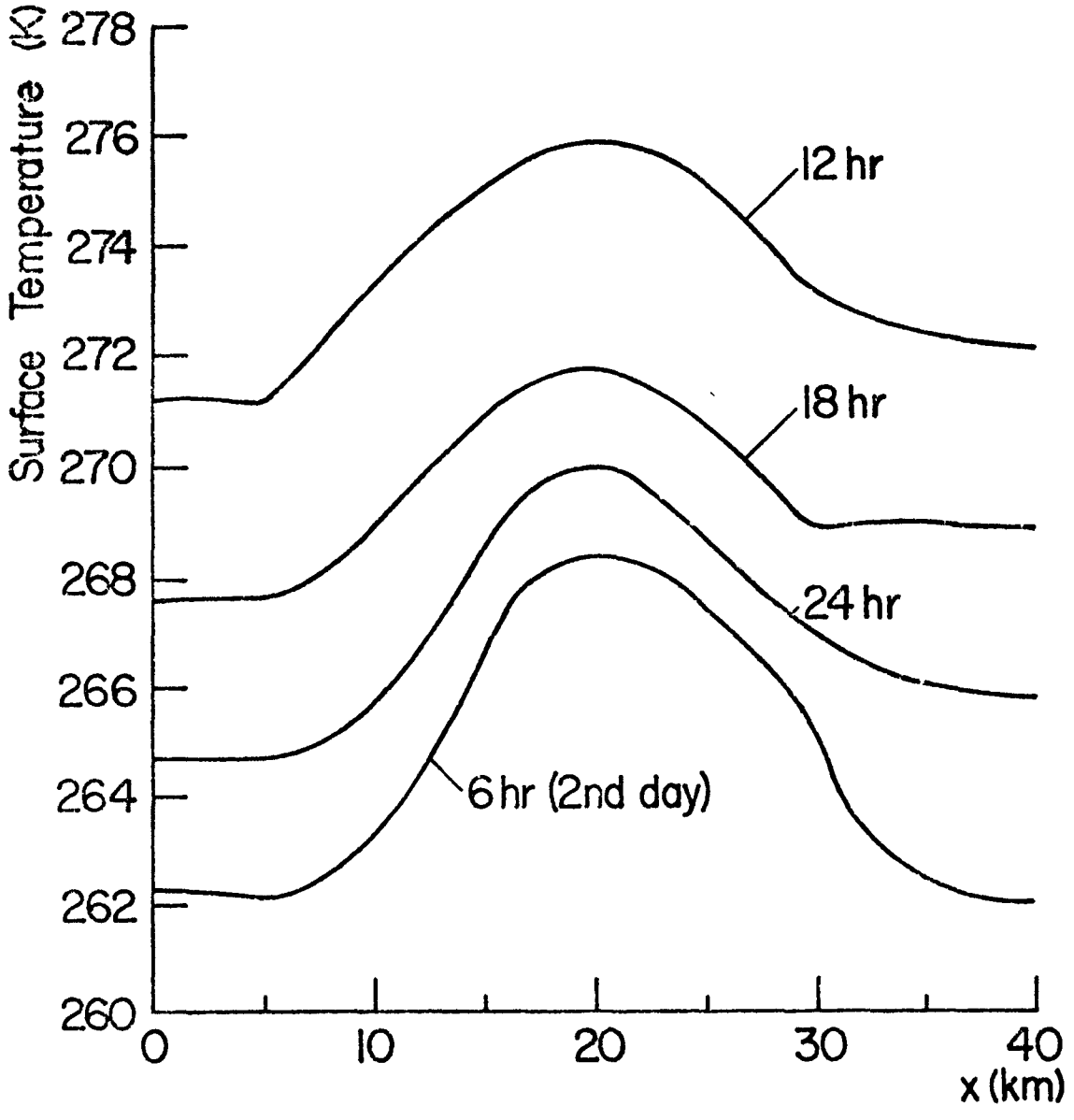

Figure 34. Surface temperature variation along the urban area for simulation W6.

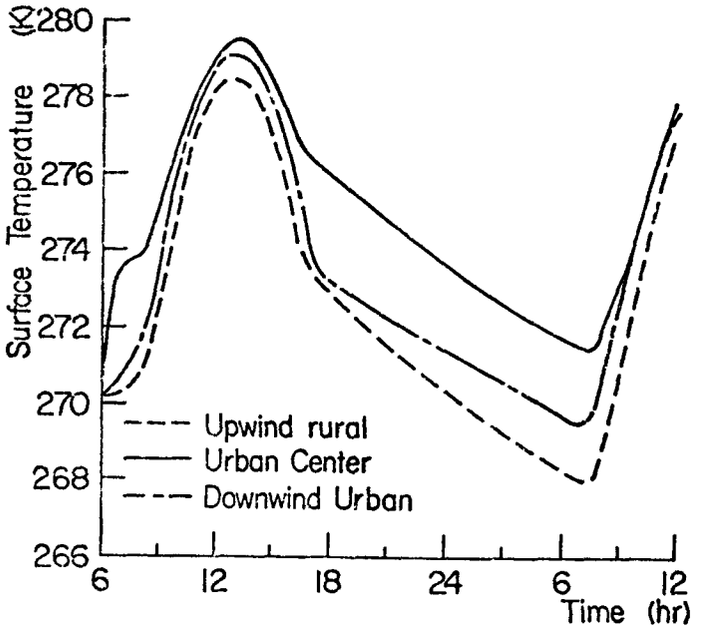

Figure 35. Diurnal surface temperature variation at upwind rural, urban center and downwind urban locations for simulation W1.

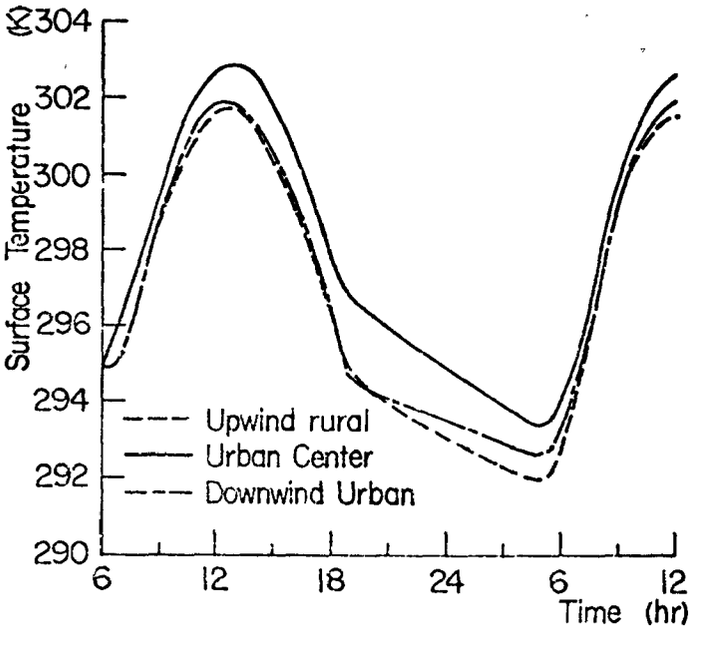

Figure 36. Diurnal surface temperature variation at upwind rural, urban center and downwind urban locations for simulation S1.

modifications of temperature show up very distinctly. The results indicate that after a 30 hour simulation period a steady diurnal cycle has not yet been established, and the earth-atmosphere continues to cool. For simulation S1, however, there is only about 0.1 K temperature difference at the urban center between noon on the first and the second days of the simulation period. This suggests that the time is too short for complete stabilization. The trends indicated in the figures agree with those reported in the literature (McElroy, 1973; Torrance and Shum, 1976) and are consistent with observations during the winter at Montreal (Oke and East, 1971) and during the summer at Columbus (McElroy, 1971). Various simulations have been performed to determine the sensitivity of the model to a change in a single parameter or group of parameters. The results are presented as surface temperature differences between two comparable simulations.

Effects of Radiatively Active Pollutants

The effects of the radiatively active pollutants on the surface temperature difference (temperature for simulation with radiatively participating pollutants minus temperature for simulation with nonparticipating pollutants) along the urban area for the base winter (W2-W1) and summer (S2-S1) simulations are presented in Figures 37 and 38, respectively. Examination of the figures shows that during the night the differences are positive and during the day they are negative. The results indicate that the surface temperatures are relatively more sensitive to pollutants for the winter than for the summer simulations. This is due to several factors. First, the thermal flux incident on the surface, which is the dominant term in the surface energy balance at night, is relatively larger during the winter than during the summer. Second, the warmer surface temperatures decrease stability of the atmosphere near the ground and in doing so increase the turbulent energy transport to the surface. This feedback is more significant in the rural areas and downwind of

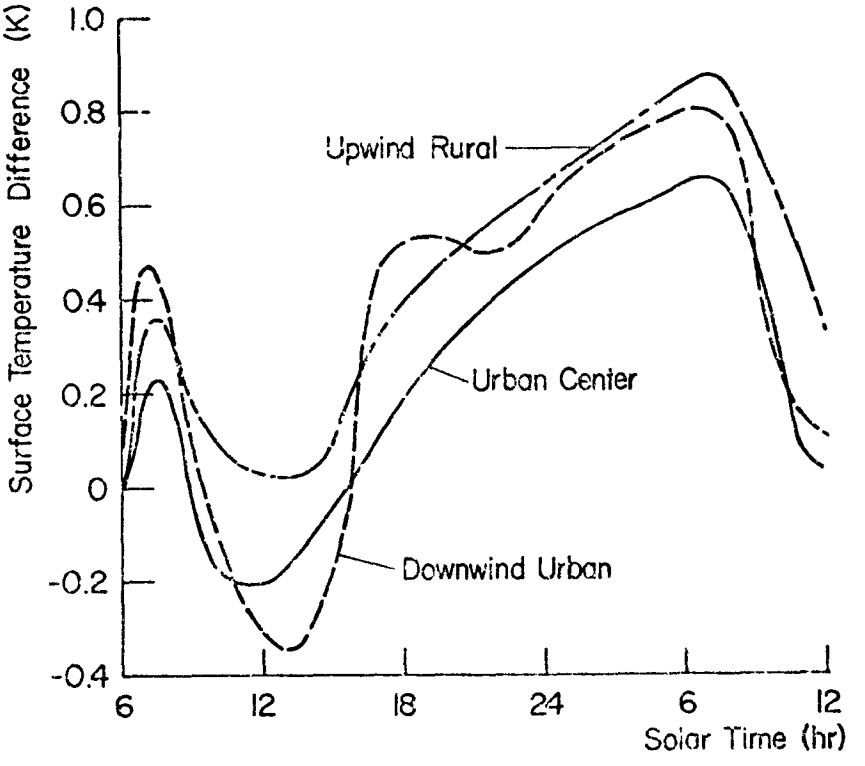

Figure 37. Diurnal variation of surface temperature differences between simulations W2 and W1 at upwind rural, urban center and downwind urban locations.

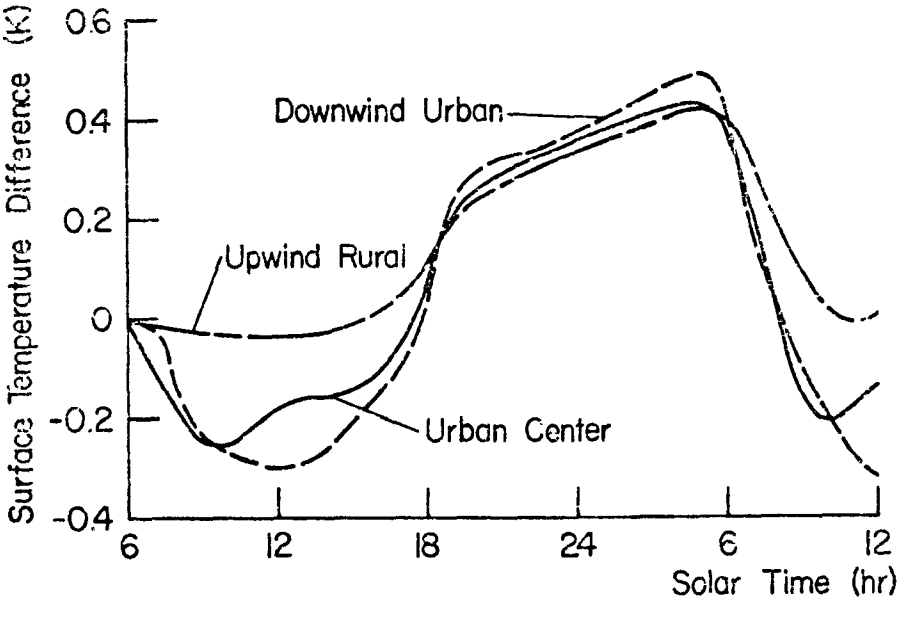

Figure 38. Diurnal variation of surface temperature differences between simulations S2 and S1 at upwind rural, urban center and downwind urban locations.

the city where the anthropogenic heat emissions into the atmosphere are relatively small in comparison to the absorbed thermal flux. The surface temperatures during the day are lower for the simulations with radiatively interacting pollutants primarily because of the attenuation of the solar radiation by anthropogenic aerosols.

The feedback between radiatively active pollutants and surface temperatures is greater for the simulations with snow covered ground (W7 and W6) than with bare ground (W2 and W1) winter simulations. Inspection of Figure 37 shows that even at noon $\Delta T_{p\text{-}NP}$ is positive at the upwind rural location. This indicates that there was an increase in the net flux heating the surface resulting from the radiatively active pollutants instead of a net decrease of the flux. Thus, the greatest feedback between pollutants and the surface temperature is expected to occur when the net flux at the surface is smallest. This is certainly the case for the winter simulations with snow covered ground.

Effects of Anthropogenic Heat Releases

Comparison of surface temperatures for simulation W2 with W3 and W2 with W8 show that the temperatures are very sensitive to the anthropogenic heat releases. Figure 39 illustrates the surface temperature difference along the urban area between simulations W2 and W8 with radiatively active pollutants. For simulation W2 the average anthropogenic heat releases in the city were50 W/m^2 while for W8 there were no heat releases (see Table 3). As a result of the decrease in this parameter the nighttime surface temperature at the urban center is approximately 3.1 K lower for simulation W8 than W2. However, during the day the difference is only 1.0 K as the anthropogenic heat release is a less significant component of the total energy balance near the surface. Because of the strong coupling of the near-surface temperature to the turbulent eddy diffusivity through the stability parameter (Richardson number Ri) the increase in q_{an} does not result in a proportional increase in the surface temperatures. This

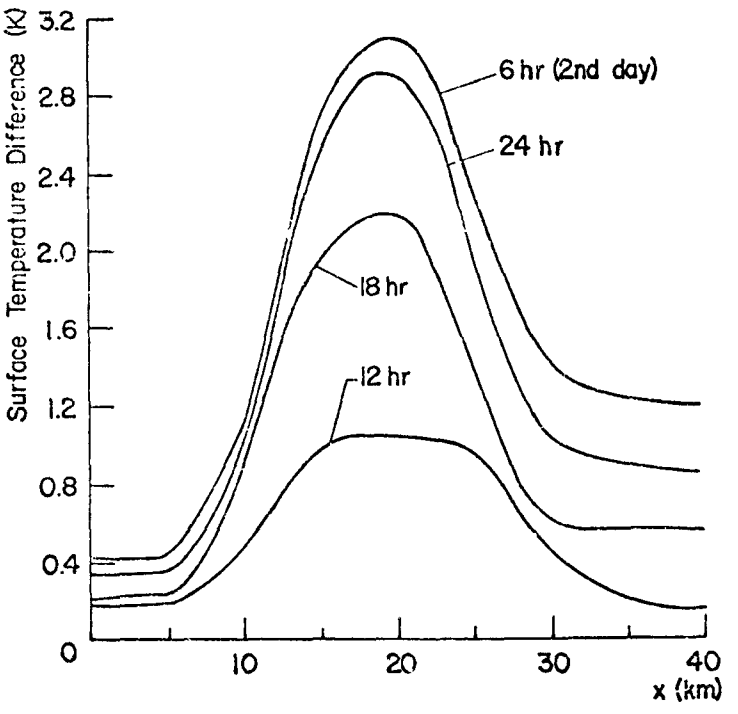

Figure 39. Surface temperature differences between simulation W2 and W8 along the urban area.

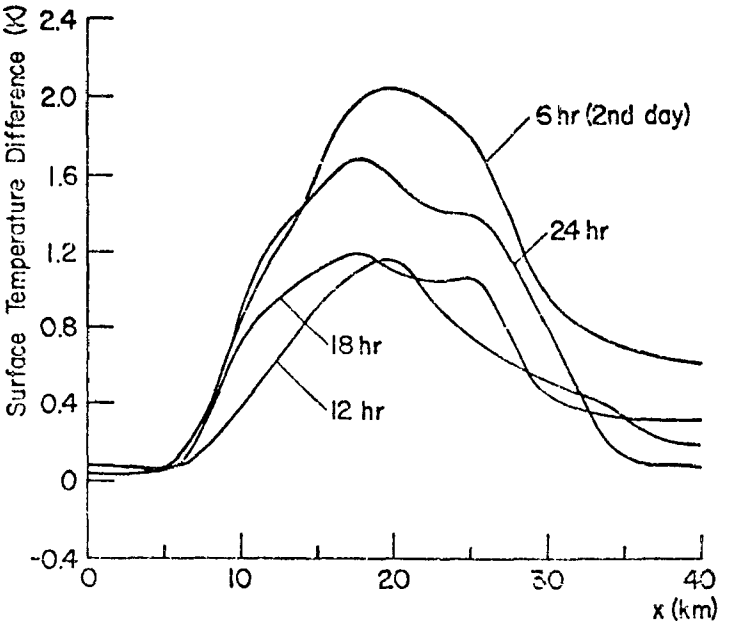

Figure 40. Surface temperature differences between simulation W3 and W2 along the urban area.

can be seen by comparing the results in Figure 40, where the anthropogenic heat releases are increased from 50 W/m^2 (simulation W2) to 100 W/m^2 (simulation W3) in the city, with those presented in Figure 39. For example, the maximum surface temperature difference at 6:00 in the center of the city for W3-W2 is about 2.1 K while for W2-W8 the maximum difference is approximately 3.1 K. Figure 41 shows that the anthropogenic heat release is also of importance for summer simulations. For simulation S2 q_{an} = 20 W/m^2 in the city while for simulation S4 q_{an} = 0 W/m^2.

Effects of Other Surface Parameters

Figure 42 shows the effect of increased surface roughness on the temperature difference. This effect is most significant during the day and is caused by the increase in the upward turbulent heat flux at the surface. Doubling z_o at the urban center from 1.0 to 2.0 m increases the surface temperature at noon by about 1 K. The trend is consistent with available results (Venkatram and Viskanta, 1976) but the magnitude of the effect predicted is smaller primarily because of the larger moisture availability parameter used for the simulations reported here.

The sensitivity of the surface temperature to the solar albedo along the urban area can be determined by examining the surface temperatures for simulations S2, S5 and S8. As expected, an increase in the ratio $r_{s,UR}/r_{s,UC}$ increases the surface temperature in the city relative to that in the rural areas. This is clearly indicated in Figure 43 where ΔT_{S5-S2} are presented along the urban area. A decrease in the solar albedo from 0.125 to 0.1 results in a surface temperature increase of about 0.2 K between the two summer simulations S5 and S2 at the urban center. At night the temperature is approximately 0.1 to 0.2 K lower for simulation S5 due to the altered temperature structure in the atmosphere and the soil during the previous day. Note that increasing the rural-urban albedo difference increases the

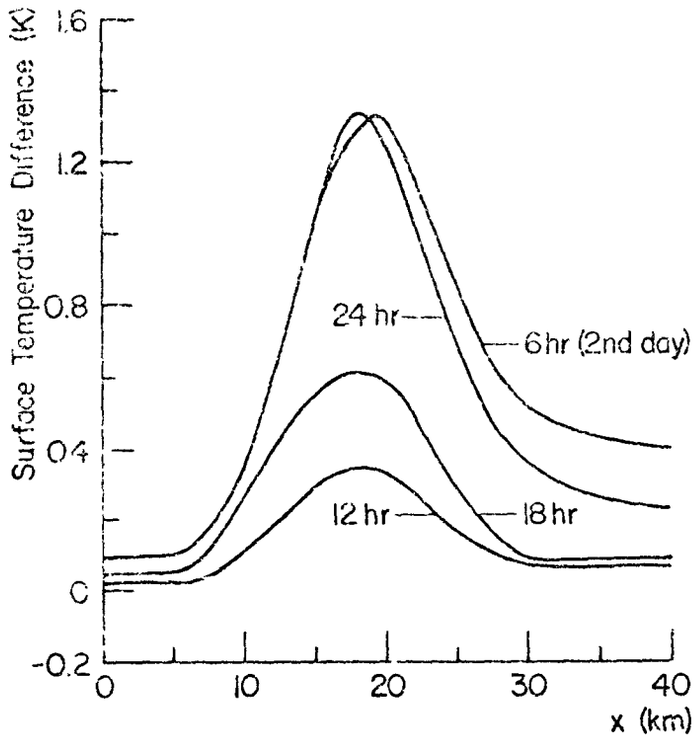

Figure 41. Surface temperature differences between simulations S2 and S4 along the urban area.

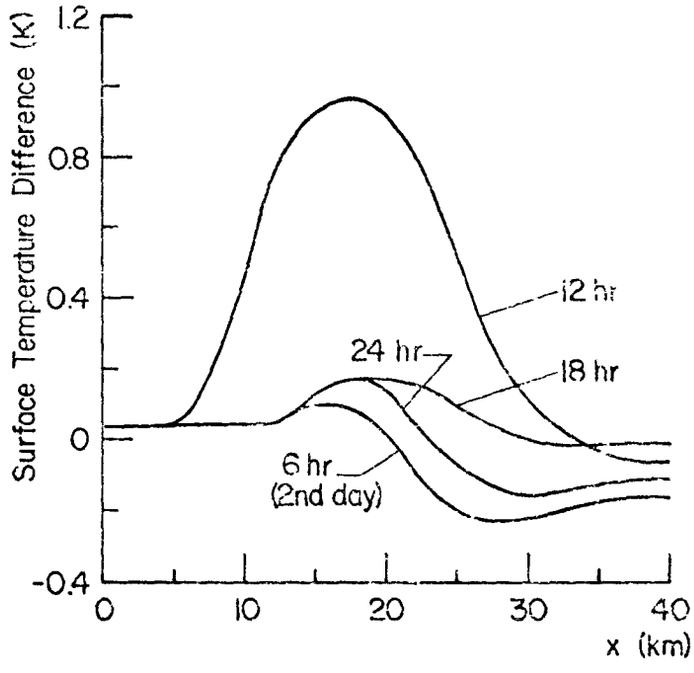

Figure 42. Surface temperature differences between simulations W2 and W9 along the urban area.

surface temperature difference during the day, but has little effect at night. Comparing temperatures of simulation S8 to simulation S2 shows that a decrease in albedo at both the rural and urban locations causes the temperature to be higher all along the urban area. The effect is greatest at noon in the upwind rural area where the temperature is 0.77 K higher and at the urban center the temperature is 0.39 K higher for simulation S8 than for S2. At night the temperature along the urban area is warmer by 0.3 to 0.4 K due to the altered temperature structure during the day.

Halstead's moisture availability parameter is also very important in determining the surface temperature. Figure 44 shows that reducing M from 0.75 to 0.5 at the rural location and from 0.2 and 0.0 at the urban center causes a relatively large difference in the surface temperature. As the latent energy flux is reduced, the surface temperature must rise to increase the turbulent heat flux and emission to compensate for the reduction in latent energy flux. The effect is the greatest at noon, when the temperature increase at the urban center is approximately 4.2 K.

In summary of surface property effects, it can be stated that increasing the solar albedo or decreasing the moisture availability parameter decreases the sensitivity of the surface temperature to the solar flux changes and hence the effects of radiatively interacting aerosols. The greater sensitivity of the earth-PBL system to the radiative participation by the aerosols when the solar albedo is increased is a well know result (Russell and Grams, 1975) which is confirmed by this study in the context of surface temperature changes.

TEMPERATURE DISTRIBUTION

Temperature Perturbation

Isopleths of potential temperature perturbation Θ' (temperature in the city minus the upwind rural temperature) are

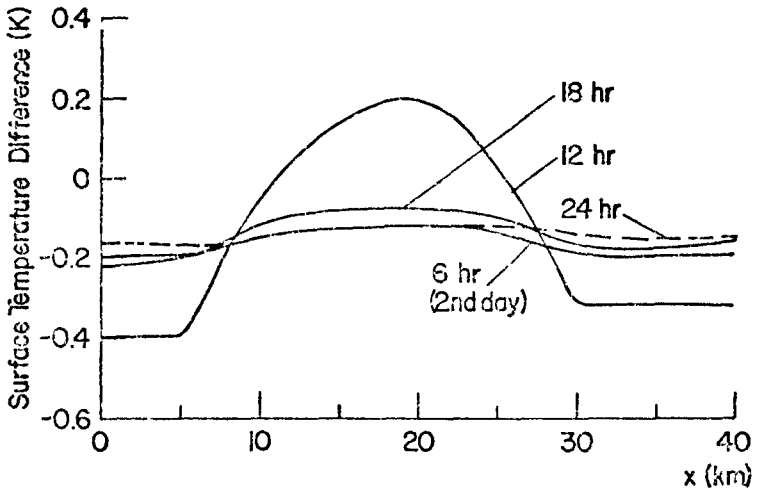

Figure 43. Surface temperature differences between simulations S5 and S2 along the urban area.

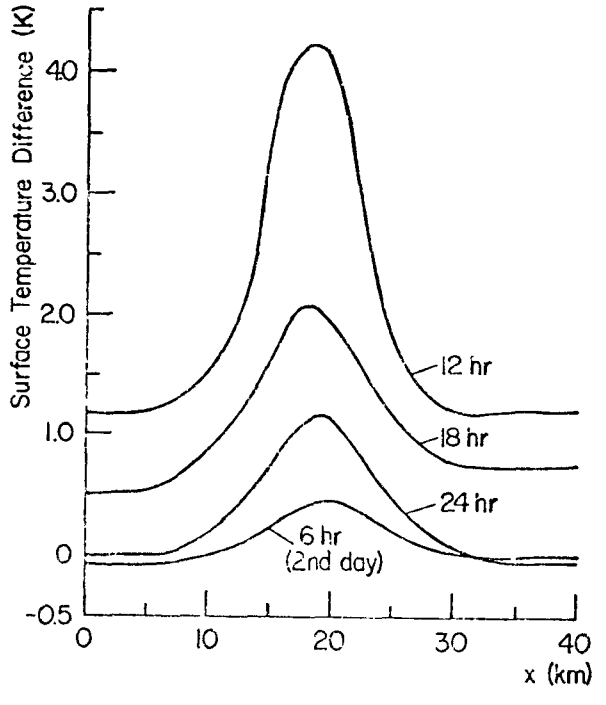

Figure 44. Surface temperature differences between simulations S6 and S2 along the urban area.

illustrated for the radiatively noninteracting simulations W1, W6 and S1 in Figures 45, 46 and 47, respectively. The left panel (part a) gives the temperature at noon and the right panel (part b) gives the temperature at midnight. It is seen from the figures that the air temperature in the city and downwind are warmer than upwind of the city. In agreement with observations (DeMarais, 1975) the perturbations are greater at midnight than at noon. The trends indicated in all three figures are the same, except the magnitudes of θ' are different. In the upper part of PBL the potential temperatures over the city and for some distance downwind are cooler than upwind of the city. This is referred to as the potential temperature "crossover effect" and has been observed by some investigators (Bornstein, 1968; Oke and East, 1971). The magnitude of the effect and the height at which the crossover occurs depends at least in part on the particular interface parameters, meteorological and boundary conditions chosen for the simulations and is greater for the winter (Figure 46) than for the summer (Figure 47) seasons.

Comparison of results in Figures 45 and 46 shows that the potential temperature excess is considerably greater at noon and midnight for simulation W6 compared to simulation W1. The maximum potential temperature excess occurs at the surface and is 4.65 K and 5.26 K at noon and midnight, respectively. The maximum potential temperature excess at noon for simulation S1 (Figure 47) occurs at some distance above the surface, and is in this respect, similar to simulation W1. Notice the crossover effect is relatively small (a maximum of 0.27 K) and occurs at a higher altitude than for the winter simulations. At midnight, the maximum potential temperature excess of 1.80 K for the simulation is rougly half of that for simulation W1, which is 3.44 K.

The results presented indicate that urbanization and human activity (even without the radiatively active pollutants in the atmosphere) increase the temperature near the ground above that in the rural environs. This finding is in agreement with the

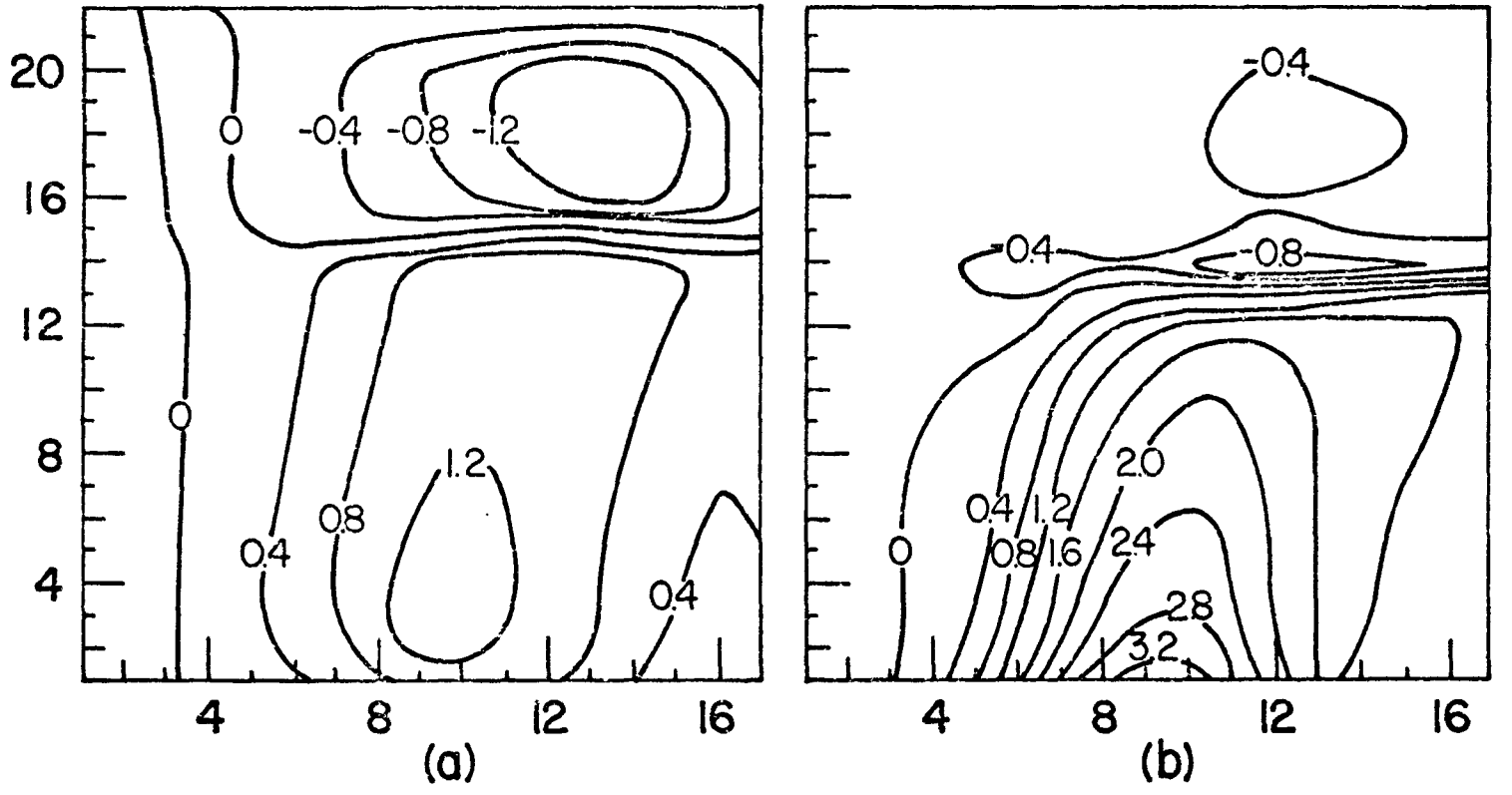

Figure 45. Isopleths of potential temperature perturbation in the urban atmosphere for simulation W1 at noon (a) and at midnight (b); the abscissa and the ordinate denote the grid points in the horizontal and vertical directions, respectively.

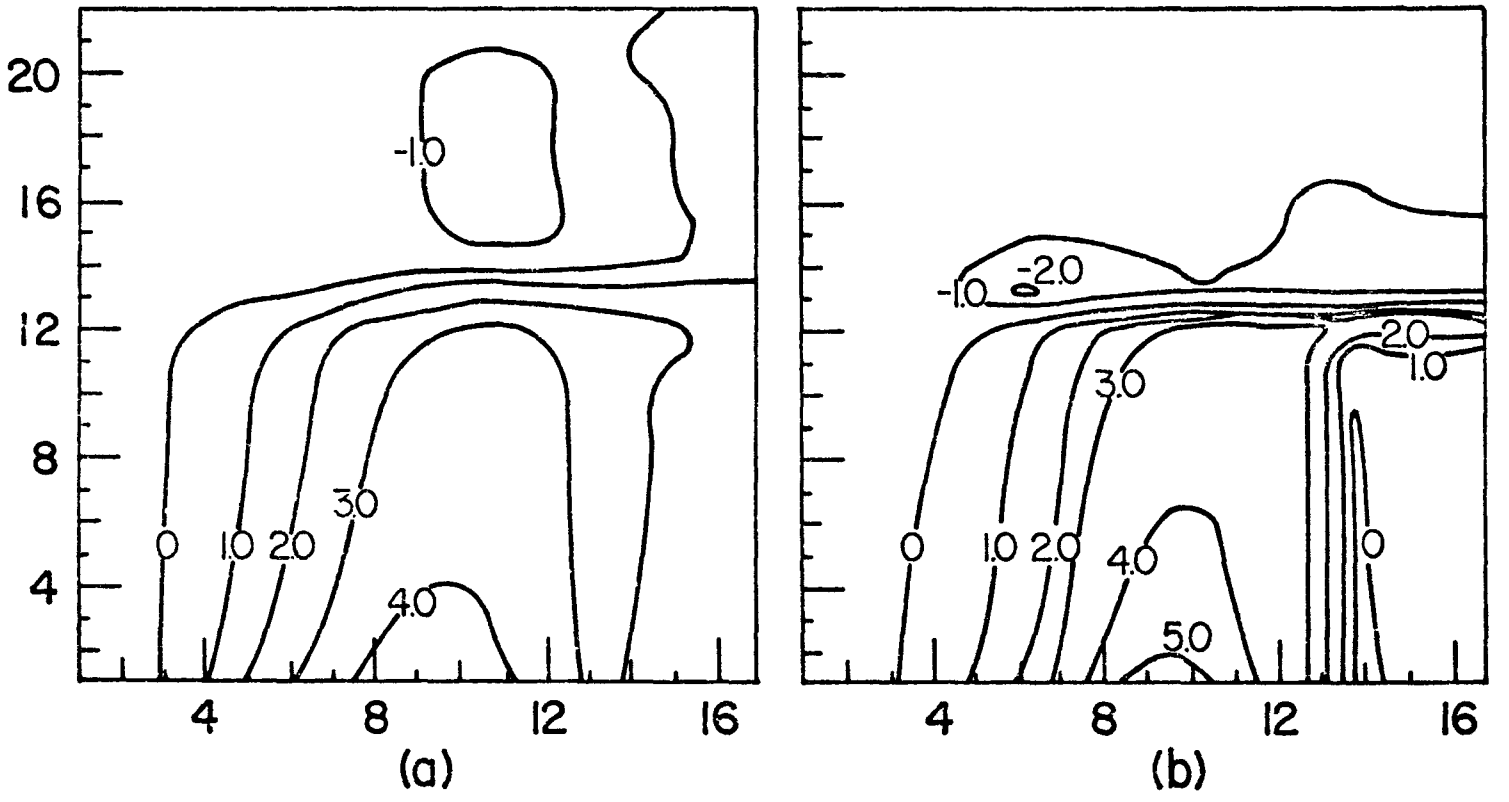

Figure 46. Isopleths of potential temperature perturbation in the urban atmosphere for simulation W6 at noon (a) and at midnight (b)

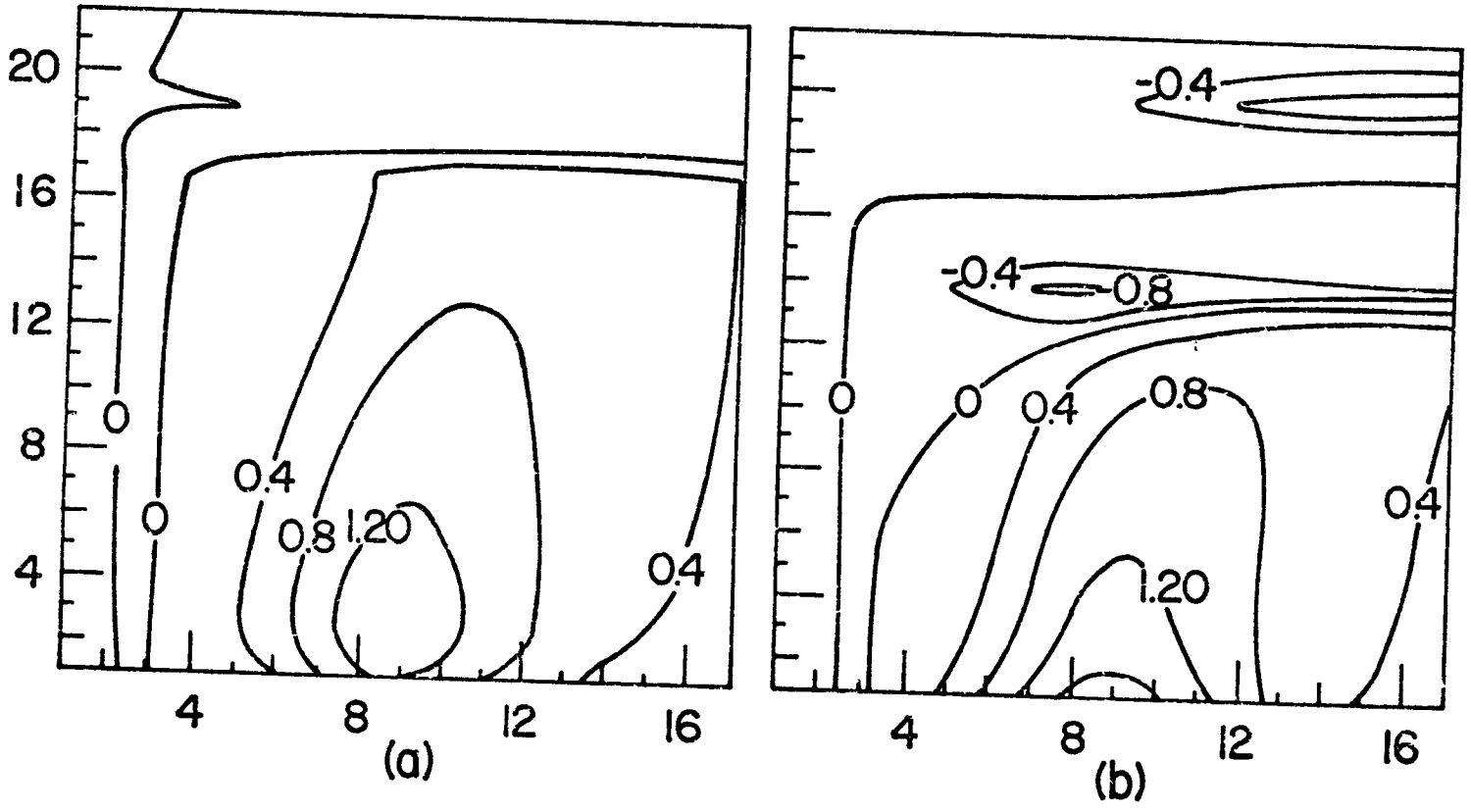

Figure 47. Isopleths of potential temperature perturbation in the urban atmosphere for simulation S1 at noon (a) and at midnight (b).

results reported by other investigators for different meteorological conditions (Garstang et al., 1975; Yu and Wagner, 1975).

Effect of Radiatively Active Pollutants on Temperature

The effects of the radiatively active pollutants on the temperature structure in the urban atmosphere are presented in Figures 48 and 49 as isopleths of the potential temperature difference $\Delta\theta$ (temperature for simulation with radiatively interacting pollutants minus temperature for simulation with noninteracting pollutants) for simulation W1 and W2, respectively, at both noon and midnight. The presence of active pollutants changes the radiative energy balance which alters the temperature structure. As expected, the effect is greater during the winter than during the summer. During the day, the potential air temperature near the surface is generally lower for simulations with radiatively participating pollutants than for the simulations with nonparticipating pollutants. The largest difference (less than 0.4 K) is downwind of the city center where the pollutant concentration is highest. The nighttime temperature differences are positive and somewhat higher in magnitude near the surface. Near the top of the PBL, the radiatively participating pollutants tend to decrease the potential temperatures slightly at both noon and midnight.

A small surface inversion upwind of the city was predicted by the model at night, but no surface inversion developed near the city center. This is in agreement with the observations of Clarke and McElroy (1974) in Columbus, Ohio and St. Louis, Missouri. The warmer near-surface temperatures in the city decrease the stability of the atmosphere and increase turbulent heat flux to the surface, see Table 4. The results clearly show that the pollutants have not only a direct influence on the temperature near the ground through the reduction of the infrared cooling rate, see Table 5, but also indirectly through the feedback between temperature, stability and turbulent heat transport to the surface. Near-surface temperatures at noon for

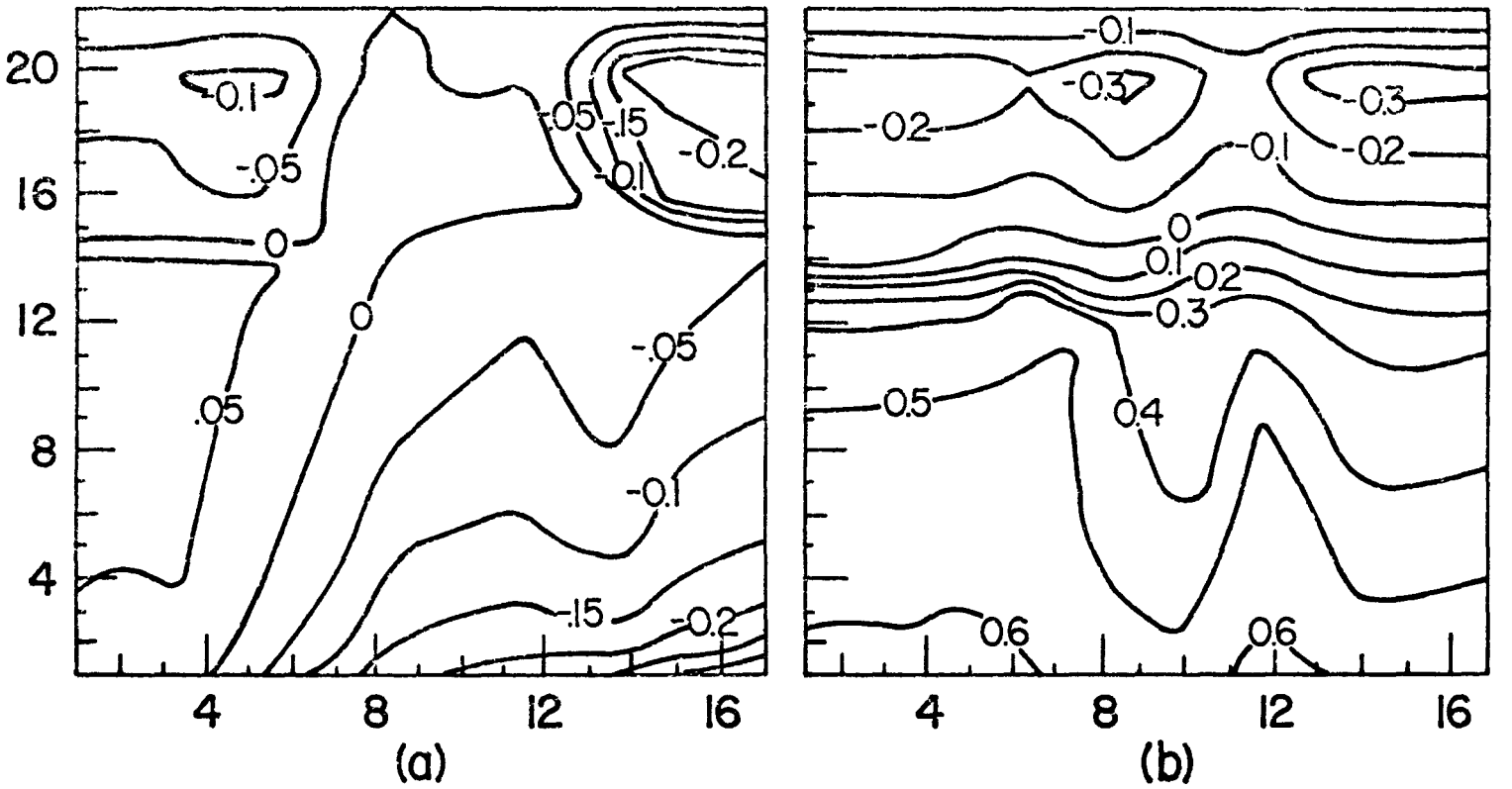

Figure 48. Isopleths of potential temperature difference in the urban atmosphere between simulations W2 and W1 at noon (a) and at midnight (b)

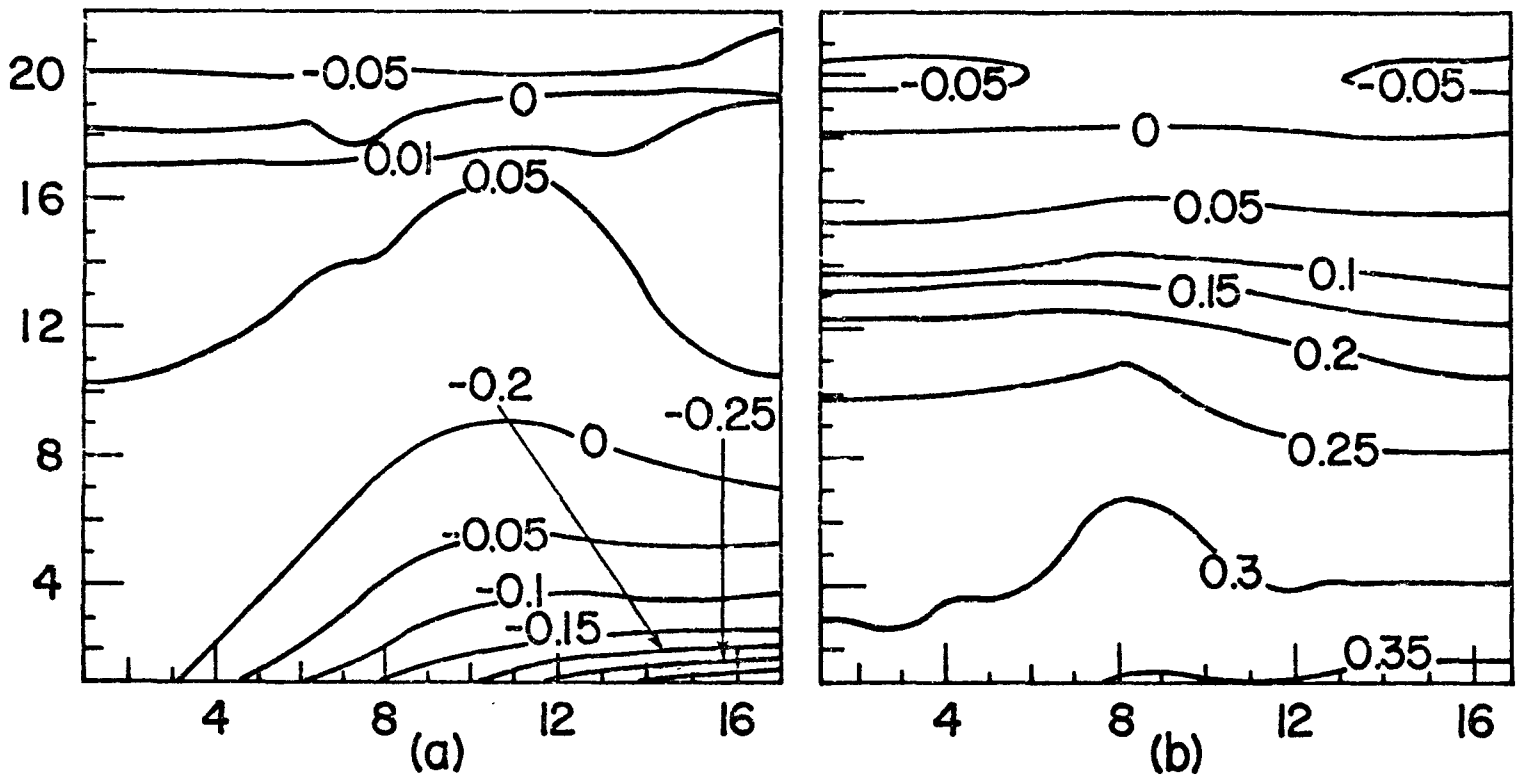

Figure 49. Isopleths of potential temperature difference in the urban atmosphere between simulations S2 and S1 at noon (a) and at midnight (b).

simulation W1 in and downwind of the city primarily because of the attenuation of solar radiation by the aerosols in the PBL.

The net effect of radiatively active pollutants on the temperature structure is more clearly illustrated in Figure 50 where the temperature differences between simulations W7 and W6 with snow covered ground are plotted. The temperature differences between these two simulations are rather significant. Clearly, the air pollutants increase the temperature in the surface region and decrease it slightly near the top of the PBL. The most dramatic increase in the temperature is at night downwind of the city where the gaseous pollutant concentrations are largest. Results presented in Figures 45 and 50 allow us to conclude that under certain meteorological conditions, surface and

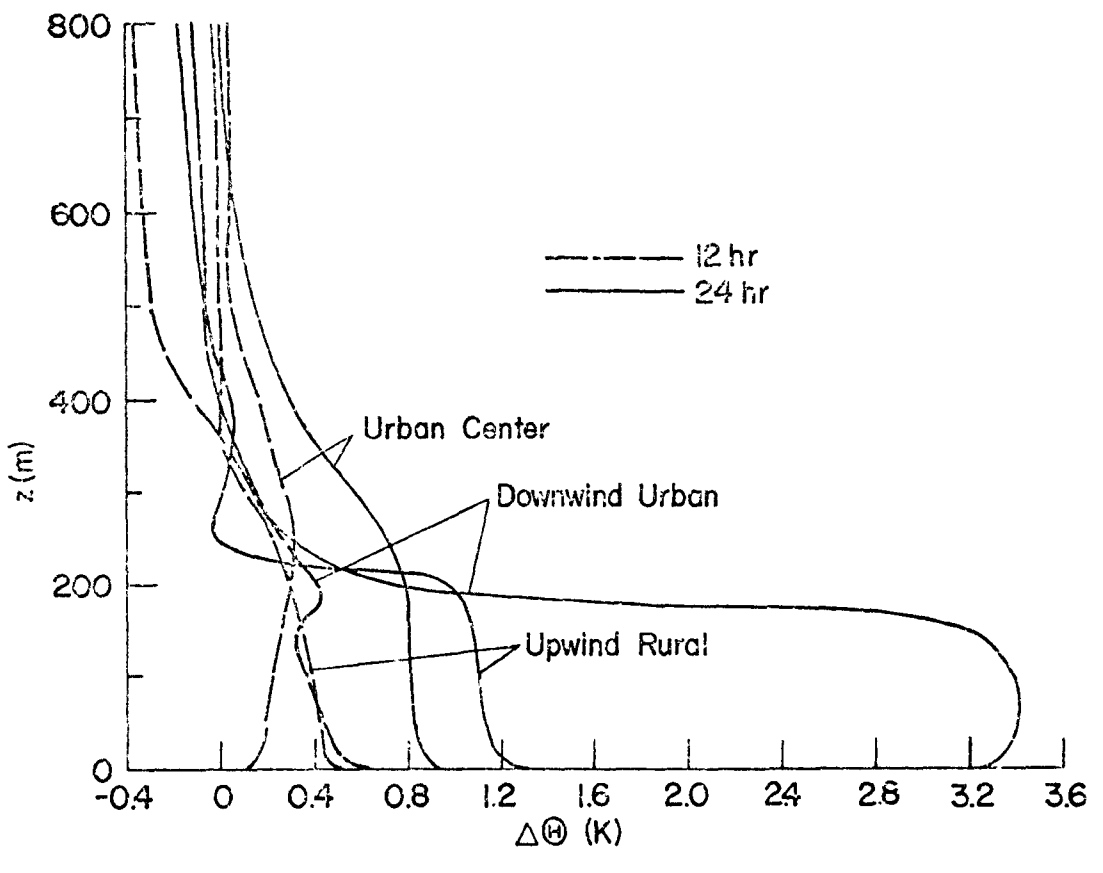

Figure 50. Potential temperature differences in the urban atmosphere between simulations W7 and W6 at the upwind rural, urban center and downwind urban locations.

urban parameters, the effects of radiatively active pollutants on the temperature structure near the surface may be of the same order of magnitude as effects of urbanization.

The Crossover Effect

The temperature crossover effect is associated with the existence of lower temperatures around 400 m over the city (Bornstein, 1968). Below 400 m city temperatures are generally higher than those over the countryside. Two physical mechanisms have been suggested to explain the potential temperature crossover effect. Lee and Olfe (1974) believe that the effect is caused by the lifting of stable air over the city. Lee and Olfe have conducted numerical experiments using a constant turbulent eddy diffusivity. They obtain crossover temperatures as great as 0.7 K. It should be noted that the results of Bornstein (1974), which are based on a more sophisticated numerical model, do not show the crossover effect. A second possible explanation is radiative cooling due to pollutants. However, the results of this study and those of Atwater (1975) and Venkatram and Viskanta (1976) indicate that the effect cannot be explained by radiative cooling due to the gaseous pollutants as nonparticipating simulations S1 and W1 both exhibit the crossover effect, see Figures 51 and 52. It appears that the prediction of the effect is dependent on the particular turbulence model used in the numerical calculations.

The diurnal variation of the vertical potential temperature perturbation θ' for simulation W1 and S1 are shown in Figures 51 and 52, respectively. The height at which the crossover occurs depends on the time during the diurnal cycle but is never lower than 200 m. The magnitude of the temperature deficit increases as the night progresses. The summer simulation S1 (Figure 52) does not exhibit formation of the temperature crossover during the day.

The effects of radiative participation on the daytime temperature crossover is shown in Fig. 53. Simulation W2 with

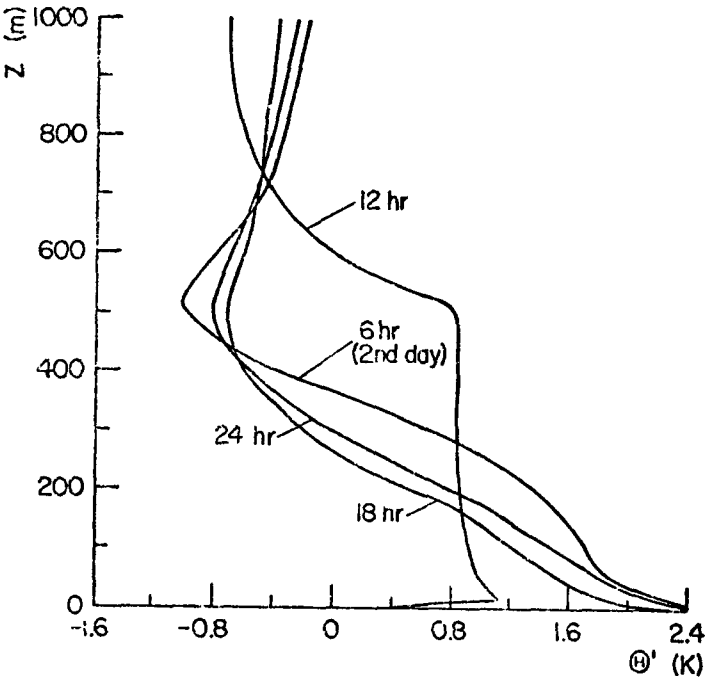

Figure 51. Potential temperature perturbation at the urban center for simulation W1.

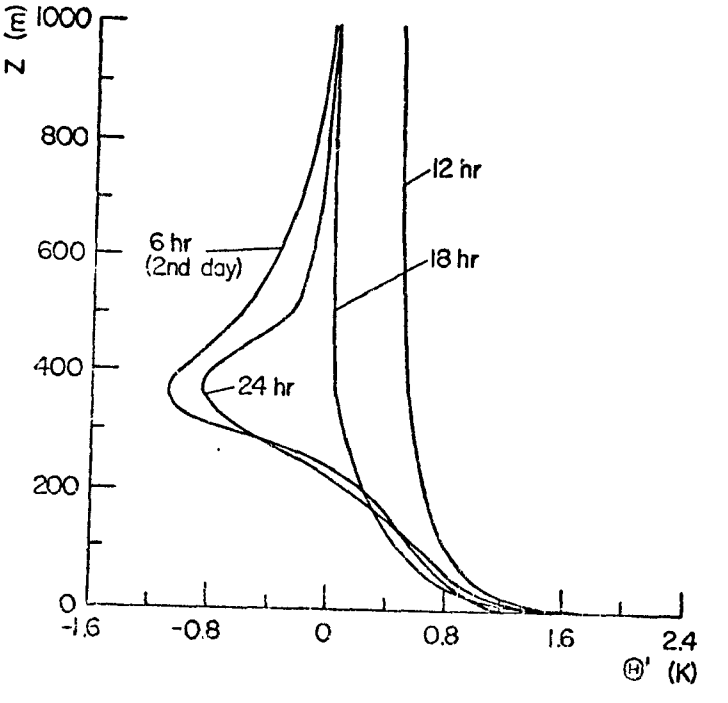

Figure 52. Potential temperature perturbation at the urban center for simulation S1.

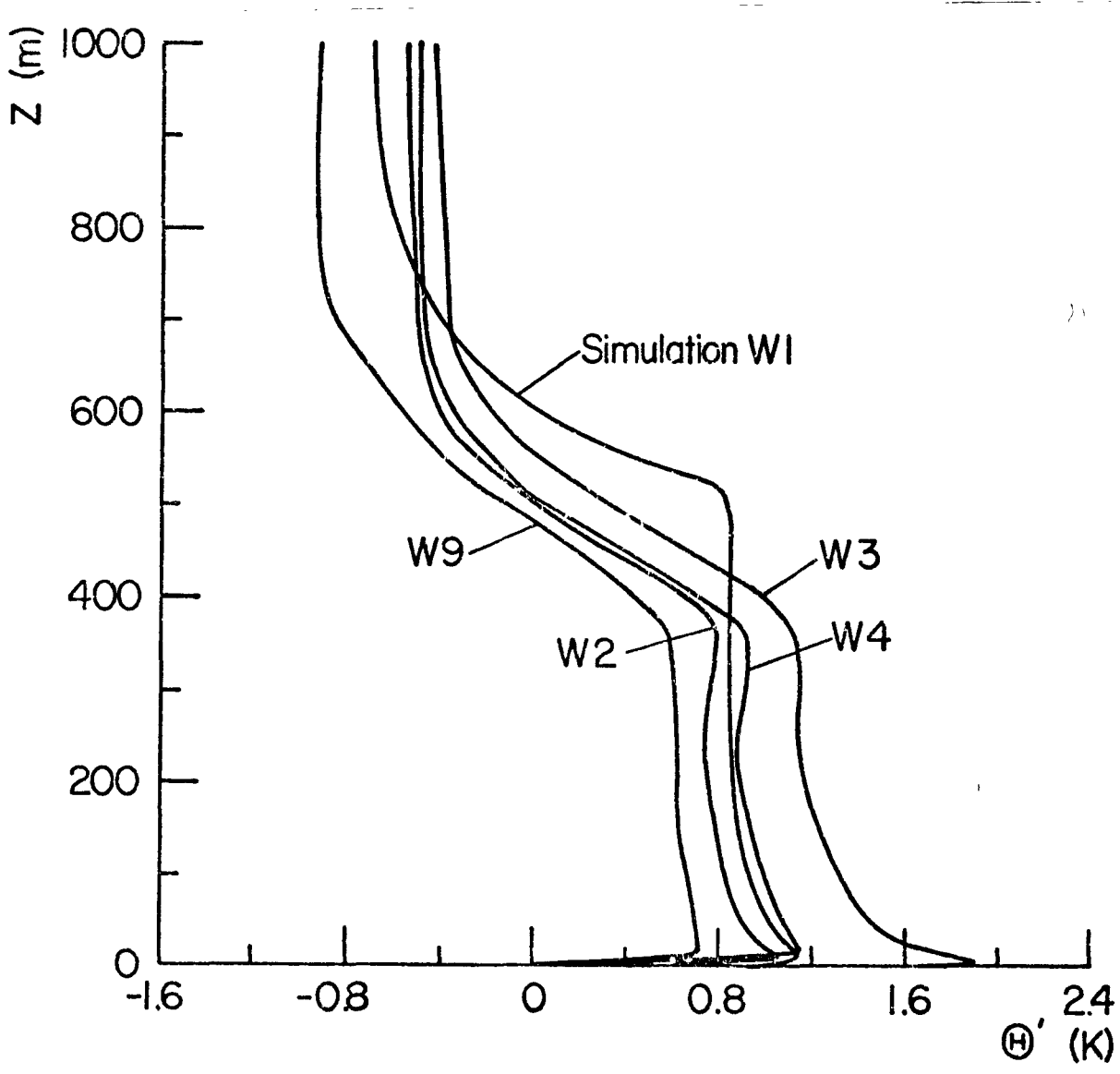

Figure 53. Comparison of potential temperature perturbations at the urban center for some winter simulations at the urban center.

radiatively participating pollutants shows a decrease in the crossover effect of approximately 0.2 K compared to simulation W1. Also note that the temperature deficit first occurs at about 500 m as compared to 600 m for nonparticipating simulation W1. The effect is due to lower surface temperature and turbulent diffusivity. At night the crossover effect is also reduced. This is caused by the altered temperature structure during the day. Increasing the anthropogenic heat emissions as in simulation W3 is seen to have an effect of less than 0.1 K when compared to simulation W2. The warmer surface temperature causes the decrease in the crossover effect. The effect of volumetrically distributing the anthropogenic heat (simulation W4) is seen to have an even smaller effect. At night, the effects are similarly small. Increasing the surface roughness from 1.0 m (simulation W2) to 2.0 m (simulation W9) is seen to have the greatest influence. The temperature deficit is partially due to the reduced surface temperature.

The maximum temperature crossover of about 1 K predicted in this study for the base simulations agrees fairly well with observations made by Clarke and McElroy (1974) over Columbus, Ohio and St. Louis, Missouri. The measurements were made in September and March and direct comparisons are not possible because of different meteorological conditions used in the numerical experiments. The observations are consistent with the predictions of this study.

POLLUTANT CONCENTRATIONS

Concentration Distributions

As indicated in Table 2 the initial aerosol and gaseous pollutant concentration distributions as well as the emissions were arbitrarily assumed to be the same in order to reduce the number of independent parameters. Therefore, the concentrations of the two pollutants are identical, and hence only the gaseous pollutant concentrations will be discussed. Isopleths of the

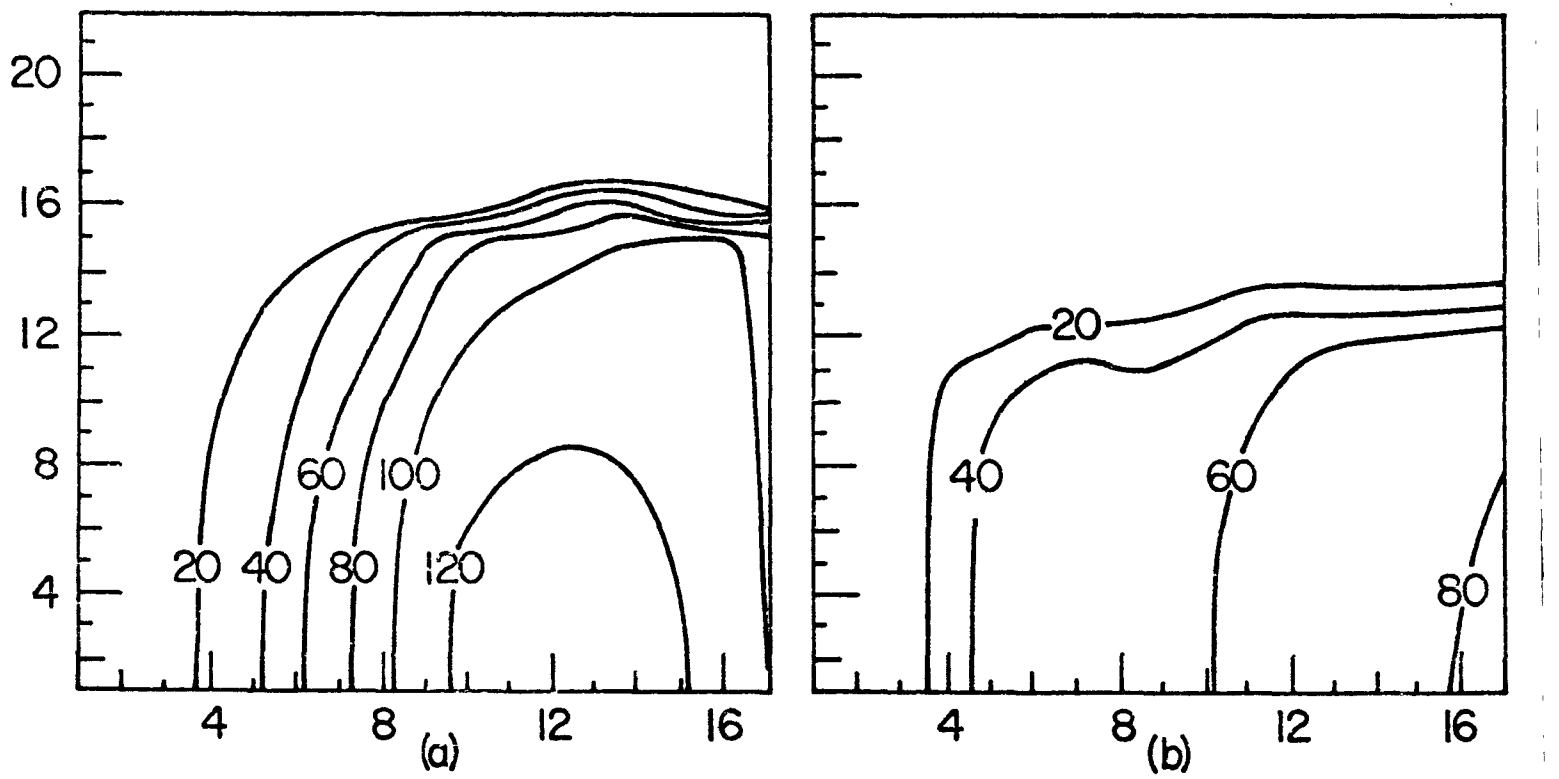

Figure 54. Isopleths of pollutant concentration perturbation in the urban atmosphere for simulation W1 at noon (a) and at midnight (b).

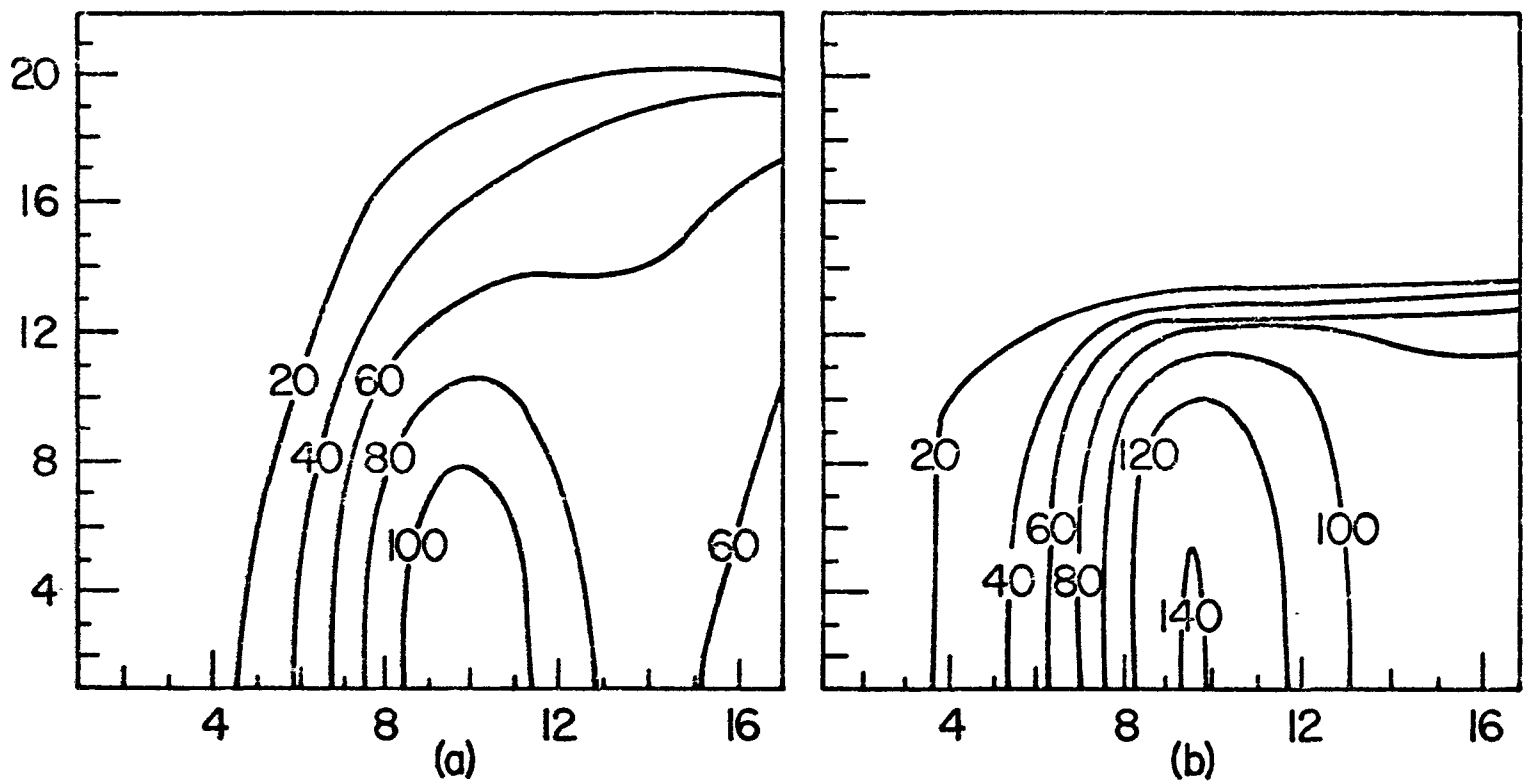

Figure 55. Isopleths of pollutant concentration perturbation in the urban atmosphere for simulation S1 at noon (a) and at midnight (b).

concentration perturbations are illustrated for the radiatively noninteracting simulations W1 and S1 in Figures 54 and 55, respectively. The left panel (part a) gives the concentration at noon and the right panel (part b) the concentration at midnight. The background pollutant concentration at the upwind countryside was assumed to decrease exponentially with height from 20 $\mu g/m^3$ at the surface to about 10 $\mu g/m^3$ at the top of the PBL.

Inspection of Figures 54 and 55 reveals a pollutant plume formation downwind of the urban center. This finding agrees with that of Atwater (1975) who also predicted higher concentrations downwind of the city center. The diurnal variation of the pollutant emissions and mixed layer height influence very strongly pollutant concentrations during the daily cycle. During the day the pollutants disperse more effectively throughout the PBL for the summer simulation S1 than for the winter simulation W1. This is due primarily to the fact that the mixed layer height is larger for S1 than W1. Even though the emission sources were assumed to be larger for S1 (see Table 2) the concentrations for W1 are higher due to more limited vertical mixing. During the night the mixed layer height decreases more drastically for simulation S1 than for W1. As a consequence the concentrations increase for S1 and decrease for W1 in comparison to those at noon. The decrease in mixed layer height and the decrease in pollutant releases in the evening, for example, have opposite effects on pollutant concentrations. Their net influence is to dampen the concentration variations during the diurnal cycle.

The pollutant concentration near the ground (say, at z = 2m) is important to human health and comfort. For this reason, the diurnal variation of pollutant concentrations along the city are given for simulations W1 and S1 in Figures 56 and 57, respectively, at a height of z = 2m. It is seen from the figures that the concentrations reach a maximum late in the afternoon when the emissions are still high (see Figure 2) and the turbulent eddy diffusivities have decreased to a minimum (see Figure 14). The collapse of the mixed layer at this time contributes also to

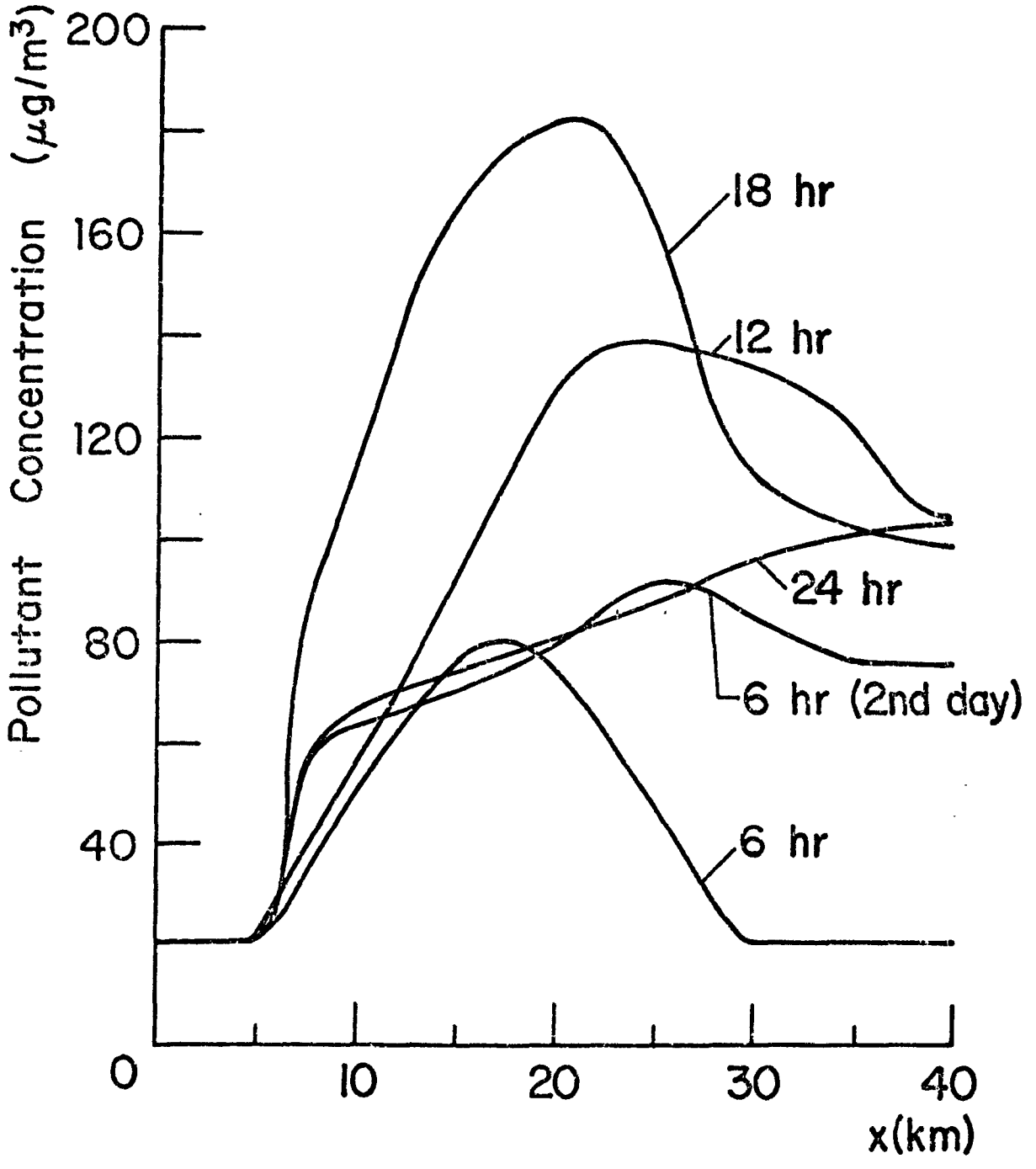

Figure 56. Pollutant concentration variation along the urban area during the diurnal cycle at a height of 2 m for simulation W1.

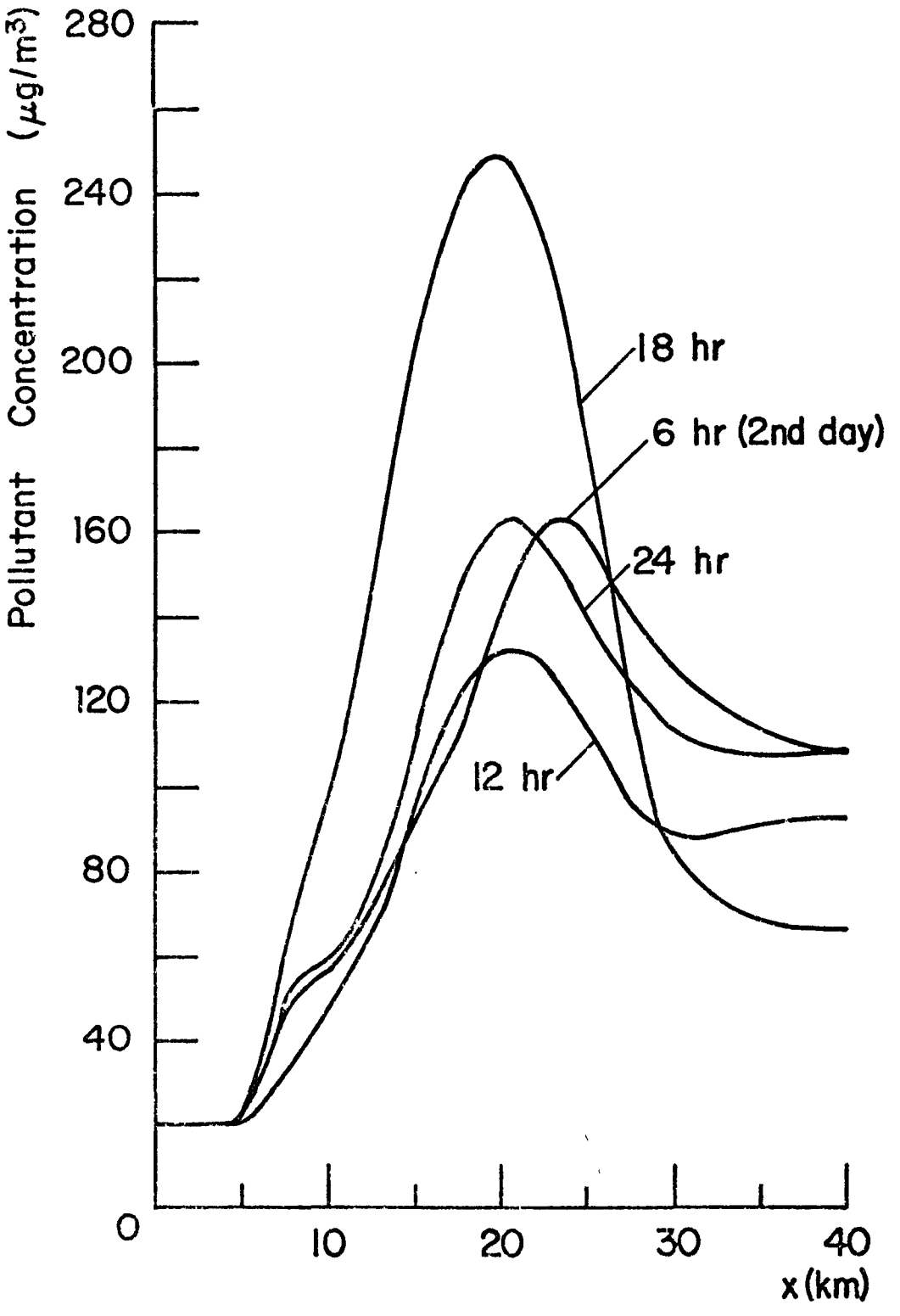

Figure 57. Pollutant concentration variation along the urban area during the diurnal cycle at a height of 2 m for simulation S1.

increased pollutant concentrations.

The two worst times for pollutant dispersion are early in the morning just after sunrise and before sunset. This is clearly seen from Figure 58 where the pollutant concentrations at a height of z = 2m are presented along the city as a function of time. The concentrations near the ground are most sensitive to the turbulent diffusivities at the first few grid points above the ground. The diurnal trends in pollutant concentrations can be explained on the basis of the diurnal variation of turbulent diffusivity near the surface. For example, as the stability of the atmosphere near the ground decreases the pollutants are dispersed more effectively by vertical mixing. The concentrations are seen to decrease and reach a minimum after noon. The trends predicted agree with observations. The worst times for dispersion are at night while the middle of the day is generally the best (Stern et al., 1972).

Concentration Differences

While the presence of radiatively interacting pollutants alters the radiant and total energy balances and therefore the temperature distribution directly, the pollutant concentration is only indirectly modified through the turbulent eddy diffusivity. By modifying the potential temperature and velocity (through the eddy diffusivity) gradients, radiatively active pollutants alter the eddy diffusivity, which in turn affects the pollutant concentrations. Thus, the effect of pollutants on their own dispersal is expected to be rather sensitive to the turbulence model used.

The effect of radiatively active pollutants on their own dispersion can be most clearly indicated by examining the differences between simulations with participating and nonparticipating pollutants. Such differences between simulations W2 and W1 and between simulations S2 and S1 are depicted in Figures 59 and 60, respectively. Examination of the figures reveals that the concentration differences are larger for the winter than for

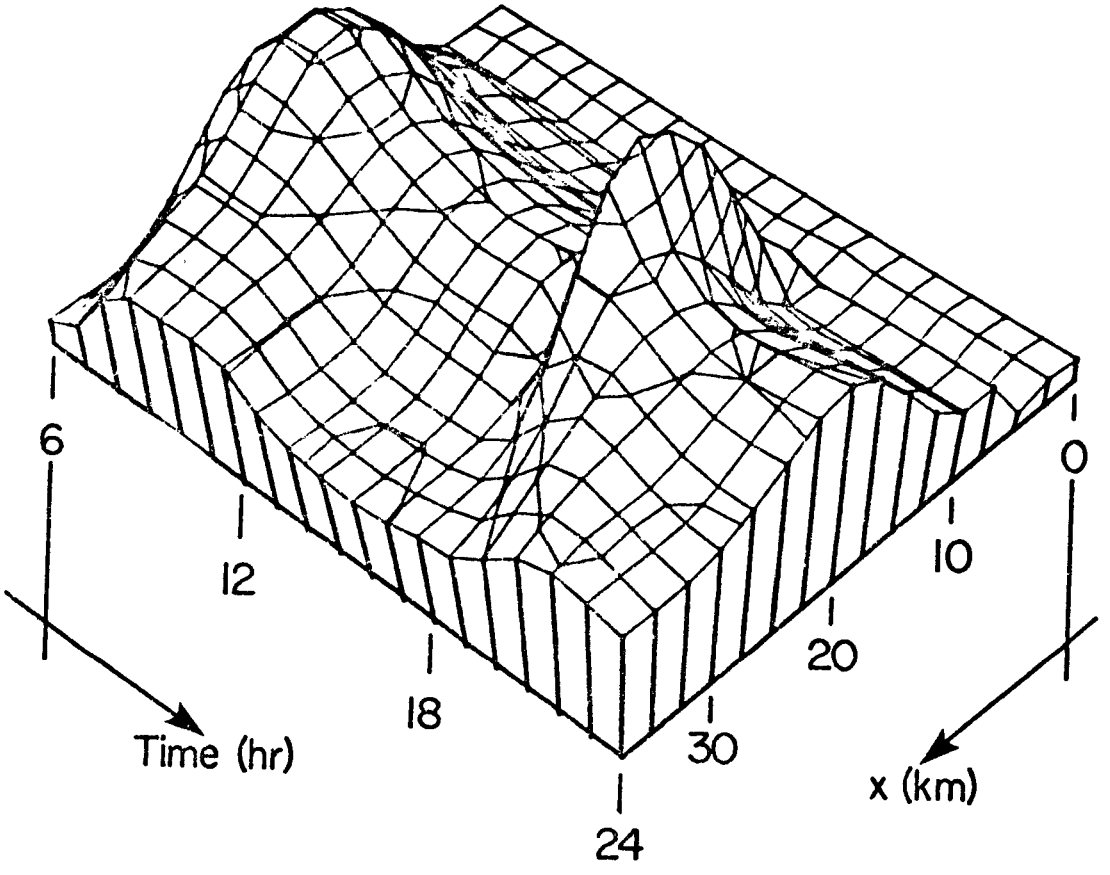

Figure 58. Three dimensional representation of pollutant concentration at a height of 2 m along the urban area with time for simulation S1.

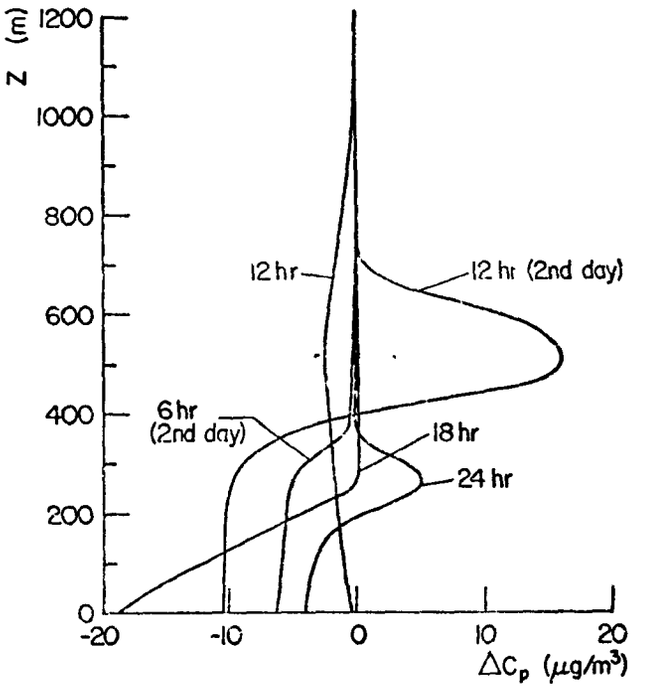

Figure 59. Pollutant concentration difference between simulation W2 and W1 at the urban center.

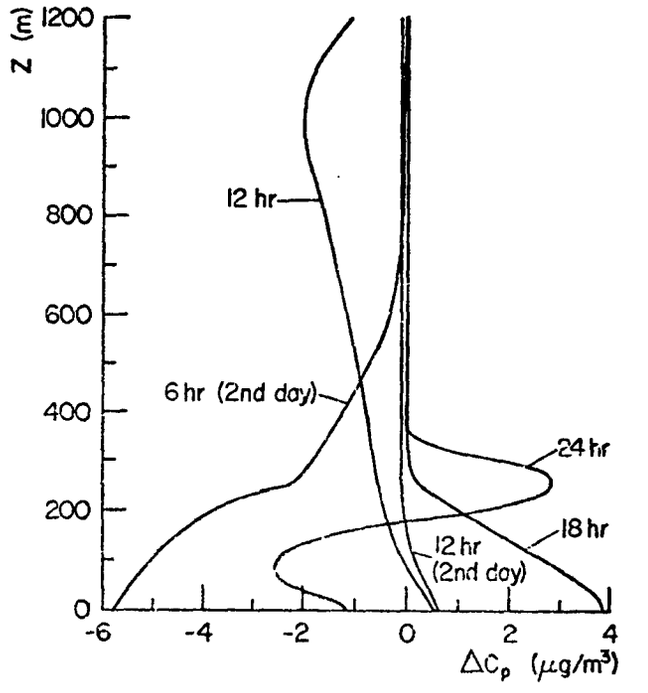

Figure 60. Pollutant concentration difference between simulation S2 and S1 at the urban center.

the summer simulations. This is not surprising and is due to the greater sensitivity of the temperature structure to the radiatively active pollutants in the PBL for the winter simulations. The temperature structure in turn modifies turbulent diffusivities and pollutant concentrations.

The sensitivity of the pollutant concentrations to the urban parameter changes is highlighted in Table 9. The results clearly show that radiatively active pollutants reduce significantly (about 15%) pollutant concentrations near the surface at the urban center for the winter simulations (e.g. W2-W1, W7-W6). The maximum percent reduction occurs in the evening at 18:00 hours. For the summer simulations (S2-S1) the modification of pollutant concentrations by the radiatively active pollutants is not as significant. Examination of Table 9a and 9b reveals that, in general, the decrease in pollutant concentration downwind of the city center is substantially greater than at the urban center. This is primarily due to greater turbulent diffusivities which result from decreased atmospheric stability caused by warmer ground temperatures (see Figure 37). The feedback between pollutant concentrations, temperature structure and pollutant dispersion is greatest downwind of the city where the concentrations are largest.

The increased anthropogenic heat emissions (W3-W2) are seen to decrease pollutant concentrations whereas decreased emissions (W8-W2, S4-S2) cause a very substantial increase in pollutant concentrations, particularly for the winter simulations when q_{an} represents a substantial contribution to the energy balance near the ground. Greater surface roughness height and associated cooler surface temperatures (simulations W9-W2) increase the pollutant concentrations near the ground both at the urban center and downwind of the city.

The results obtained cannot be compared directly with those reported earlier (Viskanta et al., 1977a) for different meteorological conditions with time independent pollutant emissions. The effects of anthropogenic heat releases on pollutant

TABLE 9. POLLUTANT CONCENTRATION DIFFERENCES (IN $\mu g/m^3$) AT THE HEIGHT OF 2 m

a) Urban Center, x = 17.5 km

Time (hr)	W2-W1	W7-W6	S2-S1	S8-S7	W3-W2	W8-W2	S4-S2	W9-W2
06	0	0	0	0	0	0	0	0
08	-6.2	-7.6	1.7	20.5	-34.0	77.8	9.7	3.6
10	-5.0	-21.6	0.5	1.6	-46.8	99.8	9.0	-4.2
12	-0.4	-22.7	0.5	0.4	-13.1	45.7	2.3	11.6
14	0.3	-6.8	0.2	0.8	-8.1	9.0	2.0	1.3
16	-1.6	-7.9	1.5	1.5	-8.5	73.8	3.4	3.5
18	-18.7	-15.8	3.8	0.6	-17.5	129.5	3.7	25.6
20	-8.1	-13.9	1.7	1.6	-22.3	84.8	10.0	5.2
22	-5.3	-9.4	0.8	1.6	-17.5	49.9	4.3	1.1
24	-3.9	-10.4	-1.2	0.2	-12.8	37.6	4.7	-1.4
02	-7.1	-9.7	-11.7	-14.9	-19.8	36.7	26.9	0.2
04	-5.2	-6.1	-7.6	-7.9	-9.2	38.0	38.5	2.2
06	-6.2	-7.1	-5.7	-6.3	-6.1	42.3	52.4	5.0
08	-7.1	-27.7	-2.9					
10	-7.2	-39.1	-6.6					
12	-14.8	-10.8	-0.6					

b) Downwind Urban, x = 30 km

Time (hr)	W2-W1	W7-W6	S2-S1	S8-S7	W3-W2	W8-W2	S4-S2	W9-W2
06	0	0	0	0	0	0	0	0
08	-0.4	-0.6	-8.5	0.6	-2.4	-0.7	2.5	-2.5
10	-4.7	-1.9	0.6	1.6	-17.5	13.9	5.1	-2.7
12	-4.2	-14.8	-1.3	-0.6	-35.9	46.4	5.0	8.1
14	-0.8	-34.4	-0.1	0.1	-10.4	45.7	0.7	19.8
16	0.7	-42.7	1.4	0.6	-7.4	14.6	0.3	7.5
18	-1.5	-48.8	2.8	3.1	-14.8	28.9	5.4	9.0
20	-8.2	-52.5	3.0	3.6	-41.3	39.5	10.4	10.6
22	-22.5	-58.8	1.8	2.5	-53.0	45.2	12.1	26.6
24	-16.4	-48.3	0.5	0.8	-31.7	33.0	5.8	23.3
02	-6.5	-44.7	0.6	0.6	-21.3	18.9	2.0	14.7
04	-5.6	-40.5	1.0	1.2	-14.1	14.8	-0.7	10.5
06	-6.9	-42.5	-0.1	0.6	-12.4	14.5	-1.8	9.6
08	-7.1	-32.8	-1.8					
10	-6.5	-27.3	-15.4					
12	-9.0	-29.5	-2.0					

concentrations, however, agree in trend with those found in the present numerical experiments. Atwater (1975) predicted an increase in the daytime pollutant concentrations of about 20% near the surface due to the radiative active pollutants in the PBL. Our results do not show such large changes probably because the pollutant concentrations were considerably smaller as compared to those used by Atwater.

URBAN HEAT ISLAND

One of the better known features of urban climatology is the existence of the urban heat island. The heat island intensity (the maximum difference between the upwind rural and the highest urban surface temperature, $\Delta T_{u-r,max}$) is shown as a function of time for some representative numerical simulations in Figures 61 and 62. Results of numerical modeling efforts (Myrup, 1969; Atwater, 1972; McElroy, 1973; Yu and Wagner, 1975; Torrance and Shum, 1976) show that the urban heat island is caused primarily by the surface parameters and anthropogenic heat release differences between urban and rural areas. Comparison of $\Delta T_{u-r,max}$ values for simulations W2 and W1 shows that the radiatively interacting pollutants decrease the urban heat island intensity. For example, just before sunrise the intensity is 3.59 K for simulation W1 while it is 3.38 K for simulation W2. In the simulation with radiatively participating pollutants the presence of background pollutants increased the downward thermal flux incident upon the surface, see Figure 14. This causes slightly higher surface temperatures at the upwind rural area. Background pollutants were introduced in the upwind rural area as the atmosphere is not free of pollutants a few kilometers upwind or downwind of the city. Note that for the summer simulations (Figure 62) the peak intensity occurs at sunset, and then decreases during the night. Similar behavior has been observed for Johannesburg, South Africa (Garstang et al., 1975) during July, 1971. This behavior is markedly different than that for the winter simulations and is due to the different mechanisms causing the

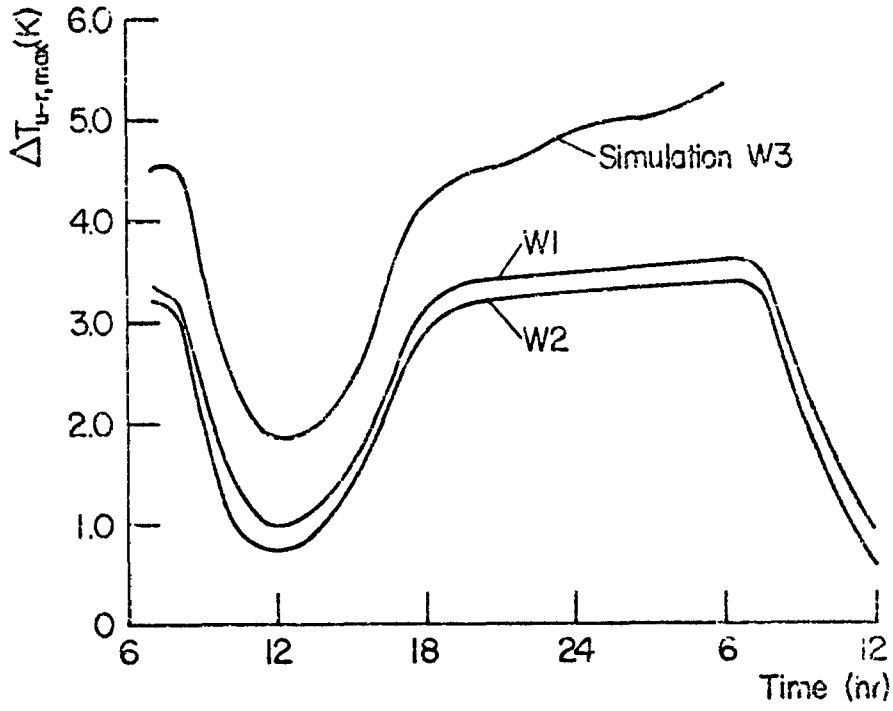

Figure 61. Maximum urban minus upwind rural surface temperature difference variation with time for some winter simulations.

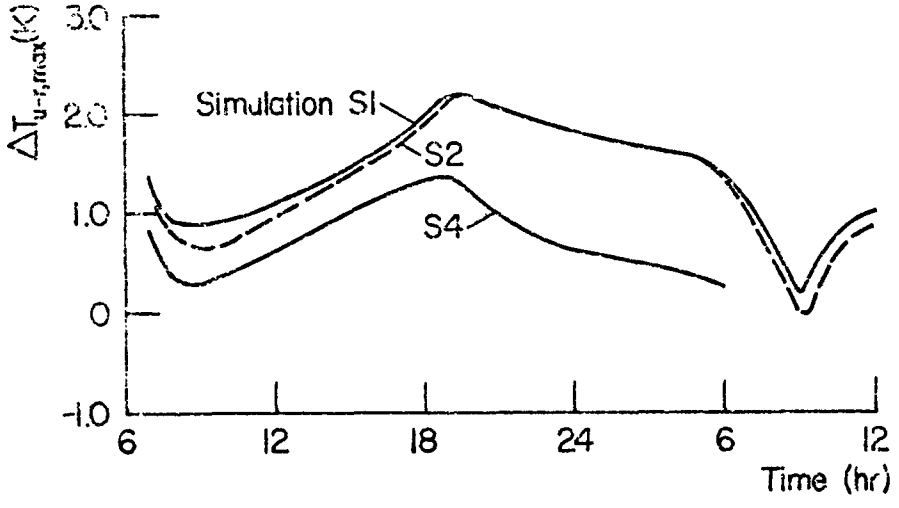

Figure 62. Maximum urban minus upwind rural surface temperature differences for some summer simulations.

heat island. In the summer during the day, the city absorbs and stores more solar energy than the surrounding countryside. This happens because the city itself possesses a higher thermal admittance than the vegetation and soil characteristic of the surrounding countryside. This stored energy causes the temperature in the city to decrease more slowly than in the rural area toward sunset. At night, the temperature difference decreases as the city cools by emission of thermal radiation. In the winter, the insolation is considerably smaller. Hence, man-made heat emission becomes a more significant factor in the formation of the urban heat island during the winter. As these emissions are assumed constant throughout the night, the heat island remains relatively constant.

The urban heat island intensity depends on the extent of urbanization and is seen from Figures 61 and 62 to be a positive temperature anomaly. The magnitude of the effect depends on meteorological conditions and is partly caused by changes in the responses of the earth's surface to solar and thermal radiation, the storage of sensible heat, moisture transfer and anthropogenic heat releases. The effect therefore exhibits considerable diurnal variation as indicated in the figures. Because of the greater admittance of the surface materials in the city than in the surroundings, the temperature anomaly may be negative after sunrise, but it will be warmer in the evening and at night. If the moisture availability parameter is relatively large, $\Delta T_{u-r,max}$ may be negative (Venkatram and Viskanta, 1976). The sensitivity of the urban heat island to different mechanisms which contribute to its formation by making reference to Table 10.

Comparing values of $\Delta T_{u-r,max}$ for simulation W2 (with q_{an} = 50 W/m^2 as an average emission in the city) to simulation W3 (with q_{an} = 100 W/m^2) shows the importance of anthropogenic heat releases in the city. A more dramatic comparison is between simulation W2 and W8 for which q_{an} = 0. For simulations W5,

W6 and W7 with snow covered ground, the urban heat island intensities are considerably higher than those with bare ground. The reason is the heat island intensity continues to increase throughout the simulation period. This is felt to be due to the initial conditions as the rural temperature continues to fall throughout the cycle. The heat island intensity predicted is not unrealistically high, however, since values of this magnitude have been observed (DeMarrais, 1975). Again, results of simulations W7 and W6 show that the radiatively active pollutants decrease the magnitude of $\Delta T_{u-r,max}$. For all simulations except simulation W4, the anthropogenic heat is assumed to be emitted into the atmosphere within the first two meters of the surface. This approach is oversimplified, as in reality most of this heat is released into the atmosphere through chimneys and through the sides of buildings. Comparison of results presented in Table 10 shows the effect of distibuting q_{an} through the lower 50 or so meters of atmosphere. A relatively small difference in the heat island intensity (less than 0.5 K at any time) is noted when the results of simulation W4 are compared with those of W2. Other urban PBL models (Yu and Wagner, 1975; Atwater, 1975) have assumed the

TABLE 10. DIURNAL VARIATION OF THE URBAN HEAT ISLAND INTENSITY (IN K)

Time (hr)	W1	W2	W3	W4	W6	W7	W8	W9	S1	S2	S4	S5	S6	S7	S8
06	0	0	0	0	0	0	0	0	0	0	0	0	0	0	0
08	3.2	3.1	4.5	2.8	3.9	3.8	1.2	2.8	0.9	0.8	0.3	1.1	2.0	0.7	0.5
10	1.6	1.4	2.8	1.3	4.5	4.2	0.4	0.8	0.9	0.7	0.4	1.2	2.3	0.5	0.3
12	1.0	0.7	1.9	0.6	4.6	4.4	0.0	0.2	1.2	1.0	0.7	1.6	4.6	0.8	0.6
14	1.2	1.1	2.1	0.9	4.6	4.2	.0	0.3	1.4	1.2	0.9	1.8	5.7	1.1	1.0
16	2.0	1.9	3.0	1.9	4.4	4.1	0.7	1.5	1.6	1.5	1.1	1.8	3.7	1.4	1.3
18	3.1	2.9	4.1	2.8	4.2	3.9	0.9	2.8	1.9	1.8	1.3	2.0	3.4	1.8	1.7
20	3.4	3.1	4.4	3.2	4.5	4.2	0.9	3.1	2.1	2.1	1.1	2.2	3.8	2.1	2.1
22	3.4	3.1	4.7	3.3	4.8	4.5	0.8	3.1	2.0	2.0	0.9	2.0	3.3	1.9	1.9
24	3.4	3.3	4.8	3.3	5.7	4.8	0.7	3.2	1.8	1.8	0.7	1.9	3.0	1.8	1.8
02	3.5	3.3	5.0	3.4	5.7	5.2	0.7	3.2	1.7	1.7	0.5	1.8	2.6	1.6	1.6
04	3.6	3.3	5.1	3.4		5.9	5.5	0.7	1.6	1.6	0.4	1.6	2.3	1.5	1.5
06	3.6	3.4	5.3	3.6		6.1	5.7	0.7	1.4	1.4	0.2	1.5	1.9	1.3	1.3
08	3.3	3.1		3.5		6.2	5.8		0.8	0.6					
10	1.9	1.6		1.9		6.5	6.0		0.6	0.3					
12	0.9	0.6		0.6		6.7	6.0		1.0	0.8					

anthropogenic heat sources to enter the surface energy balance.

Even when the anthropogenic heat emissions are neglected (simulation S4) a heat island is formed due to the urban-rural parameter differences discussed above. The anthropogenic heat emissions assumed for simulation S1 increase the heat island intensity, but the importance of the heat releases is less than that for the winter simulations. Note that simulation S2 slightly negative heat island intensity is predicted in the morning of the second day. This phenomenon has been observed during the summer (Mitchell, 1961).

The effect of the surface roughness on the heat island intensity can be determined by comparing the results of simulation W2 with those of simulation W9. Increasing the surface roughness from 1 m to 2 m at the urban center decreases the urban heat island intensity by a maximum of about 0.5 K at noon. In general, the winter simulations have their minimum heat island intensity around noon. There is a rapid increase in heat island intensity toward evening, then a small increase during the night. A maximum is reached just before sunrise, with the heat island decreasing rapidly thereafter. This variation in heat island intensity is consistent with experimental observations of Oke and Maxwell (1974) over Montreal and Vancouver, Canada.

Results show (compare $\Delta T_{u-r,max}$ for simulations S2 and S6) that the magnitude of the heat island intensity is quite sensitive to the decrease in the moisture availability parameter M in the city, particularly during the noon hours. It is seen that the reduced evaporation in the urban area leads to a heat island intensity of 5.72 K. It is noted that this temperature excess occurs in the early afternoon rather than after sunset. Although this situation has not been observed, it has been predicted theoretically (Myrup, 1969).

The solar albedo is also seen to have an effect on the heat island intensity during the day. An increase in the urban-rural albedo difference (simulation S5, see Table 10 for values)

causes an increase in heat island intensity. A decrease in the urban-rural albedo difference (simulations S7 and S8) is seen to have the opposite effect.

The urban heat island is just one measure of the inadvertent climate and weather modification. The intensities predicted are of sufficient magnitude to be of social and economic significance. The results obtained indicate that urbanization together with anthropogenic heat and pollutant emissions into the atmosphere may affect energy demand for space heating and cooling. The practical implications do not appear to have been considered previously. There may be a saving in the energy demand for heating if the heat island intensity is sufficienty large (a few degrees Kelvin as for some simulations predicted) during the winter, but this benefit would be nullified in summer if energy demand for space cooling is increased. The net effect of pollutants on the energy demand for space heating and cooling in an urban area during a diurnal or a yearly cycle are by no means clear, and a more complete investigation appears to be warranted. There are also secondary effects and impacts of the urban heat island. For example, one would mention lower costs for snow removal and increased human mobility during winter months in urban areas.

REFERENCES

Abrams, C. The Uses of Land in Cities. Cities, A Scientific American Book. Alfred A. Knopf, New York, 1966, 122-132.

Ackerman, T. P., K. N. Liou, and C. B. Levoy. Infrared Radiative Transfer in Polluted Atmospheres. J. Appl. Meteor. 15: 28-35, 1976.

Atwater, M. A. Radiation Budget for Polluted Layers of the Urban Environment. J. Appl. Meteor. 10: 205-214, 1971a.

Atwater, M. A. Radiative Effects of Pollutants in the Atmospheric Boundary Layer. J. Atm. Sci. 28: 1367-1373, 1971b.

Atwater, M. A. Thermal Effects of Urbanization and Industrialization: A Numerical Study. Boundary-Layer Meteor. 3: 229-245, 1972.

Atwater, M. A. Thermal Changes Induced by Pollutants for Different Climatic Regions. Symposium on Atmospheric Diffusion and Air Pollution, American Meteorological Society, Boston, 1974, pp. 147-150.

Atwater, M. A. Thermal Changes Induced by Urbanization and Pollutants. J. Appl. Meteor. 14: 1061-1071, 1975.

Atwater, M. A. Urbanization and Pollutant Effects on the Thermal Structure in Four Climatic Regions. J. Appl. Meteor. 16: 888-895, 1977.

Avaste, O. A., and G. M. Vainikko. A Method of Calculating Radiative Transfer in Broken Clouds. In: Proceedings of the Symposium on Radiation in the Atmosphere, H. J. Bolle, ed., Science Press, Princeton, N. J., 1977, pp. 220-224.

Bakan, S., and H. Quenzel. Path Length Distributions of Photons Scattered in Turbid Atmospheres. Cont. Atmosph. Phys. 49: 272-284, 1976.

Bartholomew, H. Land Uses in American Cities. Harvard University Press, Cambridge, MA, 1955. 166 pp.

Bergstrom, R. W. Predictions of the Spectral Absorption and Extinction Coefficients of an Urban Air Pollution Aerosol Model. Atmos. Envir. 6: 247-258, 1972.

Bergstrom, R. W., and R. Viskanta. Prediction of the Solar Radiant Flux and Heating Rates in a Polluted Atmosphere. Tellus 25: 486-498, 1973a.

Bergstrom, R. W., and R. Viskanta. Modeling of the Effects of Gaseous and Particulate Pollutants in the Urban Atmosphere. Part I: Thermal Structure. J. Appl. Meteor. 12: 901-912, 1973b.

Bergstrom, R. W., and R. Viskanta. Modeling of the Effects of Gaseous and Particulate Pollutants in the Urban Atmosphere. J. Appl. Meteor. 12: 913-918, 1973c.

Bergstrom, R. W., and R. Viskanta. Spherical Harmonics Approximation for Radiative Transfer in Polluted Atmospheres. In: Thermophysics and Spacecraft Thermal Control, R. G. Hering, ed., MIT Press, Cambridge, MA, 1974. pp. 23-40.

Bergstrom, R. W., and J. T. Peterson. Comparison of Predicted and Observed Solar Radiation in an Urban Area. J. Appl. Meteor. 16: 1107-1116, 1977.

Bhardwaja, P. S., J. Herbert, and R. J. Charlson. Refractive Index of Atmospheric Particulate Matter: An in Situ Method for Determination. Appl. Opt. 13: 731-734, 1974.

Blackadaar, A. K. The Vertical Distribution of Wind and Turbulent Exchange in a Neutral Atmosphere. J. Geophys. Res. 67: 3095-3102, 1962.

Bornstein, R. D. Observations of the Urban Heat Island Effect in New York City. J. Appl. Meteor. 7: 575-582, 1968.

Bornstein, R. D. The Two-Dimensional URMBET Urban Boundary Layer Model. J. Appl. Meteor. 14 : 1459-1477, 1975.

Businger, J. A. Turbulent Transfer in the Atmospheric Surface Layer. Workshop in Micrometeorology, D. A. Haugen, ed. American Meteorological Society, Boston, 1972, pp. 67-100.

Butcher, S. S., and R. J. Charlson. An Introduction to Air Chemistry. Academic Press, New York, 1972. 241 pp.

Chandrasekhar, S. Radiative Transfer. Dover Publications, New York, 1960. 393 pp.

Charlson, R. J., A. H. Vanderpol, D. S. Covert, A. P. Waggoner,

and N. C. Alquist. H_2SO_4 $(NH_4)_2$ SO_4 Background Aerosol: Optical Detection in the St. Louis Region. Science 184: 156-158, 1974.

Clarke, J. F., and J. L. McElroy. Effects of Ambient Meteorology and Urban Meteorological Features on the Vertical Temperature over Cities. Air Pollution Control Association Annual Meeting Paper No. 74-73, 1974.

Clarke, R. H., A. J. Dyer, R. R. Book, D. G. Reid, and A. J. Troup. "The Wangara Experiment: Boundary Layer Data". CSIRO Division of Meteorological Physics Technical Report No. 19, 1971.

Clawson, M. America's Land and Its Use. The Johns Hopkins University Press, Baltimore, 1972. 166 pp.

Coulson, K. L., and R. S. Fraser. Radiation in the Atmosphere. Rev. Geophys. Space Phys. 13: 732-737, 1975.

Dabbert, J. W., and P. A. Davis. Determination of Enegetic Characteristics of Urban-Rural Surfaces in the Greater St. Louis Area. EPA-650/4-74-007, U. S. Environmental Protection Agency, Research Triangle Park, NC, 1974. 105 pp.

Davis, R., and J. A. Weinman. Results from Two Models of the Three Dimensional Transfer of Solar Radiation in Finite Clouds. In: Proceedings of the Symposium on Radiation in the Atmosphere, H. J. Bolle, ed., Science Press, Princeton, NJ, 1977, pp. 225-227.

DeMarrais, G. A. Nocturnal Heat Island Intensities and Relevance to Forecasts of Mixing Heights. Monthly Weather Review 104: 235-245, 1975.

Dzubay, T., and R. K. Stevens. Ambient Air Analysis with Dichotomous Sampler and x-ray Fluorescence Spectrometer. Env. Sci. and Tech. 9: 663-668, 1975.

Eagleson, P. S. Dynamic Hydrology. McGraw-Hill, New York, 1978. 462 pp.

Estoque, M. A., and C. M. Bhumralkar. A Method for Solving the Planetary Boundary Layer Equations. Boundary-Layer Meterol. 1: 169-194, 1969.

Fischer, K. Bestimmung der Absorption von Sichtbarer Strahlung durch Aerosolpartikeln. Cont. Atm. Phys. 43: 244-254, 1970.

Fischer, K. Mass Absorption Coefficients of Natural Aerosol

Particles in the 0.4 μm - 2.4 μm Wavelength Interval. Beitr. Phys. Atm. 46: 89-100, 1973.

Garstang, M., P. D. Tyson, and G. D. Emitt. The Structure of Heat Islands. Rev. Geophys. Space Phys. 13: 139-165, 1975.

Gertis, K., and U. Wolfseher. Veränderung des termischen Mikroklimas durch Bebaung. Gesundheits-Inegenieur 90: 1-10, 1977.

Goody, R. M. Atmospheric Radiation. Oxford University Press, Oxford, 1964. 436 pp.

Gutman, D. P., and K. E. Torrance. Response of the Urban Boundary Layer to Heat Addition and Surface Roughness. Boundary-Layer Meteorology 9: 217-233, 1975.

Halstead, R. H., R. L. Richman, M. Covery, and J. D. Merryman. Preliminary Design of a Computer for Micrometeorology. J. Meteor. 14: 308-325, 1957.

Hänel, G. The Real Part of the Mean Complex Refractive Index and the Mean Density of Samples of Atmospheric Aerosol Particles. Tellus 20: 371-379, 1968.

Irving, J., and N. Mullineux. Mathematics in Physics and Engieering. Academic Press, New York, 1959. 883 pp.

Kaimal, J. C., D. A. Haugen, J. C. Readings, and R. Rayment. A Comparison of Balloon-Borne and Tower-Mounted Instrumentation for Probing the Atmospheric Boundary Layer. J. Appl. Meteor. 14: 540-545, 1975.

Kondratyev, K. Ya. Radiation in the Atmosphere. Oxford University Press, Oxford, 1969. 436 pp.

Kondratyev, K. Ya. A Complete Atmospheric Energetics Experiment. Global Research Programme (GARP, GARP Publication Series No. 12, ICSU-WMU, Geneva, 1973.

Kondratyev, K. Ya. Meteorology and Climatology. Vinitin, Moskva, Volume IV, 1977. 202 pp. (in Russian).

Kuhn, P. M. Radiosonde Observations of Infrared Flux Emissivity of Water Vapor. J. Appl. Meteor. 2: 368-378, 1963.

Kunkel, B., F. Wolz, H. J. Bolle, and E. Redemann. Air Quality Measurements from Space Platforms. European Space Agency Report No. ESA CR-577, 1975. 290 pp.

Landsberg, H. Inadvertent Atmospheric Modification through Urbanization. In: Weather and Climatic Modification,

W. N. Hess, ed. John Wiley & Sons, New York, 1974. pp. 726-763.

Landsberg, H. E. Actual and Potential Effects of Pollutants on Climate. International Conference on Environment and Assessment (ICESA), Paper No. 32-1, Las Vegas, 1975.

Landsberg, H. E. Effect of Man's Activity on Climate. Contribution No. 154 of the Graduate Program in Meteorology, University of Maryland, College Park, Maryland, 1977.

Launder, B. E., and D. B. Spalding. Lectures in Mathematical Models of Turbulence. Academic Press, New York, 1972. 169 pp.

Leahey, D. M., and J. P. Friend. A Model for Predicting the Depth of the Mixing Layer over an Urban Heat Island with Applications to New York City. J. Appl. Meteor. 10: 1162-1173, 1971.

Lee, R. L., R. W. Bergstrom, and R. D. Bornstein. Workshop on Modeling the Urban Boundary Layer, Las Vegas, Nevada, 5 May 1975. Bull Amer. Meteor. Soc. 57: 313-314, 1976.

Leighton, P. H. Photochemistry of Air Pollution. Academic Press, New York, 1961. 300 pp.

Lettau, H. H., and B. Davidson. Exploring the Atmosphere's First Mile. Volumes 1 and 2, New York, Pergamon Press, 1957.

Liou, K.-N., and T. Sasamori. On the Transfer of Solar Radiation in Aerosol Atmospheres. J. Atm. Sci. 32: 2166-2177, 1975.

Ludwig, C. B., R. Bartle, and M. Griggs. Study of Air Pollution Detection by Remote Sensors. General Dynamics Corporation, Report NASA CR-1380, 1969.

McElroy, J. L. A Numerical Study of the Nocturnal Heat Island over a Medium-Sized Mid-Altitude City (Columbus, Ohio). Boundary-Layer Meteorology 3: 442-453, 1973.

Myrup, L. O. A Numerical Model of the Urban Heat Island. J. Appl. Meteor. 8: 908-918, 1969.

Mitchell, J. M. The Temperature of Cities. Weatherwise 14: 224-229, 1961.

Mitchell, J. M. The Effect of Atmospheric Aerosols on Climate with Special Reference to Temperature Near the Earth Surface. J. Appl. Meteor. 10: 703-714, 1971.

Nappo, C. J., Jr. A Numerical Study of the Urban Heat Island.

In: Conference on Urban Environment and Second Conference on Biometeorology. American Meteorological Society, Boston, MA, 1972. 1-4 pp.

Oke, T. R., and C. East. The Urban Boundary Layer in Montreal. Boundary-Layer Meteor. 1: 411-437, 1971.

Oke, T. R., and F. R. Fuggle. Comparison of Urban/Rural Center and Net Radiation at Night. Boundary-Layer Meteor. 2: 290-308, 1972.

Oke, T. R., and G. B. Maxwell. Urban Heat Island Dynamics in Montreal and Vancouver. Atmospheric Environment 9: 191-200, 1975.

Olfe, D. B., and R. L. Lee. Linearized Calculations of Urban Heat Island Convection Effects. J. Atm. Sci. 28: 1374-1382, 1971.

Orlanski, I., B. B. Ross, and L. J. Polinsky. Diurnal Variation of the Planetary Boundary Layer. J. Atm. Sci. 31: 965-989, 1974.

Peterson, J. T. The Climate of Cities: A Survey of Recent Literature. Publication No. AP-59, U. S. Public Health Service, National Air Pollution Control Administration, 1969, Washington.

Peterson, J. T., and E. C. Flowers. Interactions between Air Pollution and Solar Radiation. Solar Energy 19: 23-37, 1977.

Robinson, G. D. Some Determinations of Atmospheric Aerosol, As Revealed by Measurements at the Ground. Arch Meteor. Geophys. Biokl. B12: 19-40, 1962.

Rouse, W. R., D. Noad, and J. McCutcheon. Radiation Temperature and Atmospheric Emissivities in a Polluted Atmosphere of Hamilton, Ontario. J. Appl. Meteor. 12: 798-807, 1973.

Russell, P., and G. Grams. Application of Soil Dust Optical Properties in Analytical Models of Climatic Change. J. Appl. Meteor. 14: 1037-1043, 1975.

Sasamori, T. A Numerical Study of Atmospheric and Soil Boundary Layers. J. Atm. Sci. 27: 1122-1137, 1970.

Shir, C. C., and R. D. Bornstein. Eddy Exchange Coefficients in Numerical Models of the Planetary Boundary Layer. Boundary-Layer Meteor. 11: 171-185, 1977.

Sisterton, D. L., and R. A. Dirks. The Urban Moisture Climate.

In: Proceedings of the Conference on Metropolitan Physical Environment. USDA Forest Service General Technical Report No. NE-25, Upper Darby, PA, 1977, pp. 26-35.

Spangler, T. C., and R. A. Dirks. Meso-Scale Variations of the Urban Mixing Height. Boundary-Layer Meteorol. 6: 423-441, 1974.

Stankowski, S. J. Population Density as an Indirect Indication of Urban and Suburban Land-Surface Modification. U. S. Geological Survey Professional Paper 800-13, 1972. pp. 219-224.

Stern, A. C., H. L. Wholers, R. W. Boubel, and W. P. Lowry. Fundamentals of Air Pollution. Academic Press, New York, 1972.

Torrance, K. E., and J. S. W. Shum. Time-varying energy consumption as a factor in urban climate. Atmospheric Environment 10: 329-337, 1976.

Venkatram, A., and R. Viskanta. Radiative Effects of Pollutants on the Planetary Boundary Layer. Report No. EPA-600/4-76-039, U. S. Environmental Protection Agency, Research Triangle Park, NC, 1976. 243 pp.

Viskanta, R., R. W. Bergstrom, Jr., and R. O. Johnson. Modeling the Effects of Pollutants and Dispersion in Urban Atmospheres. EPA-600/4-76-002, U. S. Environmental Protection Agency, Research Triangle Park, NC, 1976. 106 pp.

Viskanta, R., R. W. Bergstrom, and R. O. Johnson. Effects of Air Pollution on Thermal Structure and Dispersion in an Urban Planetary Boundary Layer. Contributions to Atmospheric Physics 50: 419-440, 1977a.

Viskanta, R., R. W. Bergstrom, and R. O. Johnson. Radiative Transfer in a Polluted Urban Planetary Boundary Layer. J. Atm. Sci. 34: 1091-1103, 1977b.

Vukovich, F. M. A Study of the Atmospheric Response due to a Diurnal Heating Function Characteristic of an Urban Complex. Mon. Wea. Rev. 99: 916-929, 1973.

Yu, T.-W., and N. K. Wagner. A Numerical Study of the Nocturnal Urban Boundary Layer. Boundary-Layer Meteorol. 9: 143-162, 1975.

Welch, R., and W. Zdunkowski. A Radiation Model of the Polluted Atmospheric Boundary Layer. J. Atm. Sci. 33: 2170-2184, 1976.

Zdunkowski, W. G., and N. D. McQuage. Short-Term Effects of Aerosols on the Layer Near the Ground in a Cloudless Atmosphere. Tellus 3; 237-254.

Zdunkowski, W. G., R. M. Welch, and J. Paegle. One-Dimensional Numerical Simulations of the Effects of Air Pollution on the Planetary Boundary Layer. J. Atm. Sci. 33: 239-2414, 1976.

APPENDIX

PUBLICATIONS

Venkatram, A., and R. Viskanta. Radiative Effects of Pollutants on the Planetary Boundary Layer. EPA-600-4-76-039, U. S. Environmental Protection Agency, Research Triangle Park, NC, 1976. 243 pp.

Venkatram, A. and R. Viskanta. Effect of Elevated Pollutant Layers on Mixed Layer Growth. In: Preprints of the Third Symposium on Atmospheric Turbulence, Diffusion and Air Quality, American Meteorological Society, Boston, MA, 1976, pp. 528-532.

Venkatram, A. and R. Viskanta. The Contribution of Pollutants to the Urban Heat Island 'Crossover' Effects. In: Preprints of the Third Symposium on Atmospheric Turbulence, Diffusion and Air Quality, American Meteorological Society, Boston, MA, 1976, pp. 536-542.

Viskanta, R., R. O. Johnson and R. W. Bergstrom. Effect of Urbanization on the Thermal Structure in the Atmosphere. In: Proceedings of the Conference on METROPOLITAN PHYSICAL ENVIRONMENT, USDA Forest Service General Technical Report NE-25, Upper Darby, PA, 1977, pp. 62-76. (Paper presented at The Conference on METROPOLITAN PHYSICAL ENVIRONMENT; Syracuse, New York, 25-29 August 1975).

Viskanta, R., R. W. Bergstrom, and R. O. Johnson, Effects of Pollutants on Radiative Transfer in an Urban Boundary Layer. In: Proceedings of the SYMPOSIUM ON RADIATIVE TRANSFER IN THE ATMOSPHERE, Science Press, Princeton, NJ, 1977, pp. 460-462. (Paper presented at the Symposium on the Radiative Transfer in the Atmosphere, Garmisch-Partenkirchen, Federal Republic of Germany, 19-28 August 1976).

Viskanta, R., R. W. Bergstrom, and R. O. Johnson. Radiative Transfer in a Polluted Urban Planetary Boundary Layer. J. Atm. Sci., 34 (7): 1991-1103, 1977.

Viskanta, R., R. W. Bergstrom, and R. O. Johnson. Effects of

Air Pollution on Thermal Structure and Dispersion in an Urban Planetary Boundary Layer. Cont. Atm. Phys., 50 (7): 419-440, 1977.

Venkatram, A., and R. Viskanta. Effects of Aerosol-Induced Heating on the Convective Boundary Layer. J. Atm. Sci., 34 (12): 1918-1933, 1977.

Venkatram, A., and R. Viskanta. Radiative Effects of Elevated Pollutant Layers. J. Appl. Meteor., 16 (12): 1256-1272, 1977.

Viskanta, R., T. L. Weirich, and R. A. Daniel. Effects of Pollutant and Heat Emissions on Temperature in an Urban Area. In: Environmental Effects of Atmospheric Heat/Moisture Releases, American Society of Mechanical Engineers, New York, 1978, pp. 107-117.

Viskanta, R., and T. L. Weirich. Feedback Between Radiatively Interacting Pollutants and Their Dispersion in the Urban Planetary Boundary Layer. In: Papers Presented at the WMO Symposium on Boundary Layer Physics Applied to Specific Problems of Air Pollution, WMO-No. 510, World Meteorological Organization, Geneva, 1978, pp. 31-38.

Viskanta, R., and R. A. Daniel. Radiative Effects of Elevated Pollutant Layers on Temperature Structure and Dispersion in an Urban Atmosphere. J. Appl. Meteor. (submitted for publication).

TECHNICAL REPORT DATA
(Please read Instructions on the reverse before completing)

1. REPORT NO.	2.	3. RECIPIENT'S ACCESSION NO.
EPA-600/4-79-012		

4. TITLE AND SUBTITLE	5. REPORT DATE
EFFECTS OF POLLUTANTS AND URBAN PARAMETERS ON ATMOSPHERIC DISPERSION AND TEMPERATURE	February 1979
	6. PERFORMING ORGANIZATION CODE
7. AUTHOR(S)	8. PERFORMING ORGANIZATION REPORT NO.
R. Viskanta and T. L. Weirich	
9. PERFORMING ORGANIZATION NAME AND ADDRESS	10. PROGRAM ELEMENT NO.
School of Mechanical Engineering Purdue University West Lafayette, IN 47907	1AA603A AG-02(FY-77)
	11. CONTRACT/GRANT NO.
	R803514
12. SPONSORING AGENCY NAME AND ADDRESS	13. TYPE OF REPORT AND PERIOD COVERED
Environmental Sciences Research Laboratory - RTP,NC Office of Research and Development U. S. Environmental Protection Agency Research Triangle Park, NC 27711	Final 1/75-12/77
	14. SPONSORING AGENCY CODE
	EPA/600/09

15. SUPPLEMENTARY NOTES

16. ABSTRACT

Two dimensional numerical simulations of planetary boundary layer flow indicate that urbanization (increase of surface roughness, changes in surface albedo, and the addition of anthropogenic heat sources) has a greater influence on the urban heat island than the addition of pollutants (gaseous and particulate) which are active in the radiative transfer processes of the heat budget. Although mid-day surface temperatures are decreased by adding such pollutants, temperatures at other times of day are increased. These simulations also indicate that heat islands are most pronounced with a snow cover on the ground. The warmer surface temperatures enhance low level pollutant dispersal with a consequent 25% concentration reduction. These results indicate that a change in land use is an important factor in local climate and weather modification.

17. KEY WORDS AND DOCUMENT ANALYSIS

a. DESCRIPTORS	b. IDENTIFIERS/OPEN ENDED TERMS	c. COSATI Field/Group
*Air pollution		13B
*Mathematical models		12A
*Boundary layer flow		20D
*Urbanization		05J
*Diffusion		20M
*Surface temperature		

18. DISTRIBUTION STATEMENT	19. SECURITY CLASS *(This Report)*	21. NO. OF PAGES
RELEASE TO PUBLIC	UNCLASSIFIED	143
	20. SECURITY CLASS *(This page)*	22. PRICE
	UNCLASSIFIED	

EPA Form 2220-1 (9-73)